

Cyclin G and the Polycomb Repressive Complexes PRC1 and PR-DUB cooperate for developmental stability.

Delphine Dardalhon-Cuménal^{1,2}, Jérôme Deraze^{1,2}, Camille A Dupont^{1,2}, Valérie Ribeiro^{1,2}, Anne Coléno-Costes^{1,2}, Juliette Pouch⁴, Stéphane Le Crom^{4,5}, Hélène Thomassin^{1,2}, Vincent Debat³, Neel B Randsholt^{1,2} and Frédérique Peronnet^{1,2}.

¹ Sorbonne Universités, UPMC Univ Paris 06, Institut de Biologie Paris-Seine (IBPS), UMR 7622, Developmental Biology, F-75005, Paris, France

² CNRS, IBPS, UMR 7622, Developmental Biology, F-75005, Paris, France

³ Muséum national d'Histoire naturelle, Institut de Systématique, Évolution, Biodiversité, ISYEB UMR 7205, CNRS-MNHN-UPMC-EPHE, Sorbonne Universités, 45 rue Buffon, 75005 Paris, France

⁴ IBENS, Département de Biologie, Ecole Normale Supérieure, CNRS, Inserm, PSL Research University, F - 75005 Paris, France

⁵ Sorbonne Universités, UPMC Univ Paris 06, Univ Antilles, Univ Nice Sophia Antipolis, CNRS, Evolution Paris Seine - Institut de Biologie Paris Seine (EPS - IBPS), 75005 Paris, France

Keywords : *Drosophila melanogaster*, Developmental Stability, Fluctuating Asymmetry, Developmental noise, Polycomb, Cyclin G

ABSTRACT

In *Drosophila*, ubiquitous expression of a short Cyclin G isoform generates extreme developmental noise estimated by fluctuating asymmetry (FA), providing a model to tackle developmental stability. This transcriptional cyclin interacts with chromatin regulators of the Enhancer of Trithorax and Polycomb (ETP) and Polycomb families. This led us to investigate the importance of these interactions in developmental stability. Deregulation of Cyclin G highlights an organ intrinsic control of developmental noise, linked to the ETP-interacting domain, and enhanced by mutations in genes encoding members of the Polycomb Repressive complexes PRC1 and PR-DUB. Deep-sequencing of wing imaginal discs deregulating CycG reveals that high developmental noise correlates with up-regulation of genes involved in translation and down-regulation of genes involved in energy production. Most Cyclin G direct transcriptional targets are also direct targets of PRC1 and RNAPoIII in the developing wing. Altogether, our results suggest that Cyclin G, PRC1 and PR-DUB cooperate for developmental stability.

INTRODUCTION

Developmental stability has been described as the set of processes that buffer disruption of developmental trajectories for a given genotype within a particular environment (Palmer, 1994). In other words, developmental stability compensates the random stochastic variation of processes at play during development. Many mechanisms working from the molecular to the whole organism levels contribute to developmental stability (Nijhout and Davidowitz, 2003). For example, chaperones, such as heat-shock proteins, participate in developmental stability in a large variety of developmental processes by protecting misfolded proteins from denaturation (Feder and Hofmann, 1999; Queitsch et al., 2002; Rutherford et al., 2007). In *Drosophila melanogaster*, adjustment of cell growth to cell proliferation is essential to developmental stability by allowing to achieve a consistent organ size (e.g. wing size) in spite of variation in cell size or cell number (Debat et al., 2011; Debat and Peronnet, 2013).

Developmental noise, the “sum” of the stochastic part of each developmental process, can be observed macroscopically for morphological traits. In bilaterians, quantification of departure from perfect symmetry, the so-called fluctuating asymmetry (FA), is the most commonly used index to estimate developmental noise (Van Valen, 1962; Palmer and Strobeck, 1992). Indeed, the two sides of bilaterally symmetrical traits are influenced by the same genotype and environmental conditions, and differences between them are thus only due to developmental noise. The use of FA as an index of developmental noise makes analysis of the mechanistic and genetic bases of developmental stability compatible with custom genetic and molecular approaches of developmental biology.

The evolutionary role of developmental stability is subject to many speculations (e.g. Dongen, 2006) as its genetic bases remain unclear (for reviews see Leamy and Klingenberg, 2005; Debat and Peronnet, 2013). Experiments showing the role of *Hsp90* in buffering genetic variation led to the idea that developmental stability could be ensured by specific genes (Rutherford and Lindquist, 1998; Milton et al., 2003; Debat et al., 2006; Yeyati et al., 2007; Sangster et al., 2008). On the other hand, both theory and experiments show that complex genetic networks can become intrinsically robust to perturbations, notably through negative and positive feedbacks, suggesting that the topology of gene networks is of

paramount importance for developmental stability (Barabasi and Albert, 1999; Siegal and Bergman, 2002; Newman, 2003; Kitano, 2004). Several authors have further suggested that hubs, *i.e.* the most connected genes in these networks, might be particularly important for developmental stability (Rutherford et al., 2007; Levy and Siegal, 2008).

In *Drosophila*, mutants for *dLLP8* and *hid*, two genes involved in the control of systemic growth and apoptosis respectively, have been reported to display high FA as compared to wild type flies from the same genetic background (Garelli et al., 2012; Colombani et al., 2012; Neto-Silva et al., 2009), suggesting that these genes are important for developmental stability. Two studies have scanned the *Drosophila* genome for regions involved in developmental stability using FA as an estimator of developmental noise (Breuker et al., 2006; Takahashi et al., 2011). Several deletions increased FA but the genes responsible for this effect inside the deletions were not identified. Nevertheless, these studies confirm that the determinism of developmental stability could well be polygenic, as suggested by Quantitative Trait Loci analyses in mouse (Leamy et al., 2002; Leamy et al., 2005; Leamy et al., 2015). Together, these data reinforce the idea that developmental stability depends on gene networks.

We have shown that the gene *Cyclin G* (*CycG*) of *Drosophila melanogaster*, which encodes a protein involved in transcriptional regulation and in the cell cycle, is important for developmental stability (Salvaing et al., 2008a; Faradji et al., 2011; Debat et al., 2011; Dupont et al., 2015). Indeed, ubiquitous expression of a short Cyclin G version lacking the C-terminal PEST-rich domain (*CycG^{ΔP}*) generates a very high FA in several organs, notably in the wing. Interestingly, FA induced by *CycG^{ΔP}* expression correlates with high variability in cell size and loss of correlation between cell size and cell number, suggesting that the noisy process would somehow be connected to cell cycle related cell growth (Debat et al., 2011). Hence, *CycG* deregulation provides a convenient sensitized system to tackle the impact of cell growth variability on developmental stability.

We previously showed that *CycG* encodes a transcriptional cyclin and interacts with genes of the *Polycomb-group* (*PcG*), *trithorax-group* (*trxG*), and *Enhancer of Trithorax and Polycomb* (*ETP*) families (Salvaing et al., 2008a; Salvaing et al., 2008b; Dupont et al., 2015). These genes encode evolutionary conserved proteins assembled into large multimeric complexes that bind chromatin. They ensure maintenance of gene expression patterns during development (for recent

reviews see Grossniklaus and Paro, 2014; Kingston and Tamkun, 2014; Geisler and Paro, 2015). *PcG* genes are involved in long-term gene repression, whereas *trxG* genes maintain gene activation and counteract *PcG* action. *ETP* genes encode co-factors of both *trxG* and *PcG* genes, and behave alternatively as repressors or activators of target genes (Gildea et al., 2000; Grimaud et al., 2006; Beck et al., 2010). More recently, we discovered that *CycG* behaves as an *Enhancer of Polycomb* regarding homeotic gene regulation suggesting that it is involved in the silencing of these genes (Dupont et al., 2015). Importantly, Cyclin G physically interacts with the ETP proteins Additional Sex Comb (ASX) and Corto *via* its N-terminal ETP-interacting domain, and co-localizes with them on polytene chromosomes at many sites (Salvaing et al., 2008a; Dupont et al., 2015). Hence, Cyclin G and these ETPs might share many transcriptional targets and might in particular control cell growth *via* epigenetic regulation of genes involved in growth pathways.

Here, we investigate in depth the role of *CycG* in developmental stability. We first show that localized expression of *CycG*^{AP} in wing imaginal discs is necessary and sufficient to induce high FA of adult wings. Furthermore, this organ-autonomous effect increases when the ETP-interacting domain of Cyclin G is removed. We show that several mutations for *PcG* or *ETP* genes, notably those encoding members of the PRC1 and PR-DUB complexes, substantially increase *CycG*-induced FA. Next, we report analysis of the transcriptome of wing imaginal discs expressing *CycG*^{AP} by RNA-seq and find that transcriptional deregulation of genes involved in translation and energy production correlates with high FA of adult wings. By ChIP-seq, we identify Cyclin G binding sites on the whole genome in wing imaginal discs. Strikingly, we observe a significant overlap with genes also bound by ASX, by the Polycomb Repressive complex PRC1, and by RNAPolIII in the same tissue. We identify a sub-network of 222 genes centred on Cyclin G showing simultaneous up-regulation of genes involved in translation and down-regulation of genes involved in mitochondrial activity and metabolism. Taken together, our data suggest that Cyclin G and the Polycomb complexes PRC1 and PR-DUB cooperate in sustaining developmental stability. Precise regulation of genes involved in translation and energy production might be important for developmental stability.

RESULTS

Expression of *CycG*^{ΔP} in wing precursors is necessary and sufficient to induce high wing FA

We previously reported that expression of *CycG* deleted of the PEST-rich C-terminal domain (amino-acids 541 to 566) (*CycG*^{ΔP}) under control of ubiquitous drivers (*da-Gal4* or *Actin-Gal4*) generated extremely high FA, notably in wings (Debat et al., 2011) (Figure 1). The strength of this effect was unprecedented in any system or trait. Expression of *CycG*^{ΔP} thus provides a unique tool to investigate developmental stability in depth. To determine whether wing FA was due to local or systemic expression of *CycG*^{ΔP}, we tested a panel of Gal4 drivers specific for wing imaginal discs or neurons. A brain circuit which relays information for bilateral growth synchronization was recently identified (Vallejo et al., 2015). It notably involves a pair of neurons expressing the dILP8 receptor that connects with the insulin-producing cells (IPCs) and the prothoracicotrophic hormone (PTTH) neurons. This circuit was particularly appropriate to test the existence of a remote effect of *CycG*^{ΔP} expression in generating high FA in the wing. Expression of *CycG*^{ΔP} in this circuit (using *dilp3*-, *NPF*-, *pdf*-, *per*-, *phm*- and *R19B09-Gal4* drivers) did not increase FA of adult wings (Figure 2 and Table 1). Furthermore, expression of *CycG*^{ΔP} in cells of the future wing hinge using the *ts-Gal4* driver did not affect wing FA either. By contrast, expressing *CycG*^{ΔP} with 5 different wing pouch drivers (*nub*-, *omb*-, *rn*-, *sd*- and *vg-Gal4*) induced high FA. We thus concluded that *CycG*^{ΔP}-induced wing FA was due to an intrinsic response of the growing wing tissue.

The Cyclin G ETP interacting domain sustains developmental stability

The 566 amino-acid Cyclin G protein exhibits 3 remarkable domains: the ETP-interacting domain (amino-acids 1 to 130) that physically interacts with the ETPs Corto and ASX, a cyclin domain (amino-acids 287 to 360) that presents high similarity with the cyclin domain of vertebrate G-type cyclins, and a PEST-rich domain (amino-acids 541 to 566) (Salvaing et al., 2008a; Faradji et al., 2011; Dupont et al., 2015). To test whether the interaction with ETPs (and thus transcriptional regulation by Cyclin G) could be important to control FA, we generated new transgenic lines enabling to express different versions of the *CycG* cDNA: *CycG*^{FL} (encoding the full-length protein), *CycG*^{ΔE} (encoding an ETP-interacting domain deleted protein), *CycG*^{ΔP} (encoding a PEST domain deleted protein), and *CycG*^{ΔEΔP}

(encoding an ETP-interacting and PEST domain deleted protein). In order to express these different cDNAs at the same level and compare the amounts of FA induced, all transgenes were integrated at the same site using the *PhiC31* integrase system (at position 51C on the second chromosome). Expression of these transgenic lines was ubiquitously driven by *da-Gal4*. We first confirmed that expression of *CycG^{ΔP}* induced very high FA as compared to *yw* and *da-Gal4/+* controls. Furthermore, expression of *CycG^{FL}* also significantly increased FA, although to a much lesser extent. Interestingly, expression of either *CycG^{ΔE}* or *CycG^{ΔEΔP}* significantly increased FA as compared to *CycG^{FL}* or *CycG^{ΔP}*, respectively (Figure 3 and Table 2). These results show that the ETP interacting domain tends to limit Cyclin G-induced FA and suggest that the interaction between Cyclin G and chromatin regulators sustains developmental stability.

***CycG* and *PcG* or *ETP* genes interact for developmental stability**

We next addressed genetic interactions between *CycG* and *PcG* or *ETP* genes for developmental stability. The alleles used are listed in Table 3. FA of flies heterozygous for *PcG* and *ETP* loss of function alleles was not significantly different from that of control flies. However, when combined with a *da-Gal4, UAS-CycG^{ΔP}* chromosome, many of these mutations significantly increased wing FA as compared to *da-Gal4, UAS-CycG^{ΔP}* flies (Figure 4 and Table S1). This was notably the case for alleles for PRC1 and PR-DUB encoding genes, the *PcG* genes *Sex comb extra* (*Sce¹*, *Sce^{33M2}* and *Sce^{KO4}*), *calypso* (*caly¹* and *caly²*), *Sex comb on midleg* (*Scm^{D1}*), *Polycomb* (*Pc¹*), and *polyhomeotic* (*ph-p⁴¹⁰* and *ph-d⁴⁰¹ph-p⁶⁰²*). No modification of *CycG^{ΔP}*-induced FA was observed with the *Psc¹* allele. However, this allele has been described as a complex mutation with both loss and gain of function features (Adler et al., 1989).

Opposite effects were observed for different alleles of ETPs *Asx* and *corto*. *Asx^{22P4}* increased *da-Gal4, UAS-CycG^{ΔP}* FA whereas *Asx^{XF23}* decreased it. *Asx^{XF23}* behaves genetically as a null allele but has not been molecularly characterized (Simon et al., 1992), whereas the *Asx^{22P4}* allele does not produce any protein and thus likely reflects the effect of loss of ASX (Scheuermann et al., 2010). Similarly, the *corto^{L1}* allele increased *CycG^{ΔP}*-induced FA whereas the *corto⁴²⁰* allele had no effect. In order to characterize these *corto* alleles, we combined them with the *Df(3R)6-7* deficiency that uncovers the *corto* locus, amplified the region by PCR and sequenced

it. The *corto*⁴²⁰ allele corresponds to a substitution of 14,209 nucleotides starting at position -59 upstream of the *corto* Transcriptional Start Site (TSS) by a 30-nucleotide sequence. Hence, this allele does not produce any truncated protein. By contrast, *corto*^{L1} corresponds to a C towards T substitution that introduces a stop codon at position +73 downstream the TSS, generating a 24 amino-acid polypeptide. *corto*^{L1} might then behave as a dominant-negative mutation. Lastly, no modification of *CycG*^{ΔP}-induced FA was observed for *E(z)*⁶³ and *esc*²¹.

Interestingly, *Asx* and *caly* encode proteins of the Polycomb Repressive complex PR-DUB whereas *Pc*, *ph*, *Sce* and *Scm* encode proteins of the Polycomb Repressive complex PRC1, and *E(z)* and *esc* encode proteins of the Polycomb Repressive complex PRC2. Taken together, these results indicate that Cyclin G interacts with the Polycomb complexes PRC1 and PR-DUB, but not with PRC2, for developmental stability.

Expression of *CycG*^{ΔP} or *CycG*^{ΔEΔP} does not modify the bulk of H2AK118ub

Cyclin G binds polytene chromosomes at many sites and co-localizes extensively with PH and ASX suggesting a potential interaction with the PRC1 and PR-DUB complexes on chromatin (Salvaing et al., 2008a; Dupont et al., 2015). The two genes *Sce* and *caly* encode antagonistic enzymes of the PRC1 and PR-DUB complexes, respectively. SCE, aka dRing, ubiquitinates histone H2A on lysine 118 (H2AK118ub) whereas Calypso, aka dBap1, is the major deubiquitinase of the same H2A residue (Scheuermann et al., 2010; Scheuermann et al., 2012). To investigate whether Cyclin G was related to these ubiquitin ligase/deubiquitinase activities, we immunostained polytene chromosomes from *w*¹¹⁸ larvae with anti-Cyclin G and anti-human H2AK118ub antibodies (homologous to *Drosophila* H2AK118ub) (Pengelly et al., 2015). Cyclin G and H2AK118ub co-localized extensively on chromosome arms suggesting that Cyclin G transcriptional activity might somehow be connected to the presence of this histone mark (Figure S1A). However, when either *CycG*^{ΔP} or *CycG*^{ΔEΔP} was expressed in the posterior compartment of wing imaginal discs using the *en-Gal4* driver, the global amount of H2AK118ub was not markedly modified (Figure S1B, Figure S1C). We thus concluded that high FA was not related to a global perturbation of H2AK118 ubiquitination level.

Cyclin G controls the expression of genes involved in translation and energy production

Cyclin G controls the transcription of the homeotic gene *Abdominal-B* and more specifically behaves as an *Enhancer of PcG* gene in the regulation of homeotic gene expression (Salvaing et al., 2008b; Dupont et al., 2015). However, the high number of Cyclin G binding sites on polytene chromosomes suggests that this cyclin has many other transcriptional targets. We thus hypothesized that the high FA induced by expression of *CycG^{ΔP}* might be related to the deregulation of Cyclin G transcriptional targets. To further address the role of Cyclin G in transcriptional regulation, we deep-sequenced the transcripts from wing imaginal discs of *da-Gal4, UAS-CycG^{ΔP}/+* and *da-Gal4/+* third instar larvae. Sequence reads were aligned with the *Drosophila melanogaster* genome to generate global gene expression profiles. We performed differential analyses to obtain expression changes for *da-Gal4, UAS-CycG^{ΔP}/+* as compared to the *da-Gal4/+* control. With an adjusted p-value threshold of 0.05, we retrieved 530 genes whose expression was significantly different between the two genotypes (Table S2). Surprisingly, expression of *CycG* was only weakly induced in *da-Gal4, UAS-CycG^{ΔP}/+* imaginal discs as compared to *da-Gal4/+* imaginal discs (1.3 fold). In order to test the hypothesis that Cyclin G could directly or not, induce its own repression, we designed primers in the 3'UTR to measure expression of the endogenous *CycG* gene. Indeed, expression of endogenous *CycG* was significantly decreased when *CycG^{ΔP}* was expressed (Figure 5A and Table S3). Among the 530 genes deregulated in *da-Gal4, UAS-CycG^{ΔP}/+* imaginal discs, 216 were up-regulated and 314 down-regulated. Analysis of Gene Ontology (GO) revealed that up-regulated genes were enriched in the categories *cytoplasmic translation* and *translational initiation* whereas down-regulated genes were enriched in the category *mitochondrial respiratory chain complex* (Figure 5B and Table S4). By RT-qPCR, we verified that several ribosomal protein genes (*RpL15, RpL7* and *Rack1*) were over-expressed in *da-Gal4, UAS-CycG^{ΔP}/+* imaginal discs (Figure 5C and Table S5).

In conclusion, *CycG*-induced fluctuating asymmetry correlates with activation of genes involved in translation and repression of genes involved in energy production.

Cyclin G binds the Transcriptional Start Sites of many genes also bound by PRC1 and ASX

In order to determine the direct transcriptional targets of Cyclin G, we analysed by ChIP-seq the genome-wide binding sites of Cyclin G in *+ / UAS-Myc-CycG^{ΔP}; da-Gal4/+* imaginal discs. 889 genes with significant peaks at the transcriptional start site (TSS) were recovered (Table S6 and Figures 6A and 6B). ChIP-qPCR analysis of Cyclin G binding on *RPL7*, *RPL5*, and *Rack1* confirmed that Cyclin G peaked on the TSS of these genes and decreased on the gene body (Figure 6C and Table S7). Furthermore, Cyclin G bound its own TSS almost significantly. We then analysed the binding of Cyclin G on its own gene by ChIP-qPCR and verified the presence of Cyclin G on its TSS (Figure 6C and Table S7). As endogenous *CycG* was down-regulated when *CycG^{ΔP}* was expressed, this suggests that Cyclin G represses its own promoter.

The 889 Cyclin G-bound genes were enriched in GO categories *cytoplasmic translation* and *protein phosphorylation* (Figure 6D). Comparison of the 530 genes deregulated in imaginal discs expressing *CycG^{ΔP}* with the 889 genes presenting a peak at the TSS showed that only 62 genes were both deregulated (39 up- and 23 down-regulated) and bound by Cyclin G (Table S8). Strikingly, the 39 up-regulated genes were significantly enriched in the GO category *translation* (GO:0002181~cytoplasmic translation, 14 genes, enrichment score: 11.84, adjusted p-value 2.07E-16).

Using published datasets, we analysed the correlation between regions bound by Cyclin G in *+ / UAS-Myc-CycG^{ΔP}; da-Gal4/+* imaginal discs and those bound by PRC1, PR-DUB or RNAPoIII, or enriched in H3K27me3, in wild type wing imaginal discs (Table S9). Cyclin G-bound regions were significantly exclusive from H3K27me3, corroborating polytene chromosome immunostainings (Dupont et al., 2015). The same comparisons were performed gene-wise and gave the same results. Notably, 80% of Cyclin G-bound genes were bound by RNAPoIII (Figure 7). Considering RNAPoIII as a proxy for transcriptional activity, we concluded that Cyclin G-bound genes were located in open chromatin and were either paused or transcribed. However, Cyclin G-bound genes were also significantly enriched in PRC1 target genes. Given that PRC1 has the ability to block transcriptional initiation (Dellino et al., 2004), it suggests that Cyclin G-bound genes were most probably paused. Cyclin G also shared many target genes with ASX but, though ASX and Calypso belong to the PR-DUB complex, Cyclin G did not share binding sites with Calypso. This indicates either that the interaction between Cyclin G and ASX

destabilizes the PR-DUB complex or that it takes place outside PR-DUB.

Cyclin G is central in the wing imaginal disc network

These genome-wide analyses indicate that Cyclin G coordinates the expression of genes involved in translation and energy production. However, only a few Cyclin G-bound genes were deregulated in *da-Gal4, UAS-CycG^{ΔP}/+* imaginal discs. To better understand how Cyclin G orchestrates target gene expression, we developed a systems biology approach. We first built an interactome based on genes expressed in control *da-Gal4/+* wing imaginal discs (with a cutoff of 10 reads). Edges corresponding to protein-protein interactions (PPI) and transcription factor-gene interactions (PDI) were integrated into this interactome through DroID (Murali et al., 2011). The resulting wing imaginal disc interactome, further called the WID network, was composed of 9,966 nodes (proteins or genes) connected *via* 56,133 edges (interactions) (WID.xml file). We then examined the position of Cyclin G in this network. Betweenness centrality - *i.e.* the total number of non-redundant shortest paths going through a certain node – is a measure of centrality in a network (Yu et al., 2007). A node with a high betweenness centrality could control the flow of information across the network (Yamada and Bork, 2009). With 8.32E-03, Cyclin G had one of the highest value of betweenness centrality of the network, ranking at the 30th position among the 9,966 nodes. This suggests that Cyclin G represents a hub in the WID network.

In order to isolate a connected component of the WID network that showed significant expression change when *CycG^{ΔP}* is expressed, we introduced the expression matrix describing expression of the 530 significantly deregulated genes in the WID network. We next used JactiveModules to identify sub-networks of co-deregulated genes (Ideker et al., 2002). A significant sub-network of 222 nodes and 1069 edges centred on Cyclin G was isolated (Z score 48.53). This sub-network was laid out according to functional categories (Figure 8A, *CycG_subnetwork.xml*). Four modules composed of genes respectively involved in transcription, mitochondrial activity, translation, and metabolism, were found to be highly connected to Cyclin G. Strikingly, the “translation” module was mainly composed of genes up-regulated in *da-Gal4, UAS-CycG^{ΔP}/+* wing imaginal discs. On the contrary, the “mitochondrion” and “metabolism” modules were mainly composed of genes down-regulated in *da-Gal4, UAS-CycG^{ΔP}/+* wing imaginal discs. Hence, high fluctuating asymmetry of *da-*

Gal4, UAS-CycG^{ΔP}/+ flies correlated positively with the expression of genes involved in translation and negatively with the expression of genes involved in energy production and metabolism. Interestingly, Cyclin G-bound genes in this sub-network were enriched in genes bound by the PRC1 proteins PC, PH and PSC, as well as by RNAPoIII, and to a lesser extent by ASX (Figure 8B).

DISCUSSION

The *CycG* gene of *Drosophila melanogaster* encodes a cyclin involved in transcriptional control, cell growth and the cell cycle (Salvaing et al., 2008; Faradji et al., 2011). Mild overexpression of a cDNA encoding Cyclin G deleted of a short C-terminal sequence potentially involved in Cyclin G degradation (a PEST-rich domain; *da-Gal4, UAS-CycG^{ΔP}/+*) induces high fluctuating asymmetry (FA), notably of wings (Debat et al., 2011). Under laboratory conditions (*i.e.* low environmental variation combined with near isogenic lines), this FA should mainly result from developmental noise (Debat and Peronnet, 2013). Thus, *da-Gal4, UAS-CycG^{ΔP}* flies provide a unique tool to investigate the genetic bases of developmental stability. Cyclin G interacts physically with two chromatin regulators of the Enhancers of Trithorax and Polycomb family (ETP), and genetically with many *Polycomb-group* (*PcG*) and *trithorax-group* (*trxG*) genes (Dupont et al., 2015). This prompted us to re-examine *CycG*-induced developmental stability, notably by testing the effect of chromatin regulator mutations, and to investigate deeply the role of Cyclin G in transcriptional regulation.

Cyclin G maintains developmental stability through an organ-autonomous process that involves the PRC1 and PR-DUB complexes

In *Drosophila* very few mutations have been shown to induce an abnormally high FA. Among them are mutations of the gene encoding the *Drosophila* insulin-like peptide 8 (*Dilp8*). *Dilp8* participates in systemic coordination of growth. Being produced in growing tissues, it is secreted into the haemolymph and regulates hormone production *via* a well-identified neuronal circuit (Parker and Shingleton, 2011; Garelli et al., 2012; Colombani et al., 2012). Notably, the neurons that produce *Lgr3*, the *Dilp8* receptor, have been identified, and inactivation of *Lgr3* in these neurons also induces high FA. We investigated here the role of *CycG* in this process by deregulating it in the different modules of the circuit. *CycG*-induced wing FA only

occurred when the deregulation was local, *i.e.* in wing imaginal discs. More particularly, deregulation of *CycG* in the *Lgr3* neurons did not increase FA. We cannot exclude that Cyclin G induces expression of a systemic factor that is dumped into the haemolymph. However, neither *Dilp8* nor any other insulin-like peptide gene were found deregulated in *da-Gal4, UAS-CycG^{ΔP}* wing imaginal discs. Altogether, these observations suggest that *CycG* maintains developmental stability through an autonomous mechanism which would not involve the systemic *Dilp8/Lgr3* pathway. Such a mechanism recalls Garcia-Bellido's Entelechia model which proposes that local interactions between wing imaginal disc cells, or populations of these cells, orchestrate their own proliferation in order to generate an adult organ of constant size and shape, independently of global cues (García-Bellido and García-Bellido, 1998; García-Bellido 2009).

Expression of Cyclin G deleted of the ETP interacting domain doubles FA as compared to expression of Cyclin G with this domain, irrespective of whether the PEST domain is present or not. Hence, the interaction between Cyclin G and chromatin regulators might somehow participate in developmental stability. To test this hypothesis, we combined the *da-Gal4, UAS-CycG^{ΔP}* chromosome and *ETP* or *PcG* mutations. We observed that mutations of the PRC1 and PR-DUB encoding genes strongly increase FA. Moreover, many of the genes that are bound by Cyclin G in wing imaginal discs are also bound by PRC1 and by ASX. Altogether these observations suggest that transcriptional regulation of target genes shared by Cyclin G, PRC1 and ASX is of paramount importance for developmental stability. We did not observe any significant overlap between Cyclin G-bound genes and binding sites for Calypso, the second component of PR-DUB. Yet, *caly* mutations strongly increase *CycG*-induced FA. Thus, the role of PR-DUB in this context remains to be clarified.

PRC1 and PR-DUB contain antagonistic enzymes (SCE/dRing and Calypso) that respectively ubiquitinates and deubiquitinates H2A on lysine 118 in *Drosophila* (lysine 119 in human). Cyclin G co-localizes extensively with H2AK118ub on polytene chromosomes. However, no modification in the global level of H2AK118 ubiquitination was detected in tissues where Cyclin G isoforms were expressed. It was recently shown that canonical PRC1 accounts for only a small fraction of global H2AK118ub, most of this ubiquitination being due to L(3)73Ah, a homolog of mammalian PCGF3 (Lee et al., 2015). Altogether, our data suggest that H2AK118ub

is not involved in developmental stability and rather support the importance of the interaction between Cyclin G and canonical PRC1 in this process. It is tempting to speculate that PRC1 and PR-DUB are partners in the ubiquitination/deubiquitination of an unknown protein important for developmental stability.

Regulation of growth during the cell cycle might be a factor of developmental stability

Additional evidence further connects developmental stability to growth regulation during the cell cycle. Indeed, *CycG*-induced developmental noise is associated with high variance in cell size along with loss of correlation between cell size and cell number (Debat et al., 2011). As Cyclin G is involved in the control of growth in G1 phase of the cell cycle (Faradji et al., 2011), this supports the hypothesis that a mechanism linked to the regulation of cell cycle-dependent growth is essential for developmental stability (Debat et al., 2011). The fact that genes deregulated in wing imaginal discs deregulating *CycG* are involved mainly in translation, energy production and metabolism, strengthens this hypothesis.

It was shown that promoters of actively transcribed genes, notably *GAPDH* and several ribosomal protein genes, are bookmarked by ubiquitination during mitosis (Arora et al., 2012; Arora et al., 2015). This mechanism would allow post-mitotic resumption of their transcription at the very beginning of the G1 phase. Ubiquitination of these genes correlates with active histone marks such as H3K4me3 and H3K36me3 but not with the repressive histone mark H3K27me3. The enzymes responsible for this ubiquitination are the vertebrate PSC homolog BMI1, and Ring1A, one of the SCE/dRing homologs (Arora et al., 2015). In vertebrates, the major PRC1 component that catalyzes H2A ubiquitination is not Ring1A but its homolog Ring1B suggesting that the role of BMI1 and Ring1A in molecular bookmarking are independent of PRC1, and that BMI1 and Ring1A ubiquitinate another chromatin protein (Arora et al., 2015). In *Drosophila*, this role might be played by PRC1 and SCE/dRing. Cyclin G is exclusive of H3K27me3, and binds the promoter of many ribosomal protein genes (Dupont et al., 2015 and the present work). Furthermore, *CycG* deregulation impairs G1 phase progression and cell growth (Faradji et al., 2011). Lastly, the highest FA is observed when Cyclin G lacking the PEST domain, a potential ubiquitination site, is expressed. Hence, an exciting hypothesis would be that Cyclin G is ubiquitinated by PRC1, or PSC and

SCE/dRing outside PRC1, thus releasing the transcriptional standby of active genes at the end of mitosis. In agreement with this, we found that genes involved in metabolism and mitochondrial activity are down-regulated in the *CycG^{ΔP}* context. However, we observed at the same time that ribosomal protein genes are up-regulated which should rather promote growth. This foreshadows a complex relationship between Cyclin G and the PRC1 and PR-DUB complexes in the cell cycle-dependent regulation of these genes and appeals to the use of a more integrative, systems biology, approach.

Fine-tuned regulation of genes involved in translation, metabolism and mitochondrial activity is necessary for developmental stability

Cyclin G appears central in a small regulatory sub-network that connects genes involved in metabolism, mitochondrial activity and translation. Besides, many of Cyclin G's direct transcriptional targets in this network are also targets of PRC1 and RNAPoIII, and to a lesser extent of ASX. Interestingly, it was recently shown by a large scale analysis of the *Drosophila* wing imaginal disc proteome that wing size correlates with some basic metabolic functions, positively with glucose metabolism and negatively with mitochondrial activity, but not with ribosome biogenesis (Okada et al., 2016). In agreement with this, we report here that many genes involved in basic metabolism, such as for example *Gapdh1*, *Gapdh2* or *Jafrac1*, are down-regulated in the *CycG^{ΔP}* context, which also agrees with the small mean size of *CycG^{ΔP}* flies, organs and cells. However, while mitochondrial genes are negatively regulated, ribosomal biogenesis genes are simultaneously positively regulated. Although transcriptome variations are probably not a direct image of proteome variations, our data suggest that robustness of wing size correlates with the fine-tuning of these key functions relative to each other.

Noisiness of gene expression as a source of developmental noise

Cyclin G, PRC1 and PR-DUB are mainly involved in the regulation of transcription. An exciting hypothesis would be that alteration of developmental stability is due to the noisy transcription of their shared targets. *CycG*-induced high FA is associated with high variability of cell size, that might be due to variability in expression of target genes which are mainly involved in growth control. Phenotypic variations in isogenic populations of both prokaryotic and eukaryotic cells may indeed result from

stochastic gene expression mechanisms (McAdams and Arkin, 1997). An increasing corpus of data suggests that the process of gene regulation *per se* can strongly affect variability in gene expression among adjacent cells (for a review see Sanchez et al., 2013). Transcriptional noise may arise at all steps of transcription. For example, the architectural features of promoters have clear effects on mRNA and protein fluctuations in a population of genetically identical cells (Sanchez et al., 2013). RNA polymerase II pausing during elongation is also a source of transcriptional noise (Rajala et al., 2010). In particular, H3K36 methylation, that is related to transcriptional elongation, prevents spurious cryptic transcription from within the gene body (Venkatesh et al., 2012). Recently, activity of the Polycomb complex PRC2 was shown to be important to prevent spurious transcription of inactive genes and to suppress pervasive transcription of intergenic regions (Lee et al., 2015). Mutations of *E(z)* and *esc* that encode two PRC2 members had no effect on *CycG*-induced FA. Dysfunction of PRC2-dependent spurious transcription control is thus unlikely to be the cause of any *CycG*-induced developmental noise. Nevertheless, a similar but weaker effect on intergenic transcription was attributed to PRC1 (Lee et al., 2015). The binding of Cyclin G on many TSS is rather in favor of a role in limiting noisy initiation of transcription. Interestingly, in several cases, noise in gene expression specifically concerns a subset of genes (Weinberger et al., 2012). For example, H3K36 methylation hinders cryptic transcription in a subclass of genes involved in longevity in *S. cerevisiae* and *C. elegans* (Sen et al., 2015). It is thus tempting to speculate that cooperation between Cyclin G and the PRC1 and PR-DUB complexes is important to prevent spurious transcription of genes involved in growth in the broad sense. It will be very interesting to address these points in the future.

MATERIAL AND METHODS

Plasmids

The *pPMW-attB* plasmid was built as follows: Gateway® vector *pPMW* (Invitrogen, a gift from T. Murphy; (Huynh and Zieler, 1999) was linearized by digestion with *NsiI*; the *attB* sequence was amplified from *pUASTattB* (Bischof et al., 2007) using primers *attB-NsiIF* and *attB-NsiIR* (Table S10) and the PCR product was digested with *NsiI*; the digested PCR product and the linearized plasmid were ligated and sequenced. This plasmid was deposited at Addgene (plasmid # 61814).

The full-length *CycG* cDNA (*CycG^{FL}*, encoding the 566 amino-acid protein) was amplified from S2 cell cDNAs using primers *CycGnF* and *CycGnR*. cDNAs encoding truncated forms of Cyclin G (*CycG^{ΔP}*, Cyclin G deleted of the putative PEST domain corresponding to amino-acids 542 to 566; *CycG^{ΔE}*, Cyclin G deleted of the ETP-interacting domain corresponding to amino-acids 1 to 130; *CycG^{ΔEΔP}*, Cyclin G deleted of both domains) were amplified from the full-length *CycG* cDNA using primers *CycGnF* and *CycG541R*, *CycG130F* and *CycGnR*, and *CycG130F* and *CycG541R*, respectively (Table S10 and Dupont et al., 2015). The PCR products were cloned into *pENTR/D-TOPO*® (Invitrogen), transferred into *pPMW-attB* and the resulting plasmids *pPMW-attB-CycG^{FL}*, *pPMW-attB-CycG^{ΔP}*, *pPMW-attB-CycG^{ΔE}*, *pPMW-attB-CycG^{ΔEΔP}* were sequenced.

***Drosophila melanogaster* strains and genetics**

Flies were raised on standard yeast-cornmeal medium at 25°C.

Myc-CycG transgenic lines were obtained by *PhiC31*-integrase mediated insertion into strain $y^1M\{vas-int.Dm\}ZH-2Aw^*;M\{3xP3-RFP.attP\}ZH-51C$ (stock BL-24482). Plasmids *pPMW-attB-CycG^{FL}*, *pPMW-attB-CycG^{ΔP}*, *pPMW-attB-CycG^{ΔE}* and *pPMW-attB-CycG^{ΔEΔP}* were injected into embryos, G0 adults were back-crossed to *yw*, and G1 transformants were crossed to *yw* again to obtain G2 transformants (BestGene Inc.). Transformants were individually crossed with *yw*; *Sp/CyO*, and the curly wing siblings were crossed with each other. Homozygous transgenic lines were then obtained by crossing 5 females and 5 males. The resulting lines were named *UAS-Myc-CycG^{FL}*, *UAS-Myc-CycG^{ΔP}*, *UAS-Myc-CycG^{ΔE}* and *UAS-Myc-CycG^{ΔEΔP}*.

To estimate fluctuating asymmetry (FA), five replicate crosses were performed for each genotype, wherein 6 females carrying a Gal4 driver were mated with 5 males carrying a *CycG* transgene. Parents were transferred into a new vial every 48 h (three times) then discarded. 30 females were then sampled from the total offspring. Gal4 drivers used were *daughterless-Gal4* (*da-Gal4*) (Wodarz et al., 1995), *nubbin-Gal4* (*nub-Gal4*), *optomotor-blind-Gal4* (*omb-Gal4*), *rotund-Gal4* (*rn-Gal4*), *scalloped-Gal4* (*sd-Gal4*), *teashirt-Gal4* (*tsh-Gal4*), *vestigial-Gal4* (*vg-Gal4*) (from the Bloomington *Drosophila* stock center), and *Insulin-like peptide 3-Gal4* (*dILP3-Gal4*), *neuropeptide F-Gal4* (*NPF-Gal4*), *Pigment-dispersing factor-Gal4* (*Pdf-Gal4*), *period-Gal4* (*per-Gal4*), *phantom-Gal4* (*phm-Gal4*), *Prothoracicotropic hormone-Gal4* (*Ptth-Gal4*), *R10B09-Gal4*, kind gifts from Dr Maria Dominguez's lab (Ferres-Marco et al.,

2006).

The *da-Gal4, UAS-CycG^{ΔP}* third chromosome, obtained by recombination of *da-Gal4* with the original *UAS-CycG^{ΔP}* transgene (*RCG76*), was used to test genetic interactions between *CycG* and several *PcG* or *ETP* mutations (Dupont et al., 2015). Alleles used are described in (Soto et al., 1995; Beuchle et al., 2001; Salvaing et al., 2006; Gaytán de Ayala Alonso et al., 2007; Fritsch et al., 2003; Gutiérrez et al., 2012) (Table 3). To estimate FA, 5 crosses were performed for each genotype, wherein 6 *PcG* or *ETP* mutant females were mated with 5 *da-Gal4, UAS-CycG^{ΔP}* males, the parents were transferred into a new vial every 48 h (three times) then discarded. 30 females combining the *PcG* or *ETP* mutation and *da-Gal4 UAS-CycG^{ΔP}* were sampled from the offspring. *PcG* and *ETP* mutant females were crossed with *da-Gal4* in parallel to measure FA of heterozygous mutants.

Morphometrics

Right and left wings of sampled females were mounted on slides, dorsal side up, in Hoyer's medium. Slides were scanned with a Hamamatsu Nanozoomer Digital Slide scanner, running the Nanozoomer software with a 20x objective and an 8-bit camera. Wing pictures were separately exported into tif format using NDP.view and the 5x lens. All wings were oriented with the hinge to the left. Image J was used to digitize 15 landmarks or only landmarks 3 and 13 when indicated (Figure 1B). Analysis of size FA was performed as described previously (Debat et al., 2011) using the FA10 index as FA estimator, *i.e.* FA corrected for measurement error, directional asymmetry and inter-individual variation (Palmer and Strobeck, 1992). For all genotypes, the interaction individual*side was significant, indicating that FA was larger than measurement error.

RNA-seq experiments and RT-qPCR validations

Wing imaginal discs from *da-Gal4/UAS-CycG^{ΔP}* and *da-Gal4/+* third instar female larvae were dissected, and total RNAs were extracted as previously described except that 150 discs homogenized by pipetting were used for each extraction (Coléno-Costes et al., 2012). Three biological replicates were generated for each genotype. Library preparation and Illumina sequencing were performed at the Ecole Normale Supérieure Genomic Platform (Paris, France). Messenger (polyA+) RNAs were purified from 1 µg of total RNA using oligo(dT). Libraries were prepared using the

strand specific RNA-Seq library preparation TruSeq Stranded mRNA kit (Illumina). Libraries were multiplexed by 6 on 2 flowcell lanes. A 50 bp single read sequencing was performed on a HiSeq 1500 device (Illumina). A mean of 38.1 ± 4.8 million reads was obtained for each of the 6 samples (Table S11). They were aligned with the *Drosophila melanogaster* genome (dm6, r6.07) using TopHat 2 (v2.0.10) (Kim et al., 2013). Unambiguously mapping reads (a mean of 24.9 ± 4.9 million reads) were then assigned to genes and exons described by the Ensembl BDGP5 v77 assembly, by using the “summarizeOverlaps” function from the “GenomicAlignments” package (v 1.2.2) in “Union” mode (Lawrence et al., 2013). Library size normalization and differential expression analysis were both performed with DESeq 2 (v 1.6.3) and genes with adjusted p-value below 0.05 were retained as differentially expressed (Love et al., 2014). Gene Ontology analysis was performed using DAVID (Huang et al., 2009; Huang et al., 2009).

For RT-qPCR validations, RNAs were treated with Turbo DNase (Ambion), and cDNA were synthesized with SuperScript II Reverse transcriptase (Invitrogen) using random primers. RT-qPCR experiments were carried out in a CFX96 system (Bio-Rad) using SsoFast EvaGreen Supermix (Bio-Rad). Three biological replicates were performed for each genotype. Expression levels were quantified with the Pfaffl method (Bustin et al., 2009). The geometric mean of two reference genes, *Lamin* (*Lam*) and *rasputin* (*rin*), the expression of which did not vary when *CycG^{AP}* was expressed, was used for normalization (Vandesompele et al., 2002). Sequences of primer couples are listed in Table S10.

An interactome was built using Cytoscape (v 2.8.3) and the DroID plugin (v 1.5) to introduce protein-protein and transcription factor-gene interactions (Murali et al., 2011). The jActiveModules plugin (v 2.23) was used to find sub-networks of co-deregulated genes in the interactome by using “overlap threshold” 0.8, “score adjusted for size”, and “regional scoring” (Ideker et al., 2002).

ChIP-seq experiments and ChIP-qPCR validations

Wing imaginal discs from *+UAS-Myc-CycG^{AP}*; *+da-Gal4* and *+da-Gal4* third instar female larvae were used for chromatin immunoprecipitation (ChIP).

For ChIP-seq experiments, 600 wing imaginal discs were dissected (taking one disc per larva) in Schneider medium and aliquoted per 50 in 1.5 mL microtubes on ice. The 12 microtubes were treated as described in (Coléno-Costes et al., 2012)

with minor modifications. Discs were fixed at 22°C. 12 sonication cycles were performed (Diagenode Bioruptor sonifier; cycles of 30" ON, 30" OFF, high power). After centrifugation, the 12 supernatants were pooled, homogenized, and 2% were removed (Input). The remaining fragmented chromatin was redistributed into 12 tubes and each tube was adjusted to 1 mL with 140 mM NaCl, 10 mM Tris-HCl pH 8.0, 1 mM EDTA, 1% Triton X-100, 0.1% sodium deoxycholate, 0.1% BSA, Roche complete EDTA-free protease inhibitor cocktail). For immunoprecipitation, 3 µg of anti-Myc antibody (Abcam 9132) were added per tube. The of water. Two biological replicates were performed.

Library preparation and Illumina sequencing were performed at the Ecole normale supérieure Genomic Platform (Paris, France). Libraries were prepared using NEXTflex ChIP-Seq Kit (Bioo Scientific), using 38 ng of IP or Input DNA. Libraries were multiplexed by 10 on one flowcell run. A 75 bp single read sequencing was performed on a NextSeq 500 device (Illumina). Reads were filtered by the "fastq_quality_filter" command from the "fastx-Toolkit" package (http://hannonlab.cshl.edu/fastx_toolkit/), using a threshold of 90% bases with mapping quality ≥ 20 . A mean of 55.6 ± 15.2 million reads was obtained for each of the 4 samples (Table S12). Reads that successfully passed the filtering step were aligned to the *Drosophila* genome (dm6, r6.07) using Bowtie 2 (<http://bowtie-bio.sourceforge.net/bowtie2/>) (v2.1.0) with default parameters (Langmead and Salzberg, 2012). Peaks were called by MACS2 (v2.1.0) by comparing each ChIP to its input library, with fragment size fixed at 110 bp and otherwise default parameters (Zhang et al., 2008) . Peak reproducibility between the two biological replicates was then analysed with the IDR method (<https://www.encodeproject.org/software/idr/>) (Li et al., 2011). Briefly, an IDR score was assigned to each peak by the "batch-consistency-analysis" function, using the recommended parameters for MACS peaks (peak ranking based on p-value). Peaks below the 0.05 threshold were considered reproducible. The overlapping reproducible peaks from both replicates were fused using the BEDtools suite "merge" function (Quinlan and Hall, 2010), resulting in the final list of peaks kept for subsequent analysis. Cyclin G-bound genes were defined as genes from the genome annotation file (dm6, r6.07) which overlapped at least one of these Cyclin G peaks, as obtained by the BEDtools suite "intersect" function (Quinlan and Hall, 2010).

For ChIP-qPCR validations, ChIP were performed similarly with the anti-Myc antibody. Rabbit IgG (Diagenode) were used as a negative control (mock). qPCR experiments were carried out in a CFX96 system (Bio-Rad) using SsoFast EvaGreen Supermix (Bio-Rad). Sequences of primer couples are listed in Table S10. Data were normalized against Input chromatin.

Heatmaps and aggregation plots of Cyclin G signal over gene bodies and Transcription Start Sites (TSS) were generated using the `ngsplot` package. (<https://github.com/shenlab-sinai/ngsplot>) (Shen et al., 2014). Some genes with spurious signal (such as genes from the histone complex) were excluded from the analysis based on signal uniformity over the full length of the gene (cumulative derivative of Cyclin G signal over gene length = 0).

Data access

High-throughput sequencing data have been submitted to GEO under accession number ... (in progress).

Genomic association

Genomic loci enriched for Polycomb (PC), Posterior Sex Comb (PSC), Polyhomeotic (PH), RNA Polymerase II (RNAPolII) and H3K27me3 in wild type imaginal discs of third instar larvae were retrieved from GEO (GSE42106) (Schaaf et al., 2013) (H3K27me3_WholeWingDisc GSM1032567, PcRJ_AnteriorWingDisc GSM1032571, PcRJ_PosteriorWingDisc GSM1032574, Ph_WholeWingDisc GSM1032576, PolII_WholeWingDisc GSM1032577, Psc_WholeWingDisc GSM1032578). Binding sites for PC in the whole wing disc were defined as the overlap between PC binding sites in the anterior and posterior wing disc compartment, as obtained by the BEDtools "intersect" function. For ASX and Calypso, the bed files were a kind gift from Dr. Jürg Müller (Scheuermann et al., 2010). The mappability file for dm6 genome with 25 nt reads (the smallest size in the compared data) was generated using the Peakseq code (http://archive.gersteinlab.org/proj/PeakSeq/Mappability_Map/Code/). The overall size of the mappable genome was used as the effective genome size for the GAT software (<https://github.com/AndreasHeger/gat>) to assess the significance of the overlap between peaks of Cyclin G and other factors (Heger et al., 2013). As GAT performs a two-tailed test, it displays low p-values both for significant overlap and exclusion (as between Cyclin G and H3K27me3).

Gene overlap significance assessment was made as follows: under the null hypothesis, genes that are enriched for ASX, Calypso, PC, PSC, PH, RNAPoIII or H3K27me3 in wild type imaginal discs of third instar larvae should not exhibit any bias towards Cyclin G targets. Thus, the overlap between n enriched genes and K Cyclin G targets genes should be explained by random sampling without replacement of n genes within the total amount N of *Drosophila melanogaster* genes. The amount of overlap under the null hypothesis X follows a hypergeometric law: $X \sim HY(K, N, n)$. The significance of the observed overlap k was computed as the probability of observing X higher or equal to k under the null hypothesis: $P(X \geq k)$.

Acknowledgments

We thank Dr. Emmanuèle Mouchel-Vielh and Dr. Jean-Michel Gibert for stimulating discussions and critical reading of the manuscript, the Bloomington Stock Center for fly strains, Dr. Jürg Müller for the alleles of *Asx* and *caly* and for the ASX and Calypso ChIP bed files, Dr. Maria Dominguez and Dr Sergio Juarez-Carreño for the *dilp3-Gal4*, *R19B09-Gal4*, *npf-Gal4*, *pdf-Gal4*, *per-Gal4*, *ptth-Gal4* and *tsh-Gal4* drivers. This work was funded by the Centre National de la Recherche Scientifique (CNRS), Université Pierre et Marie Curie (UPMC), Sorbonne Universités (grant SU-14-R-CDV-05-1 to FP), and Fondation ARC pour la Recherche sur le Cancer (grant PJA20131200314 to FP). The École Normale Supérieure genomic platform was supported by the France Génomique national infrastructure, funded as part of the "Investissements d'Avenir" program managed by the Agence Nationale de la Recherche (contract ANR-10-INBS-09). CAD was funded by a doctoral fellowship from the MESR (Ministère de l'Enseignement Supérieur et de la Recherche). JD was funded by a doctoral fellowship from the MESR and by the Fondation pour la Recherche médicale (FDT20160435164).

References

- Adler, P.N., Charlton, J., and Brunk, B. (1989). Genetic interactions of the *suppressor 2* of *zeste* region genes. *Dev Genet* 10, 249-260. doi:10.1002/dvg.1020100314
- Arora, M., Packard, C.Z., Banerjee, T., and Parvin, J.D. (2015). RING1A and BMI1 bookmark active genes via ubiquitination of chromatin-associated proteins. *Nucleic Acids Res* 44, 2136-2144. doi:10.1093/nar/gkv1223
- Arora, M., Zhang, J., Heine, G.F., Ozer, G., Liu, H.W., Huang, K., and Parvin, J.D. (2012). Promoters active in interphase are bookmarked during mitosis by ubiquitination. *Nucleic Acids Res* 40, 10187-10202. doi:10.1093/nar/gks820
- Barabasi, A.L., and Albert, R. (1999). Emergence of scaling in random networks. *Science* 286, 509-512.
- Beck, S., Faradji, F., Brock, H., and Peronnet, F. (2010). Maintenance of Hox gene expression patterns. *Adv Exp Med Biol* 689, 41-62.
- Beuchle, D., Struhl, G., and Müller, J. (2001). Polycomb group proteins and heritable silencing of *Drosophila* Hox genes. *Development* 128, 993-1004.
- Bischof, J., Maeda, R.K., Hediger, M., Karch, F., and Basler, K. (2007). An optimized transgenesis system for *Drosophila* using germ-line-specific *varphiC31* integrases. *Proceedings of the National Academy of Sciences* 104, 3312-17.
- Breuker, C.J., Patterson, J.S., and Klingenberg, C.P. (2006). A single basis for developmental buffering of *Drosophila* wing shape. *PLoS One* 1, e7. doi:10.1371/journal.pone.0000007
- Bustin, S.A., Benes, V., Garson, J.A., Hellems, J., Huggett, J., Kubista, M., Mueller, R., Nolan, T., Pfaffl, M.W., et al. (2009). The MIQE guidelines: minimum information for publication of quantitative real-time PCR experiments. *Clin Chem* 55, 611-622. doi:10.1373/clinchem.2008.112797
- Coléno-Costes, A., Jang, S.M., de Vanssay, A., Rougeot, J., Bouceba, T., Randsholt, N.B., Gibert, J.M., Le Crom, S., Mouchel-Vielh, E., et al. (2012). New partners in regulation of gene expression: the Enhancer of Trithorax and Polycomb Corto interacts with methylated Ribosomal Protein L12 via its chromodomain. *PLoS Genet* 8, e1003006. doi:10.1371/journal.pgen.1003006
- Colombani, J., Andersen, D.S., and Léopold, P. (2012). Secreted peptide Dilp8 coordinates *Drosophila* tissue growth with developmental timing. *Science* 336, 582-85. doi:10.1126/science.1216689

- Debat, V., and Peronnet, F. (2013). Asymmetric flies: The control of developmental noise in *Drosophila*. *Fly (Austin)* 7, 1-8. doi: 10.4161/fly.23558
- Debat, V., Bloyer, S., Faradji, F., Gidaszewski, N., Navarro, N., Orozco-Terwengel, P., Ribeiro, V., Schlötterer, C., Deutsch, J.S., and Peronnet, F. (2011). Developmental Stability: A Major Role for Cyclin G in *Drosophila melanogaster*. *PLoS Genet* 7, e1002314. doi:10.1371/journal.pgen.1002314
- Debat, V., Milton, C.C., Rutherford, S., Klingenberg, C.P., and Hoffmann, A.A. (2006). Hsp90 and the quantitative variation of wing shape in *Drosophila melanogaster*. *Evolution* 60, 2529-538.
- Dellino, G.I., Schwartz, Y.B., Farkas, G., McCabe, D., Elgin, S.C., and Pirrotta, V. (2004). Polycomb silencing blocks transcription initiation. *Mol Cell* 13, 887-893.
- Dongen, S.V. (2006). Fluctuating asymmetry and developmental instability in evolutionary biology: past, present and future. *J Evol Biol* 19, 1727-743. doi:10.1111/j.1420-9101.2006.01175.x
- Dupont, C.A., Dardalhon-Cuménal, D., Kyba, M., Brock, H.W., Randsholt, N.B., and Peronnet, F. (2015). *Drosophila* Cyclin G and epigenetic maintenance of gene expression during development. *Epigenetics Chromatin* 8, 18. doi:10.1186/s13072-015-0008-6
- Faradji, F., Bloyer, S., Dardalhon-Cuménal, D., Randsholt, N.B., and Peronnet, F. (2011). *Drosophila melanogaster* Cyclin G coordinates cell growth and cell proliferation. *Cell Cycle* 10, 1-14. Erratum (2014) *Cell Cycle* 13, 2480-2480.
- Feder, M.E., and Hofmann, G.E. (1999). Heat-shock proteins, molecular chaperones, and the stress response: evolutionary and ecological physiology. *Annual review of physiology* 61, 243-282.
- Ferres-Marco, D., Gutierrez-Garcia, I., Vallejo, D.M., Bolivar, J., Gutierrez-Aviño, F.J., and Dominguez, M. (2006). Epigenetic silencers and Notch collaborate to promote malignant tumours by Rb silencing. *Nature* 439, 430-36. doi:10.1038/nature04376
- Fritsch, C., Beuchle, D., and Müller, J. (2003). Molecular and genetic analysis of the Polycomb group gene *Sex combs extra/Ring* in *Drosophila*. *Mech Dev* 120, 949-954. doi:10.1016/s0925-4773(03)00083-2
- García-Bellido, A. (2009). The cellular and genetic bases of organ size and shape in *Drosophila*. *Int J Dev Biol* 53, 1291-1303. doi:10.1387/ijdb.072459ag
- García-Bellido, A.C., and García-Bellido, A. (1998). Cell proliferation in the

- attainment of constant sizes and shapes: the Entelechia model. *Int J Dev Biol* 42, 353-362.
- Garelli, A., Gontijo, A.M., Miguela, V., Caparros, E., and Dominguez, M. (2012). Imaginal discs secrete insulin-like peptide 8 to mediate plasticity of growth and maturation. *Science* 336, 579-582. doi:10.1126/science.1216735
- Gaytán de Ayala Alonso, A., Gutiérrez, L., Fritsch, C., Papp, B., Beuchle, D., and Müller, J. (2007). A genetic screen identifies novel polycomb group genes in *Drosophila*. *Genetics* 176, 2099-2108. doi:10.1534/genetics.107.075739
- Geisler, S.J., and Paro, R. (2015). Trithorax and Polycomb group-dependent regulation: a tale of opposing activities. *Development* 142, 2876-887. doi:10.1242/dev.120030
- Gildea, J.J., Lopez, R., and Shearn, A. (2000). A screen for new trithorax group genes identified little imaginal discs, the *Drosophila melanogaster* homologue of human retinoblastoma binding protein 2. *Genetics* 156, 645-663.
- Graveley, B.R., Brooks, A.N., Carlson, J.W., Duff, M.O., Landolin, J.M., Yang, L., Artieri, C.G., van Baren, M.J., Boley, N., et al. (2011). The developmental transcriptome of *Drosophila melanogaster*. *Nature* 471, 473-79. doi:10.1038/nature09715
- Grimaud, C., Negre, N., and Cavalli, G. (2006). From genetics to epigenetics: the tale of Polycomb group and trithorax group genes. *Chromosome Res* 14, 363-375. doi:10.1007/s10577-006-1069-y
- Grossniklaus, U., and Paro, R. (2014). Transcriptional Silencing by Polycomb-Group Proteins. *Cold Spring Harb Perspect Biol* 6. doi:10.1101/cshperspect.a019331
- Gutiérrez, L., Oktaba, K., Scheuermann, J.C., Gambetta, M.C., Ly-Hartig, N., and Müller, J. (2012). The role of the histone H2A ubiquitinase Sce in Polycomb repression. *Development* 139, 117-127. doi:10.1242/dev.074450
- Heger, A., Webber, C., Goodson, M., Ponting, C.P., and Lunter, G. (2013). GAT: a simulation framework for testing the association of genomic intervals. *Bioinformatics* 29, 2046-48. doi:10.1093/bioinformatics/btt343
- Huang, D.W., Sherman, B.T., and Lempicki, R.A. (2009). Systematic and integrative analysis of large gene lists using DAVID bioinformatics resources. *Nat Protoc* 4, 44-57. doi:10.1038/nprot.2008.211
- Huang, D.W., Sherman, B.T., and Lempicki, R.A. (2009). Bioinformatics enrichment tools: paths toward the comprehensive functional analysis of large gene lists.

- Nucleic Acids Res* 37, 1-13. doi:10.1093/nar/gkn923
- Huynh, C.Q., and Zieler, H. (1999). Construction of modular and versatile plasmid vectors for the high-level expression of single or multiple genes in insects and insect cell lines. *J Mol Biol* 288, 13-20.
- Ideker, T., Ozier, O., Schwikowski, B., and Siegel, A.F. (2002). Discovering regulatory and signalling circuits in molecular interaction networks. *Bioinformatics* 18 Suppl 1, S233-240.
- Kim, D., Pertea, G., Trapnell, C., Pimentel, H., Kelley, R., and Salzberg, S.L. (2013). TopHat2: accurate alignment of transcriptomes in the presence of insertions, deletions and gene fusions. *Genome Biol* 14, R36. doi:10.1186/gb-2013-14-4-r36
- Kingston, R.E., and Tamkun, J.W. (2014). Transcriptional Regulation by Trithorax-Group Proteins. *Cold Spring Harb Perspect Biol* 6
doi:10.1101/cshperspect.a019349
- Kitano, H. (2004). Biological robustness. *Nat Rev Genet* 5, 826-837.
doi:10.1038/nrg1471
- Langmead, B., and Salzberg, S.L. (2012). Fast gapped-read alignment with Bowtie 2. *Nat Methods* 9, 357-59. doi:10.1038/nmeth.1923
- Lawrence, M., Huber, W., Pagès, H., Aboyoun, P., Carlson, M., Gentleman, R., Morgan, M.T., and Carey, V.J. (2013). Software for computing and annotating genomic ranges. *PLoS Comput Biol* 9, e1003118.
doi:10.1371/journal.pcbi.1003118
- Leamy, L., Klingenberg, C., Sherratt, E., Wolf, J., and Cheverud, J. (2015). The Genetic Architecture of Fluctuating Asymmetry of Mandible Size and Shape in a Population of Mice: Another Look. *Symmetry* 7, 146-163.
doi:10.3390/sym7010146
- Leamy, L.J., Routman, E.J., and Cheverud, J.M. (2002). An epistatic genetic basis for fluctuating asymmetry of mandible size in mice. *Evolution* 56, 642-653.
doi:10.1038/sj.hdy.6800637
- Leamy, L.J., Workman, M.S., Routman, E.J., and Cheverud, J.M. (2005). An epistatic genetic basis for fluctuating asymmetry of tooth size and shape in mice. *Heredity* (Edinb) 94, 316-325. doi:10.1038/sj.hdy.6800637
- Leamy, L.J.L., and Klingenberg, C.P.K. (2005). The genetics and evolution of fluctuating asymmetry. *Annu. Rev. Ecol. Evol. Syst.* 36, 1-21.
doi:10.1146/annurev.ecolsys.36.102003.152640

- Lee, H.G., Kahn, T.G., Simcox, A., Schwartz, Y.B., and Pirrotta, V. (2015). Genome-wide activities of Polycomb complexes control pervasive transcription. *Genome Res* 25,1170-81. doi: 10.1101/gr.188920.11
- Levy, S.F., and Siegal, M.L. (2008). Network hubs buffer environmental variation in *Saccharomyces cerevisiae*. *PLoS Biol* 6, e264. doi:10.1371/journal.pbio.0060264
- Li, Q., Brown, J.B., Huang, H., and Bickel, P.J. (2011). Measuring reproducibility of high-throughput experiments. *The annals of applied statistics* 5, 1752-779.
- Love, M.I., Huber, W., and Anders, S. (2014). Moderated estimation of fold change and dispersion for RNA-seq data with DESeq2. *Genome Biol* 15, 550. doi:10.1186/s13059-014-0550-8
- McAdams, H.H., and Arkin, A. (1997). Stochastic mechanisms in gene expression. *Proc Natl Acad Sci USA* 94, 814-19.
- Milton, C.C., Huynh, B., Batterham, P., Rutherford, S.L., and Hoffmann, A.A. (2003). Quantitative trait symmetry independent of Hsp90 buffering: distinct modes of genetic canalization and developmental stability. *Proc Natl Acad Sci USA* 100, 13396-3401. doi:10.1073/pnas.1835613100
- Murali, T., Pacifico, S., Yu, J., Guest, S., Roberts, G.G., and Finley, R.L. (2011). DroID 2011: a comprehensive, integrated resource for protein, transcription factor, RNA and gene interactions for *Drosophila*. *Nucleic Acids Res* 39, D736-743. doi:10.1093/nar/gkq1092
- Neto-Silva, R.M., Wells, B.S., and Johnston, L.A. (2009). Mechanisms of growth and homeostasis in the *Drosophila* wing. *Annu Rev Cell Dev Biol* 25, 197-220. doi:10.1146/annurev.cellbio.24.110707.175242
- Newman, M.E.J. (2003). The structure and function of complex networks. *SIAM Review* 45, 167-256.
- Nijhout, F., and Davidowitz, G. (2003). Developmental Perspectives on Phenotypic Variation, Canalization, and Fluctuating Asymmetry. In *Developmental instability, causes and consequences*, M. Polak, eds. (New York: Oxford University Press).
- Okada, H., Ebhardt, H.A., Vonesch, S.C., Aebersold, R., and Hafen, E. (2016). Proteome-wide association studies identify biochemical modules associated with a wing-size phenotype in *Drosophila melanogaster*. *Nat Commun* 7, 12649. doi:10.1038/ncomms12649
- Palmer, A.R., and Strobeck, C. (1992). Fluctuating asymmetry as a measure of developmental stability: Implications of non-normal distributions and power of

- statistical tests. *Acta Zool. Fennica* 191, 57-72.
- Palmer, R.A. (1994). Fluctuating asymmetry analysis: a primer. In *Developmental Instability: Its Origins and Evolutionary Implications* (T. A. Markow. Netherlands, Kluwer Academic Publishers).
- Parker, N.F., and Shingleton, A.W. (2011). The coordination of growth among *Drosophila* organs in response to localized growth-perturbation. *Dev Biol* 357, 318-325. doi:10.1016/j.ydbio.2011.07.002
- Pengelly, A.R., Kalb, R., Finkl, K., and Müller, J. (2015). Transcriptional repression by PRC1 in the absence of H2A monoubiquitylation. *Genes Dev* 29, 1487-492. doi:10.1101/gad.265439.115
- Queitsch, C., Sangster, T.A., and Lindquist, S. (2002). Hsp90 as a capacitor of phenotypic variation. *Nature* 417, 618-624. doi:10.1038/nature749
- Quinlan, A.R., and Hall, I.M. (2010). BEDTools: a flexible suite of utilities for comparing genomic features. *Bioinformatics* 26, 841-42.
- Rajala, T., Häkkinen, A., Healy, S., Yli-Harja, O., and Ribeiro, A.S. (2010). Effects of transcriptional pausing on gene expression dynamics. *PLoS Comput Biol* 6, e1000704. doi:10.1371/journal.pcbi.1000704
- Rutherford, S, Hirate, Y, and Swalla, BJ (2007). The Hsp90 capacitor, developmental remodeling and evolution: The robustness of gene networks and the curious evolvability of metamorphosis. *Crit Rev Biochem Mol* 42, 355-372.
- Rutherford, S., Knapp, J.R., and Csermely, P. (2007). Hsp90 and developmental networks. *Adv Exp Med Biol* 594, 190-97. doi:10.1007/978-0-387-39975-1_16
- Rutherford, S.L., and Lindquist, S. (1998). Hsp90 as a capacitor for morphological evolution. *Nature* 396, 336-342. doi:10.1038/24550
- Salvaing, J., Decoville, M., Mouchel-Vielh, E., Bussi re, M., Daulny, A., Boldyreva, L., Zhimulev, I., Locker, D., and Peronnet, F. (2006). Corto and DSP1 interact and bind to a maintenance element of the *Scr* Hox gene: understanding the role of Enhancers of trithorax and Polycomb. *BMC Biol* 4, 9. doi:10.1186/1741-7007-4-9
- Salvaing, J., Nagel, A.C., Mouchel-Vielh, E., Bloyer, S., Maier, D., Preiss, A., and Peronnet, F. (2008a). The enhancer of trithorax and polycomb corto interacts with cyclin G in *Drosophila*. *PLoS One* 3, e1658. doi:10.1371/journal.pone.0001658
- Salvaing, J., Mouchel-Vielh, E., Bloyer, S., Preiss, A., and Peronnet, F. (2008b). Regulation of Abd-B expression by Cyclin G and Corto in the abdominal epithelium of *Drosophila*. *Hereditas* 145, 138-146. doi:HRD2067

[pii]10.1111/j.0018-0661.2008.02067.x

- Sanchez, A., Choubey, S., and Kondev, J. (2013). Regulation of noise in gene expression. *Annu Rev Biophys* 42, 469-491. doi:10.1146/annurev-biophys-083012-130401
- Sangster, T.A., Salathia, N., Undurraga, S., Milo, R., Schellenberg, K., Lindquist, S., and Queitsch, C. (2008). HSP90 affects the expression of genetic variation and developmental stability in quantitative traits. *Proc Natl Acad Sci USA* 105, 2963-68. doi:10.1073/pnas.0712200105
- Schaaf, C.A., Misulovin, Z., Gause, M., Koenig, A., Gohara, D.W., Watson, A., and Dorsett, D. (2013). Cohesin and polycomb proteins functionally interact to control transcription at silenced and active genes. *PLoS Genet* 9, e1003560. doi:10.1371/journal.pgen.1003560
- Scheuermann, J.C., de Ayala Alonso, A.G., Oktaba, K., Ly-Hartig, N., McGinty, R.K., Fraterman, S., Wilm, M., Muir, T.W., and Müller, J. (2010). Histone H2A deubiquitinase activity of the Polycomb repressive complex PR-DUB. *Nature* 465, 243-47. doi:10.1038/nature08966
- Scheuermann, J.C., Gutiérrez, L., and Müller, J. (2012). Histone H2A monoubiquitination and Polycomb repression: the missing pieces of the puzzle. *Fly (Austin)* 6, 162-68. doi:10.4161/fly.20986
- Sen, P., Dang, W., Donahue, G., Dai, J., Dorsey, J., Cao, X., Liu, W., Cao, K., Perry, R., et al. (2015). H3K36 methylation promotes longevity by enhancing transcriptional fidelity. *Genes Dev* 29, 1362-376. doi:10.1101/gad.263707.115
- Shen, L., Shao, N., Liu, X., and Nestler, E. (2014). ngs.plot: Quick mining and visualization of next-generation sequencing data by integrating genomic databases. *BMC Genomics* 15, 284. doi:10.1186/1471-2164-15-284
- Siegal, M.L., and Bergman, A. (2002). Waddington's canalization revisited: developmental stability and evolution. *Proc Natl Acad Sci USA* 99, 10528-532. doi:10.1073/pnas.102303999
- Simon, J., Chiang, A., and Bender, W. (1992). Ten different Polycomb group genes are required for spatial control of the *abdA* and *AbdB* homeotic products. *Development* 114, 493-505.
- Soto, M.C., Chou, T.B., and Bender, W. (1995). Comparison of germline mosaics of genes in the Polycomb group of *Drosophila melanogaster*. *Genetics* 140, 231-243.

- Takahashi, H., Okada, Teramura, and Tsujino (2011). Deficiency mapping of the genomic regions associated with effects on developmental stability in *Drosophila melanogaster*. *Evolution* 65, 3565-577.
- Vallejo, D.M., Juarez-Carreño, S., Bolivar, J., Morante, J., and Dominguez, M. (2015). A brain circuit that synchronizes growth and maturation revealed through Dilp8 binding to Lgr3. *Science* 350, aac6767. doi: 10.1126/science.aac6767.
- Vandesompele, J., De Preter, K., Pattyn, F., Poppe, B., Van Roy, N., De Paepe, A., and Speleman, F. (2002). Accurate normalization of real-time quantitative RT-PCR data by geometric averaging of multiple internal control genes. *Genome Biol* 3, research0034.1-c0034.11.
- Van Valen, L. (1962). A study of fluctuating asymmetry. *Evolution* 16, 125-142.
- Venkatesh, S., Smolle, M., Li, H., Gogol, M.M., Saint, M., Kumar, S., Natarajan, K., and Workman, J.L. (2012). Set2 methylation of histone H3 lysine 36 suppresses histone exchange on transcribed genes. *Nature* 489, 452-55.
doi:10.1038/nature11326
- Weinberger, L., Voichek, Y., Tirosh, I., Hornung, G., Amit, I., and Barkai, N. (2012). Expression Noise and Acetylation Profiles Distinguish HDAC Functions. *Mol Cell* 47, 193-202. doi:10.1016/j.molcel.2012.05.008
- Wodarz, A., Hinz, U., Engelbert, M., and Knust, E. (1995). Expression of crumbs confers apical character on plasma membrane domains of ectodermal epithelia of *Drosophila*. *Cell* 82, 67-76.
- Yamada, T., and Bork, P. (2009). Evolution of biomolecular networks: lessons from metabolic and protein interactions. *Nat Rev Mol Cell Biol* 10, 791-803.
doi:10.1038/nrm2787
- Yeyati, P.L., Bancewicz, R.M., Maule, J., and van Heyningen, V. (2007). Hsp90 selectively modulates phenotype in vertebrate development. *PLoS Genet* 3, e43.
doi:10.1371/journal.pgen.0030043
- Yu, H., Kim, P.M., Sprecher, E., Trifonov, V., and Gerstein, M. (2007). The importance of bottlenecks in protein networks: correlation with gene essentiality and expression dynamics. *PLoS Comput Biol* 3, e59.
doi:10.1371/journal.pcbi.0030059
- Zhang, Y., Liu, T., Meyer, C.A., Eeckhoute, J., Johnson, D.S., Bernstein, B.E., Nusbaum, C., Myers, R.M., Brown, M., et al. (2008). Model-based analysis of ChIP-Seq (MACS). *Genome Biol* 9, R137. doi:10.1186/gb-2008-9-9-r137

Figures

Figure 1: Acquisition of morphometric data.

A – Superimposition of the left and right wings of a sample of *da-Gal4, UAS-CycG^{ΔP}* flies (left wings in red, right wings in green) showing high asymmetry.

B - Red dots show the 15 landmarks digitized on the wings. FA10 was computed using these landmarks obtained from the left and right wings of at least 30 females randomly sampled from the population as described (Debat et al., 2011).

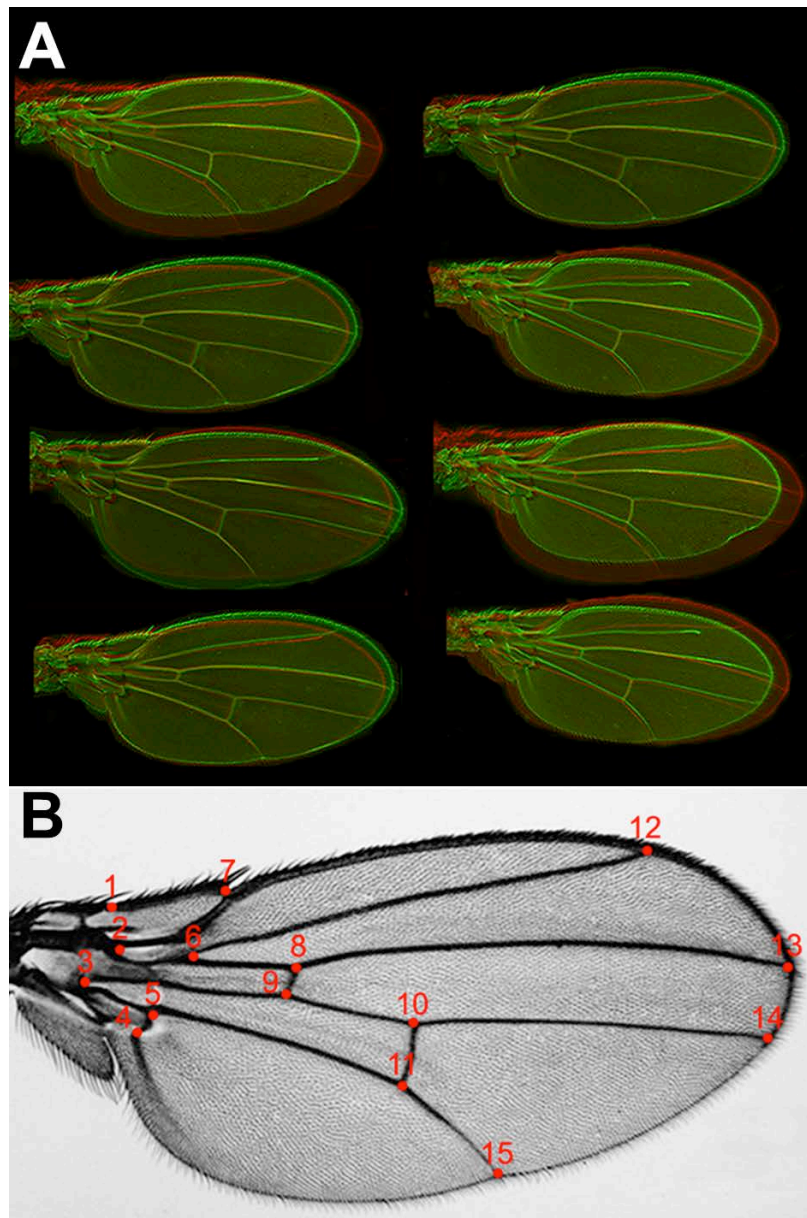


Figure 2: Local deregulation of *CycG* induces high fluctuating asymmetry.

A – Wing length fluctuating asymmetry (FA10) of females bearing a Gal4 driver either associated with *UAS-CycG^{AP}* (dark orange) or alone (light orange). Wing length was measured as the distance between landmarks 3 and 13. *** p-value<0.001.

B – Expression of the driver genes in 3rd instar larva wing imaginal discs (dark grey) and central nervous system (light grey) as indicated in modENCODE (Graveley et al., 2011).

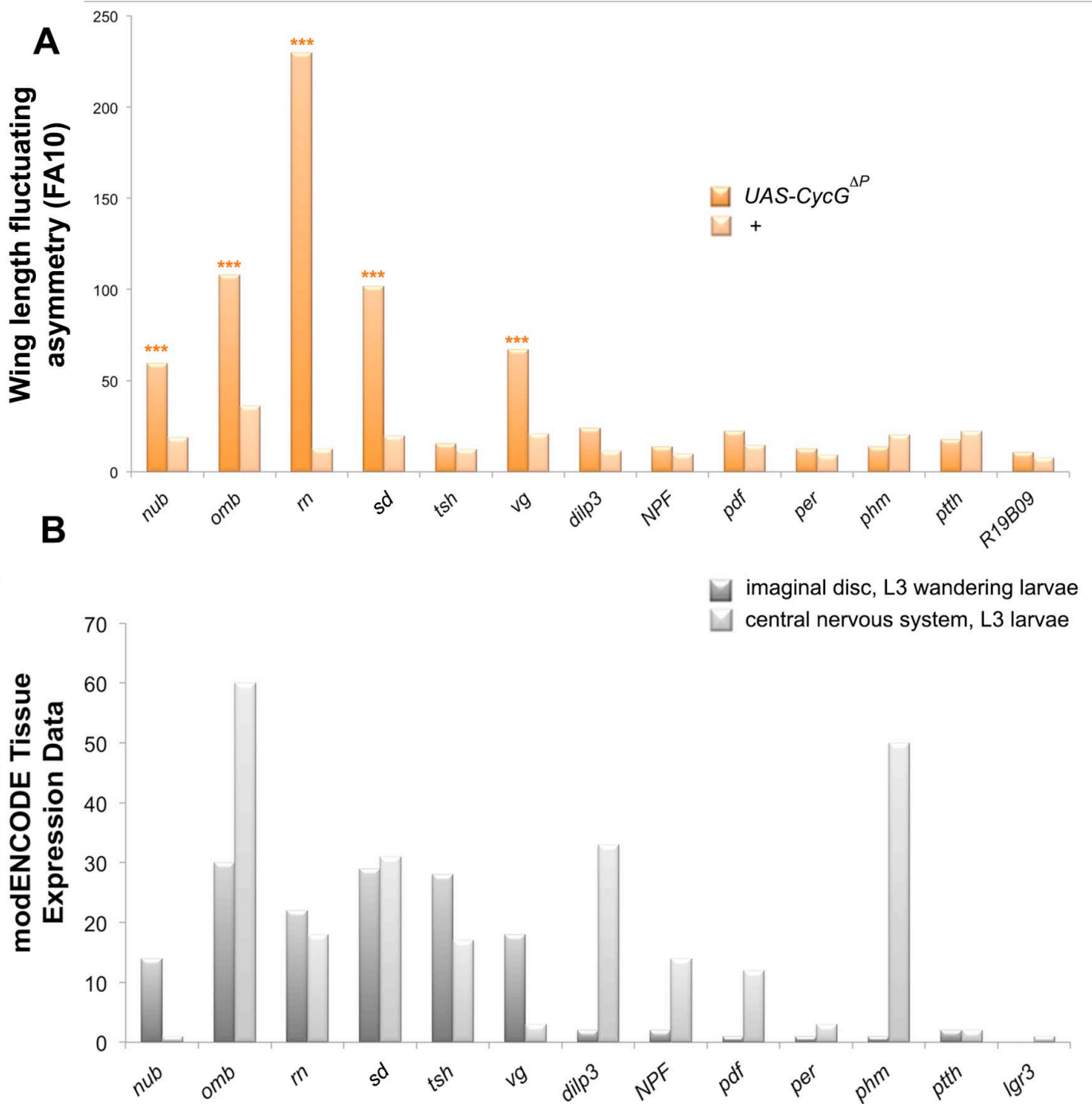


Figure 3: The ETP interacting domain limits *CycG*-induced fluctuating asymmetry

A – Centroid size fluctuating asymmetry (FA10) of females *da-Gal4/+ (+)*, *+/UAS-Myc-CycG^{FL}*; *da-Gal4/+*, (*CycG^{FL}*) and *+/UAS-Myc-CycG^{ΔE}*; *da-Gal4*, (*CycG^{ΔE}*).

B – Centroid size fluctuating asymmetry (FA10) of females *da-Gal4/+ (+)*, *+/UAS-Myc-CycG^{ΔP}*; *da-Gal4/+* (*CycG^{ΔP}*) and *+/UAS-Myc-CycG^{ΔEΔP}*; *da-Gal4/+* (*CycG^{ΔEΔP}*).

*** p-value<0.001.

Wing centroid size was calculated using the 15 landmarks described in Figure 1B.

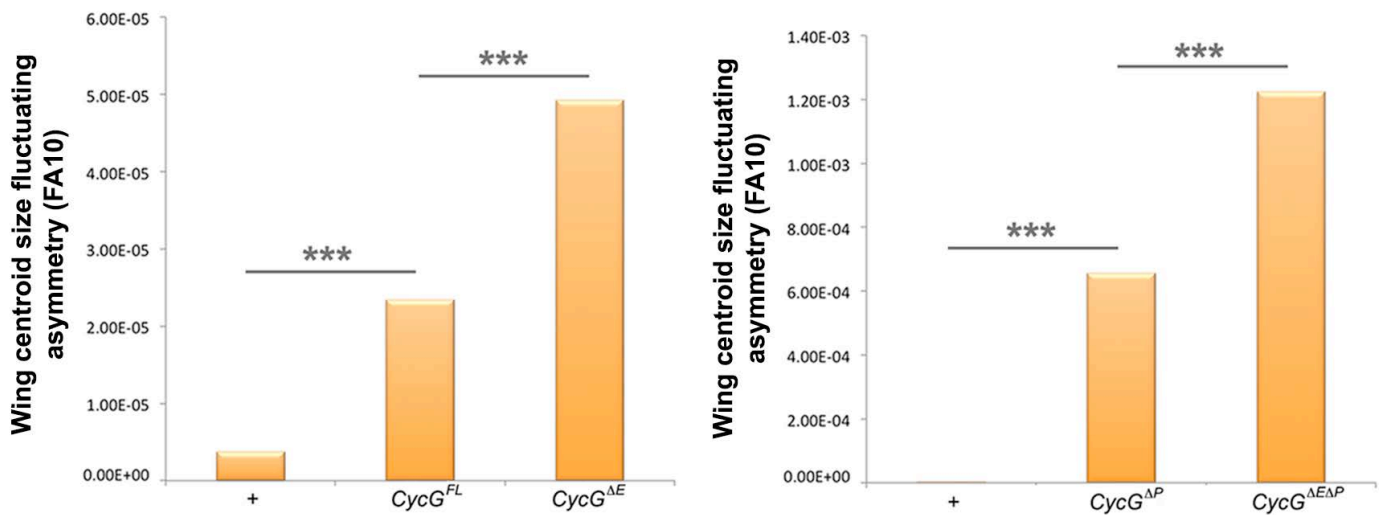


Figure 4: *CycG* interacts with several *PcG* and *ETP* genes for developmental stability.

Centroid size fluctuating asymmetry (FA10) of *ETP* or *PcG* heterozygous mutant females combined with *da-Gal4, UAS-CycG^{ΔP}* (dark orange; *da-Gal4, UAS-CycG^{ΔP}; PcG/+* or *da-Gal4, UAS-CycG^{ΔP}; ETP/+*) and *ETP* or *PcG* heterozygous mutant females combined with *da-Gal4* (light orange; *da-Gal4/+; PcG/+* or *da-Gal4; ETP/+*). In brown (+), centroid size fluctuating asymmetry of *da-Gal4, UAS-CycG^{ΔP}/+* and *da-Gal4/+* females.

*p-value<0.05; ** p-value<0.01; *** p-value<0.001.

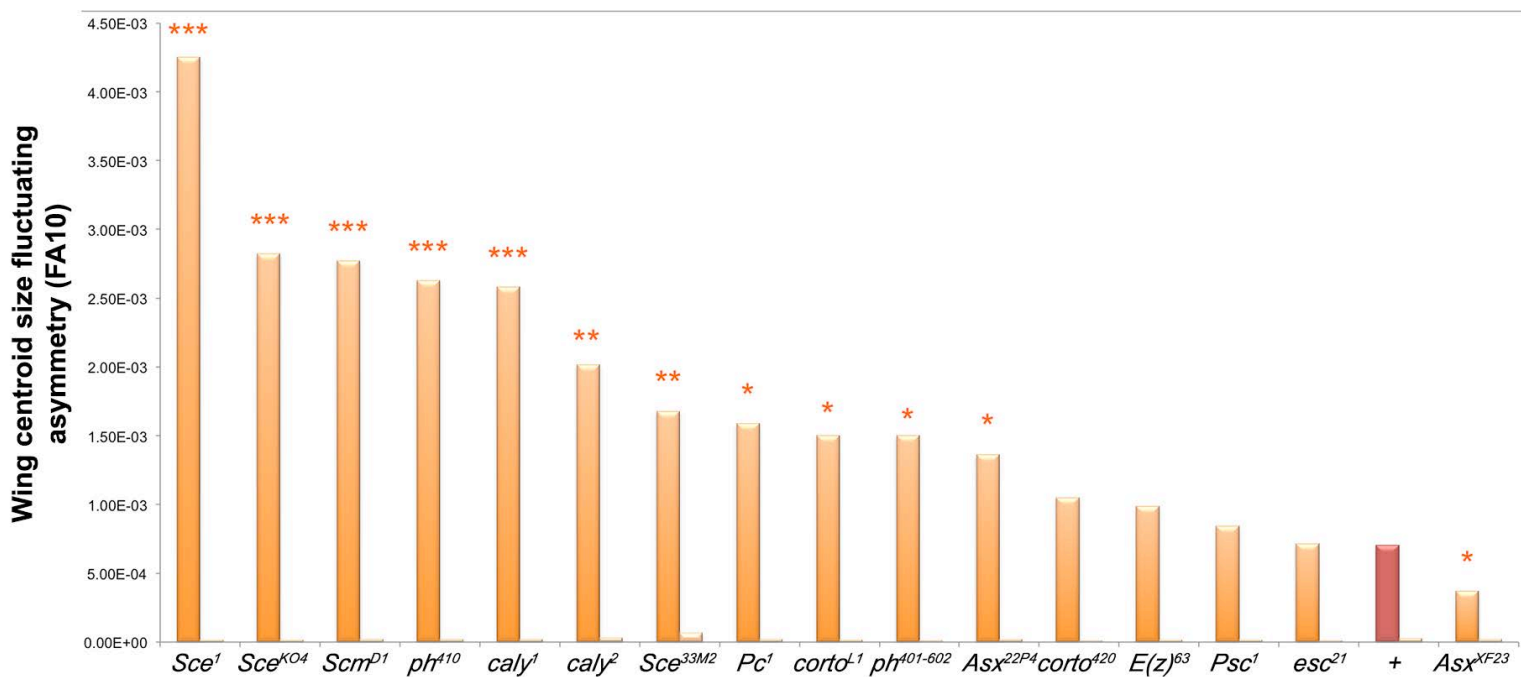


Figure 5: Genes deregulated in wing imaginal discs expressing *CycG*^{ΔP}.

A – RT-qPCR analysis of endogenous *CycG* expression in *da-Gal4,UAS-CycG*^{ΔP/+} and *da-Gal4/+* wing imaginal discs. ** p-value<0.01.

B – Ontology of up-regulated and down-regulated genes in *da-Gal4, UAS-CycG*^{ΔP/+} versus *da-Gal4/+* wing imaginal discs. Gene ontology analysis was performed with DAVID (Huang et al., 2009; Huang et al., 2009).

C – RT-qPCR analysis of *RPL15*, *RPL7* and *Rack1* expression in *da-Gal4, UAS-CycG*^{ΔP/+} and *da-Gal4/+* wing imaginal discs. ** p-value<0.01; *** p-value<0.001.

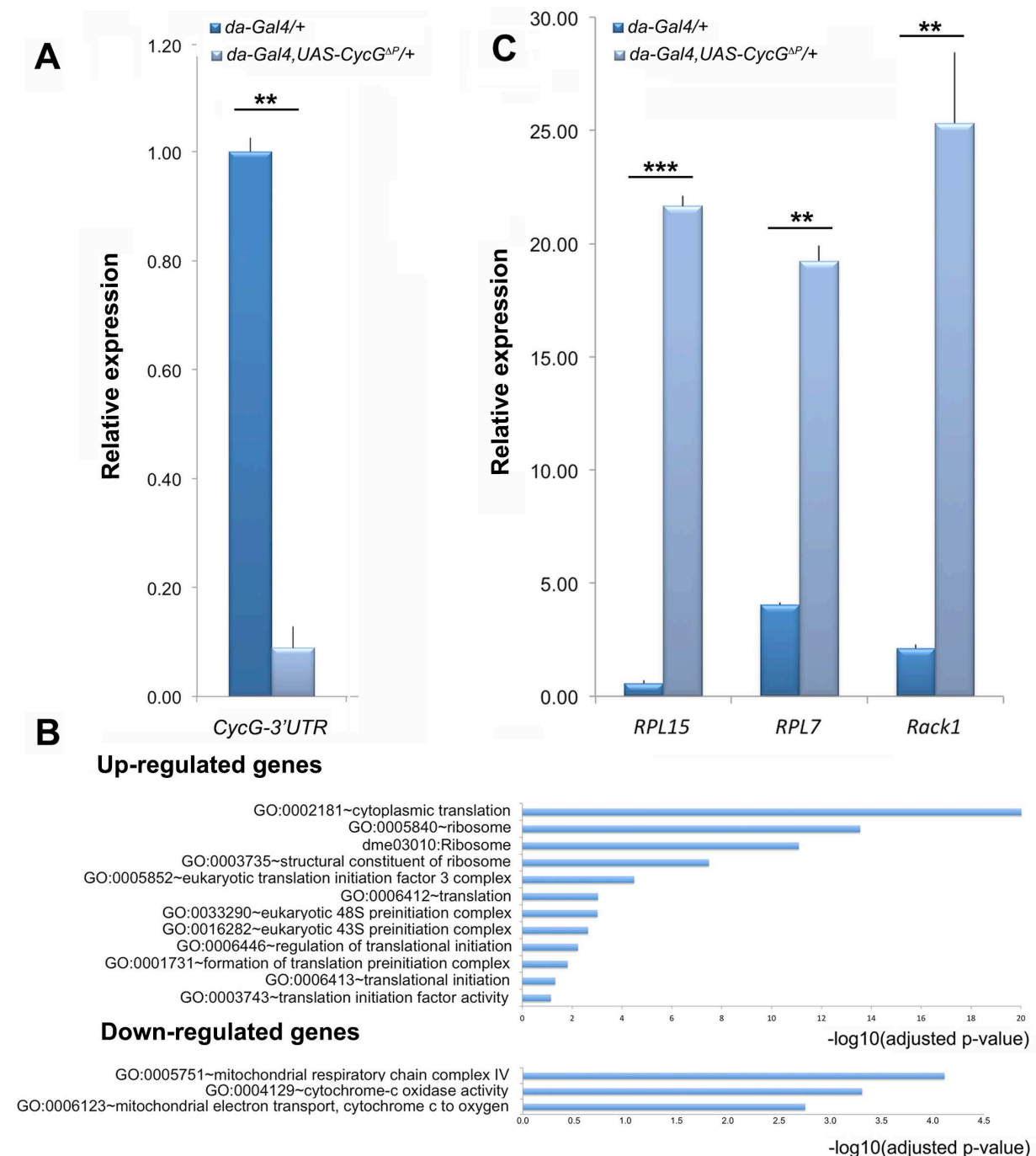


Figure 6: Identification of Cyclin G genome-wide binding sites in wing imaginal discs.

A – Heat-map showing the enrichment of Cyclin G over the Input signal on the TSS of 889 genes. TSS: Transcriptional Start Site; TES: Transcriptional End Site.

B – Average profile of Cyclin G signal over these genes shown as an aggregation plot.

C – ChIP-qPCR analysis of *RPL7*, *RPL5*, *Rack1* and *CycG*. IPs were performed either with Myc antibody (α -Myc) to reveal the presence of Cyclin G, or with rabbit IgG as negative control (mock). qPCR were performed using oligonucleotide primers located either at the TSS or in the gene body as indicated in Table S1.

D – Ontology of the 889 genes. Gene ontology analysis was performed with DAVID (Huang et al., 2009; Huang et al., 2009).

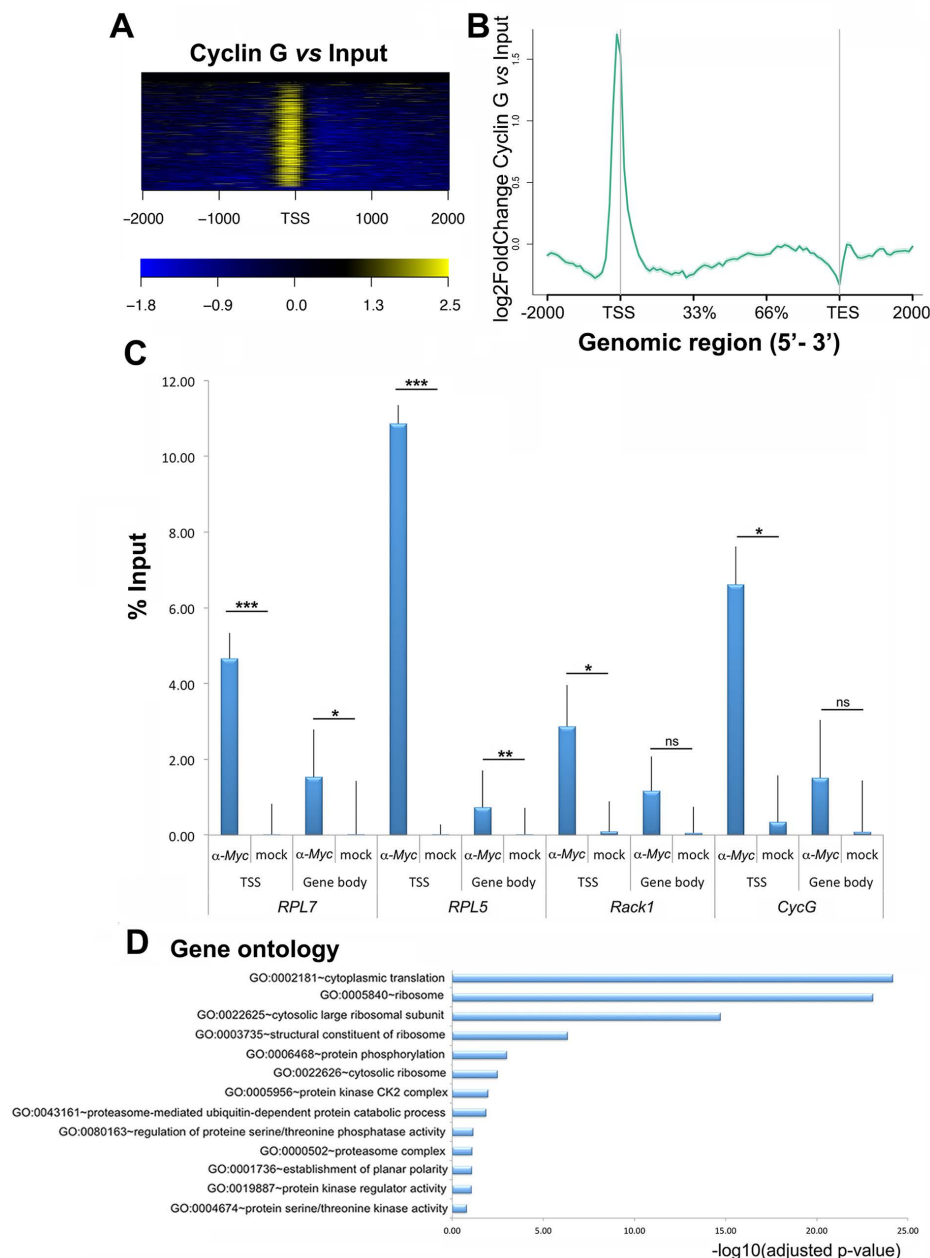


Figure 7: Cyclin G shares target genes with PRC1, ASX and RNAPoIII but not with Calypso.

Venn diagrams showing the intersection between Cyclin G-bound genes in $+/\text{UAS-Myc-CycG}^{\Delta P}$; $da-Gal4/+$, wing imaginal discs and PH, PC, PSC, ASX, Calypso and RNAPoIII in wild-type wing imaginal discs.

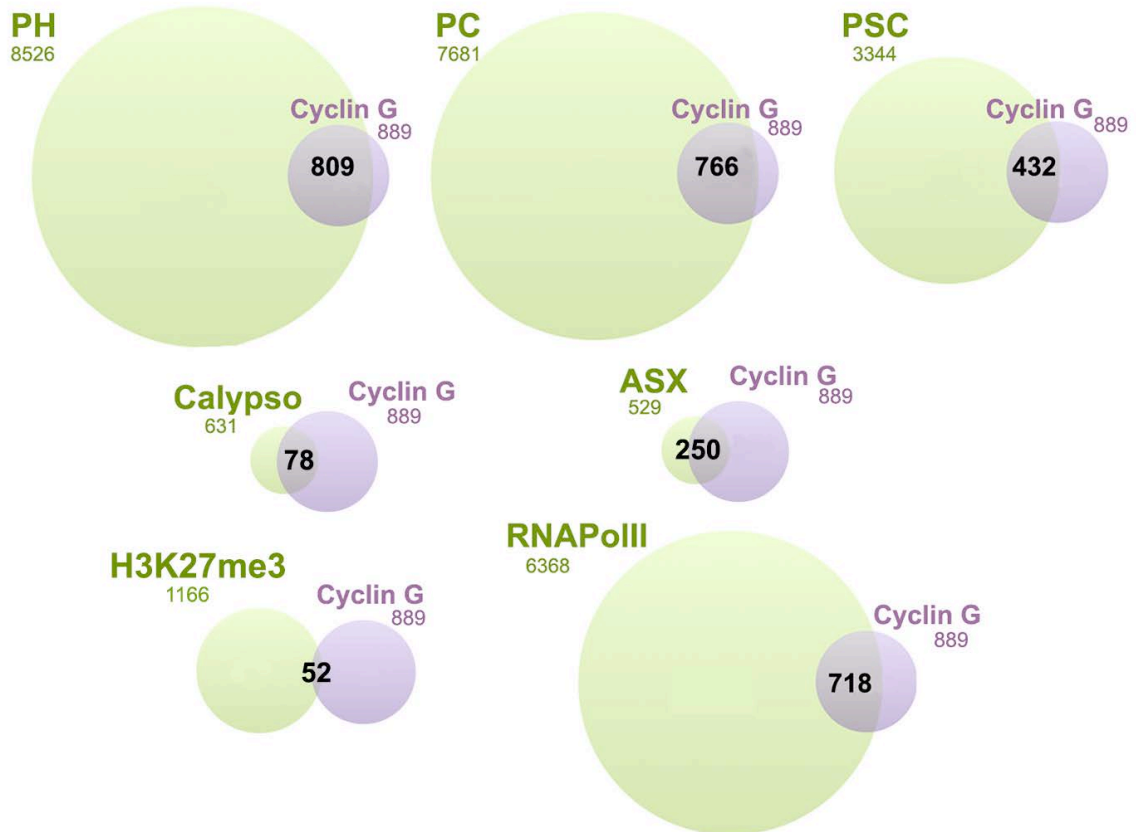


Figure 8: Functional subnetwork identified in wing imaginal discs expressing *CycG^{ΔP}*.

A – Schematic representation of a sub-network of 222 genes centred on Cyclin G and identified using JactiveModules (Z score 48.53) (Ideker et al., 2002). In this sub-network, 65 genes were up-regulated in *da-Gal4, UAS-CycG^{ΔP} versus da-Gal4/+* wing imaginal discs (green gradient), 124 genes were down-regulated (red gradient), and 33 genes were not significantly deregulated (grey). Genes bound by Cyclin G are circled in red. Transcription factor genes are represented by squares. Genes were clustered depending on their function. Black edges correspond to interactions discovered in the present study. Grey edges correspond to interactions described in the literature and imported into the WID network using DroID (Murali et al., 2011).

B – Genes bound by ASX, Calypso, PC, PH, PSC, or RNAPoIII, or enriched in H3K27me3 in the sub-network are represented in red.

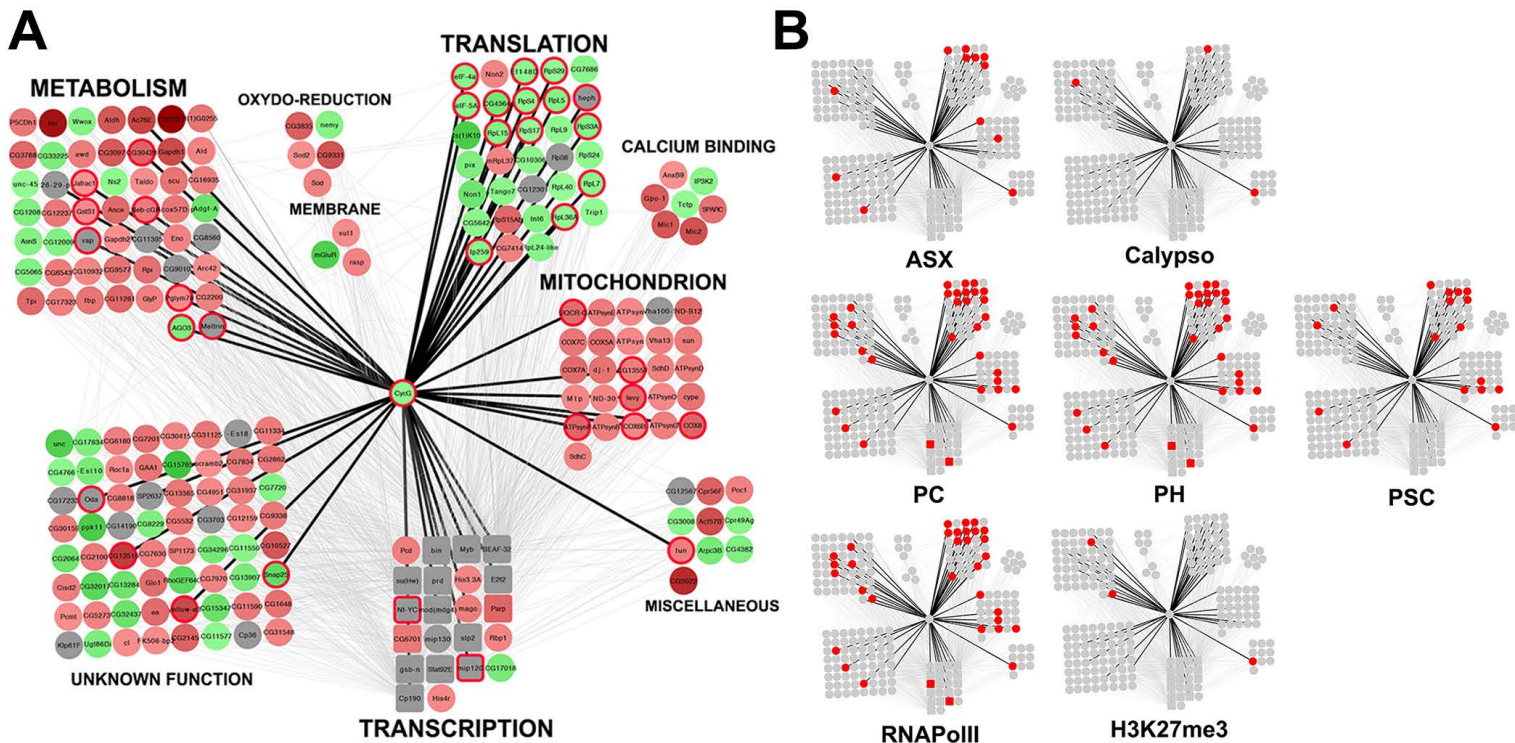


Figure S1: Cyclin G co-localizes with H2AK118ub at many sites on polytene chromosomes; expression of *CycG* ^{ΔP} does not modify the bulk of H2AK118ub.

A, A', A'' – Immunostaining of polytene chromosomes from *w*¹¹¹⁸ third instar larvae. H2AK118ub (red), Cyclin G (green), DAPI (blue). **A'''** – Close-up of the box showed in A''.

B, B' – Wing imaginal discs of 3rd instar larvae expressing *CycG* ^{ΔP} in the posterior compartment under control of the *engrailed-Gal4* driver, stained with anti-Cyclin G (green) and anti-H2AK118ub (red).

C, C' – Wing imaginal discs of 3rd instar larvae expressing *CycG* ^{$\Delta E\Delta P$} in the posterior compartment under control of the *engrailed-Gal4* driver, stained with anti-Cyclin G (green) and anti-H2AK118ub (red).

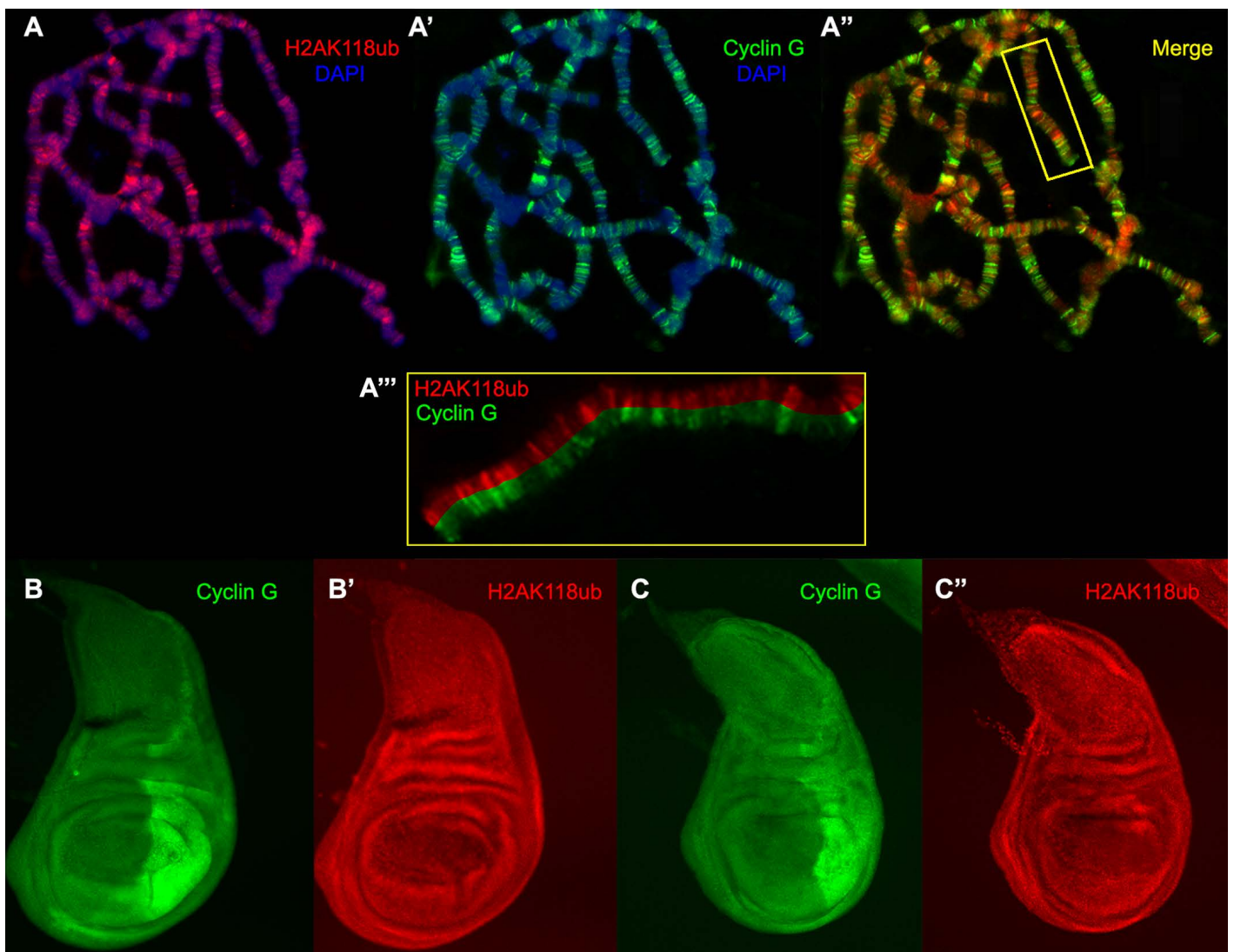


Table 1: Size fluctuating asymmetry of flies expressing *CycG*^{ΔP} with different Gal4 drivers.

Size fluctuating asymmetry was estimated with the FA10 index using landmarks 3 and 13 (Palmer and Strobeck, 1992) as described previously (Debat et al., 2011). 30 females of each genotype were measured.

Standard F-tests were used to compare FA values between genotypes. Df: degrees of freedom. *CycG*^{ΔP}: cDNA encoding the protein deleted of the PEST domain.

	FA10		Df		F	p-value
	<i>UAS-CycG</i> ^{ΔP}	+	<i>UAS-CycG</i> ^{ΔP}	+		
<i>nub-Gal4</i>	59.34	18.80	26.25	26.45	3.1561	2.34E-03
<i>omb-Gal4</i>	107.90	36.17	28.41	27.88	2.9829	2.87E-03
<i>m-Gal4</i>	229.69	12.59	28.80	25.30	18.2390	9.60E-11
<i>sd-Gal4</i>	101.85	19.83	28.56	26.45	5.1367	3.64E-05
<i>tsh-Gal4</i>	15.49	12.32	23.89	22.27	1.2576	2.97E-01
<i>vg-Gal4</i>	67.11	20.90	28.45	26.67	3.2107	1.88E-03
<i>dilp3-Gal4</i>	23.90	11.51	26.97	23.71	2.0776	4.02E-02
<i>NPF-Gal4</i>	13.90	9.90	25.09	22.98	1.4048	2.12E-01
<i>pdf-Gal4</i>	22.14	14.75	24.60	25.09	1.5012	1.60E-01
<i>per-Gal4</i>	12.69	9.09	23.12	21.53	1.3963	2.23E-01
<i>phm-Gal4</i>	13.81	20.18	23.86	27.06	1.4609	1.80E-01
<i>ptth-Gal4</i>	17.62	22.14	25.17	26.30	1.2565	3.39E-01
<i>R19B09-Gal4</i>	10.76	7.81	23.15	21.87	1.3782	2.32E-01

Table 2: Centroid size fluctuating asymmetry of flies expressing different versions of Cyclin G.

Centroid size fluctuating asymmetry was estimated with the FA10 index using the 15 landmarks (Palmer and Strobeck, 1992) as described previously (Debat et al., 2011). Standard F-tests were used to compare FA values between genotypes. Df: degrees of freedom. n: number of females analysed. *CycG^{FL}*: cDNA encoding the full-length protein; *CycG^{ΔE}*: cDNA encoding a protein deleted of the ETP-interacting domain; *CycG^{ΔP}*: cDNA encoding a protein deleted of the PEST domain; *CycG^{ΔEΔP}*: cDNA encoding a protein deleted of both domains.

Genotype	n	FA10	Df	<i>yw; +/da-Gal4</i>		<i>yw; +/UAS-CycG^{FL}; da-Gal4/+</i>		<i>yw; +/UAS-CycG^{ΔE}; da-Gal4/+</i>		<i>yw; +/UAS-CycG^{ΔP}; da-Gal4/+</i>	
				F	p-value	F	p-value	F	p-value	F	p-value
<i>yw; da-Gal4/+</i>	146	3.73E-06	16.37	-	-						
<i>yw; +/UAS-CycG^{FL}; da-Gal4/+</i>	89	2.34E-05	72.82	6.27	9.30E-05	-	-				
<i>yw; +/UAS-CycG^{ΔE}; da-Gal4/+</i>	88	4.92E-05	85.78	13.19	4.49E-07	2.10	6.96E-04	-			
<i>yw; +/UAS-CycG^{ΔP}; da-Gal4/+</i>	111	6.57E-04	108.76	176.01	7.08E-16	28.06	4.52E-35	13.34	6.63E-28	-	-
<i>yw; +/UAS-CycG^{ΔEΔP}; +/da-Gal4</i>	95	1.22E-03	93.28	328.22	5.34E-18	52.32	7.18E-44	24.88	1.12E-37	1.86	9.32E-04

Table 3: Polycomb and Enhancer of Polycomb and Trithorax alleles used in this study.

Class	Gene	Allele	Allele class	Reference
<i>ETP</i>	<i>Additional sex combs</i>	<i>Asx</i> ^{22P4}	no protein detected	Scheuermann et al., 2010
		<i>Asx</i> ^{XF23}	loss of function	Simon et al., 1992
	<i>corto</i>	<i>corto</i> ⁴²⁰	loss of function	Salvaing et al., 2006
		<i>corto</i> ^{L1}	amorphic	Salvaing et al., 2006
<i>PcG</i>	<i>calypso</i>	<i>caly</i> ¹	no protein detected	Gaytán de Ayala Alonso et al., 2007; Scheuermann et al., 2010
	<i>calypso</i>	<i>caly</i> ²	no protein detected	Gaytán de Ayala Alonso et al., 2007; Scheuermann et al., 2010
	<i>Enhancer of zeste</i>	<i>E(z)</i> ⁶³	loss of function	Beuchle et al., 2001
	<i>extra sexcombs</i>	<i>esc</i> ²¹	amorphic	Gindhart and Kaufman, 1995
	<i>Polycomb</i>	<i>Pc</i> ¹	amorphic	Capdevilla et al., 1986
	<i>polyhomeotic</i>	<i>ph-d</i> ⁴⁰¹ <i>ph-p</i> ⁶⁰²	null	Dura et al., 1987
	<i>polyhomeotic proximal</i>	<i>ph-p</i> ⁴¹⁰	loss of function	Dura et al., 1987
	<i>Posterior sex combs</i>	<i>Psc</i> ¹	hypomorphic	Adler et al., 1989
	<i>Sex combs extra</i>	<i>Sce</i> ¹	null	Gorfinkiel et al., 2004
	<i>Sex combs extra</i>	<i>Sce</i> ^{33M2}	loss of function	Fritsch et al., 2003
	<i>Sex combs extra</i>	<i>Sce</i> ^{KO4}	null	Gutiérrez et al., 2012
	<i>Sex comb on midleg</i>	<i>Scm</i> ^{D1}	amorphic	McKeon and Brock, 1991,

Table S1: Centroid size fluctuating asymmetry of flies expressing *CycG*^{ΔP} combined with different *PcG* or *ETP* mutant alleles

Centroid size fluctuating asymmetry was estimated with the FA10 index using the 15 landmarks (Palmer and Strobeck, 1992) as described previously (Debat et al., 2011). Standard F-tests were used to compare FA values between genotypes. Df: degrees of freedom.

Genotype	FA	Df	F	p-value
+/ <i>daGal4</i>	2.87E-05	27.71		
+/ <i>da-Gal4</i> ; <i>UAS-CycG</i> ^{ΔP}	7.05E-04	28.91		
<i>corto</i> ⁴²⁰ / <i>da-Gal4</i>	1.05E-05	19.48	2.73	1.23E-02
<i>corto</i> ⁴²⁰ / <i>da-Gal4</i> ; <i>UAS-CycG</i> ^{ΔP}	1.05E-03	28.98	1.49	1.46E-01
<i>corto</i> ^{L1} / <i>da-Gal4</i>	1.74E-05	25.78	1.00	1.02E-01
<i>corto</i> ^{L1} / <i>da-Gal4</i> ; <i>UAS-CycG</i> ^{ΔP}	1.50E-03	28.97	2.13	2.30E-02
<i>Asx</i> ^{22P4} /+; +/ <i>da-Gal4</i>	2.31E-05	28.31	1.65	2.87E-01
<i>Asx</i> ^{22P4} /+; +/ <i>da-Gal4</i> ; <i>UAS-CycG</i> ^{ΔP}	1.36E-03	26.94	1.93	4.26E-02
<i>Asx</i> ^{XF23} /+; +/ <i>da-Gal4</i>	1.86E-05	27.62	2.21	1.30E-01
<i>Asx</i> ^{XF23} /+; +/ <i>da-Gal4</i> ; <i>UAS-CycG</i> ^{ΔP}	3.68E-04	28.93	1.92	4.29E-02
<i>caly</i> ¹ /+; +/ <i>da-Gal4</i>	2.15E-05	27.85	1.77	2.27E-01
<i>caly</i> ¹ /+; +/ <i>da-Gal4</i> ; <i>UAS-CycG</i> ^{ΔP}	2.58E-03	28.97	3.66	4.06E-04
<i>caly</i> ² /+; +/ <i>da-Gal4</i>	3.03E-05	26.31	2.05	4.43E-01
<i>caly</i> ² /+; +/ <i>da-Gal4</i> ; <i>UAS-CycG</i> ^{ΔP}	2.01E-03	28.95	2.86	3.10E-03
<i>E(z)</i> ⁶³ / <i>da-Gal4</i>	1.70E-05	27.86	2.89	8.60E-02
<i>E(z)</i> ⁶³ / <i>da-Gal4</i> ; <i>UAS-CycG</i> ^{ΔP}	9.87E-04	28.96	1.40	1.86E-01
<i>esc</i> ²¹ /+; +/ <i>da-Gal4</i>	1.21E-05	26.91	1.62	1.38E-02
<i>esc</i> ²¹ /+; +/ <i>da-Gal4</i> ; <i>UAS-CycG</i> ^{ΔP}	7.14E-04	26.82	1.01	4.86E-01
<i>Pc</i> ¹ / <i>da-Gal4</i>	2.08E-05	26.26	1.15	2.07E-01
<i>Pc</i> ¹ / <i>da-Gal4</i> ; <i>UAS-CycG</i> ^{ΔP}	1.59E-03	29.93	2.25	1.58E-02
<i>ph-d</i> ⁴⁰¹ <i>ph-p</i> ⁶⁰² /+; +/ <i>da-Gal4</i>	1.11E-05	19.16	1.98	1.76E-02
<i>ph-d</i> ⁴⁰¹ <i>ph-p</i> ⁶⁰² /+; +/ <i>da-Gal4</i> ; <i>UAS-CycG</i> ^{ΔP}	1.50E-03	28.95	2.13	2.33E-02
<i>ph-p</i> ⁴¹⁰ /+; +/ <i>da-Gal4</i>	1.98E-05	18.29	1.06	2.08E-01
<i>ph-p</i> ⁴¹⁰ /+; +/ <i>da-Gal4</i> ; <i>UAS-CycG</i> ^{ΔP}	2.63E-03	27.88	3.72	3.72E-04
<i>Psc</i> ¹ /+; +/ <i>da-Gal4</i>	1.38E-05	27.10	1.89	3.04E-02
<i>Psc</i> ¹ /+; +/ <i>da-Gal4</i> ; <i>UAS-CycG</i> ^{ΔP}	8.45E-04	28.85	1.20	3.15E-01
<i>Sce</i> ¹ / <i>da-Gal4</i>	1.66E-05	23.20	1.31	9.28E-02
<i>Sce</i> ¹ / <i>da-Gal4</i> ; <i>UAS-CycG</i> ^{ΔP}	4.25E-03	28.93	6.03	3.15E-06
<i>Sce</i> ^{33M2} / <i>da-Gal4</i>	6.68E-05	28.71	1.59	1.44E-02
<i>Sce</i> ^{33M2} / <i>da-Gal4</i> ; <i>UAS-CycG</i> ^{ΔP}	1.68E-03	28.97	2.38	1.14E-02
<i>Sce</i> ^{KO4} / <i>da-Gal4</i>	1.83E-05	26.40	6.37	1.26E-01
<i>Sce</i> ^{KO4} / <i>da-Gal4</i> ; <i>UAS-CycG</i> ^{ΔP}	2.82E-03	29.97	4.00	1.72E-04
<i>Scm</i> ^{D1} / <i>da-Gal4</i>	2.22E-05	28.22	1.75	2.53E-01
<i>Scm</i> ^{D1} / <i>da-Gal4</i> ; <i>UAS-CycG</i> ^{ΔP}	2.77E-03	28.96	3.93	2.15E-04

Table S2: List of the 530 genes deregulated in *da-Gal4/+;UAS-CycG^{ΔP}* wing imaginal discs as compared to *da-Gal4/+* wing imaginal discs.

Gene ID	Gene name	baseMean	log2foldChange	foldChange	logfoldStandard Error	wald-statistics	p-value	adjusted p-value
FBgn0004852	<i>Ac76E</i>	157.95	-1.06	0.48	0.16	-6.73	1.71E-11	3.64E-09
FBgn0034628	<i>Acox57D-p</i>	493.37	-0.54	0.69	0.12	-4.51	6.54E-06	3.24E-04
FBgn0002855	<i>Acp26Aa</i>	62.15	2.09	4.26	0.19	11.27	1.75E-29	2.43E-26
FBgn0002856	<i>Acp26Ab</i>	40.44	1.40	2.65	0.18	7.94	1.99E-15	7.50E-13
FBgn0000043	<i>Act42A</i>	48484.83	-0.31	0.81	0.10	-3.13	1.76E-03	3.24E-02
FBgn0000044	<i>Act57B</i>	1298.53	-0.95	0.52	0.18	-5.33	9.81E-08	9.38E-06
FBgn0036752	<i>Adgf-A</i>	165.24	1.02	2.03	0.17	5.98	2.25E-09	3.19E-07
FBgn0250816	<i>AGO3</i>	205.37	0.69	1.61	0.16	4.29	1.81E-05	7.70E-04
FBgn0024912	<i>agt</i>	212.27	0.49	1.41	0.15	3.32	9.06E-04	1.99E-02
FBgn0014455	<i>Ahcy13</i>	8016.68	-0.38	0.77	0.10	-3.98	6.85E-05	2.30E-03
FBgn0000064	<i>Ald</i>	9857.00	-0.42	0.75	0.09	-4.55	5.29E-06	2.73E-04
FBgn0012036	<i>Aldh</i>	582.55	-0.85	0.56	0.16	-5.28	1.32E-07	1.16E-05
FBgn0015569	<i>alpha-Est10</i>	105.48	0.77	1.70	0.18	4.38	1.20E-05	5.47E-04
FBgn0003884	<i>alphaTub84B</i>	131635.85	-0.35	0.78	0.09	-3.96	7.51E-05	2.49E-03
FBgn0003885	<i>alphaTub84D</i>	7305.60	-0.34	0.79	0.09	-3.79	1.53E-04	4.50E-03
FBgn0003886	<i>alphaTub85E</i>	158.98	0.83	1.78	0.18	4.73	2.25E-06	1.27E-04
FBgn0011746	<i>ana</i>	2067.08	-0.37	0.77	0.12	-3.19	1.43E-03	2.82E-02
FBgn0012037	<i>Ance</i>	17205.19	-0.68	0.63	0.11	-6.06	1.34E-09	2.02E-07
FBgn0000084	<i>AnxB10</i>	422.93	-0.54	0.69	0.16	-3.30	9.68E-04	2.09E-02
FBgn0000083	<i>AnxB9</i>	9633.78	-0.29	0.82	0.07	-4.35	1.33E-05	5.96E-04
FBgn0038742	<i>Arc42</i>	2401.99	-0.34	0.79	0.08	-4.43	9.34E-06	4.46E-04
FBgn0065032	<i>Arpc3B</i>	85.14	0.78	1.72	0.19	4.19	2.77E-05	1.09E-03
FBgn0031781	<i>Arpc4</i>	1644.28	-0.41	0.75	0.12	-3.41	6.54E-04	1.54E-02
FBgn0270926	<i>AsnS</i>	534.27	0.55	1.46	0.12	4.42	9.70E-06	4.55E-04
FBgn0037989	<i>ATP8B</i>	518.41	0.40	1.32	0.13	3.02	2.52E-03	4.22E-02
FBgn0020236	<i>ATPCL</i>	7452.69	-0.32	0.80	0.09	-3.60	3.24E-04	8.43E-03
FBgn0019644	<i>ATPsynB</i>	5227.18	-0.46	0.73	0.11	-4.15	3.38E-05	1.30E-03
FBgn0010217	<i>ATPsynbeta</i>	38872.94	-0.20	0.87	0.07	-3.06	2.19E-03	3.79E-02
FBgn0016120	<i>ATPsynD</i>	6664.75	-0.46	0.72	0.07	-6.28	3.29E-10	5.47E-08
FBgn0028342	<i>ATPsyndelta</i>	4618.13	-0.38	0.77	0.08	-4.47	7.72E-06	3.75E-04
FBgn0038224	<i>ATPsynE</i>	3642.27	-0.49	0.71	0.10	-5.04	4.62E-07	3.23E-05
FBgn0035032	<i>ATPsynF</i>	3082.49	-0.71	0.61	0.15	-4.89	1.03E-06	6.28E-05
FBgn0010612	<i>ATPsynG</i>	4277.38	-0.46	0.73	0.09	-5.30	1.15E-07	1.05E-05
FBgn0020235	<i>ATPsyngamma</i>	8921.67	-0.36	0.78	0.07	-5.27	1.40E-07	1.21E-05
FBgn0016691	<i>ATPsynO</i>	5921.97	-0.37	0.77	0.07	-4.97	6.83E-07	4.58E-05
FBgn0000150	<i>awd</i>	34753.24	-0.49	0.71	0.11	-4.68	2.90E-06	1.58E-04
FBgn0038494	<i>beat-llb</i>	120.27	0.53	1.44	0.18	3.00	2.73E-03	4.46E-02
FBgn0039258	<i>beta4GalT7</i>	904.97	-0.41	0.75	0.12	-3.51	4.50E-04	1.12E-02
FBgn0013753	<i>Bgb</i>	1979.15	-0.30	0.81	0.10	-2.98	2.92E-03	4.68E-02
FBgn0035625	<i>Blimp-1</i>	2451.04	0.58	1.50	0.18	3.24	1.19E-03	2.42E-02
FBgn0001090	<i>bnb</i>	18175.81	-0.83	0.56	0.16	-5.21	1.92E-07	1.55E-05
FBgn0053653	<i>Cadps</i>	210.94	0.49	1.41	0.16	3.11	1.89E-03	3.41E-02
FBgn0264607	<i>CaMKII</i>	5338.07	0.24	1.18	0.07	3.37	7.41E-04	1.71E-02
FBgn0032685	<i>CG10211</i>	1429.48	-0.43	0.74	0.12	-3.43	6.11E-04	1.44E-02
FBgn0032783	<i>CG10237</i>	608.83	-0.68	0.63	0.12	-5.82	6.03E-09	7.96E-07
FBgn0034654	<i>CG10306</i>	7984.95	0.42	1.34	0.07	5.98	2.26E-09	3.19E-07
FBgn0035452	<i>CG10359</i>	3628.29	0.19	1.14	0.06	3.07	2.16E-03	3.77E-02
FBgn0034583	<i>CG10527</i>	578.41	-0.87	0.55	0.12	-7.22	5.21E-13	1.35E-10
FBgn0036314	<i>CG10754</i>	2049.32	-0.22	0.86	0.07	-3.01	2.63E-03	4.36E-02
FBgn0038804	<i>CG10877</i>	382.12	-0.56	0.68	0.14	-4.06	4.87E-05	1.70E-03
FBgn0029969	<i>CG10932</i>	2090.24	-0.39	0.76	0.09	-4.12	3.75E-05	1.40E-03
FBgn0030035	<i>CG11190</i>	1968.54	-0.33	0.80	0.09	-3.64	2.78E-04	7.38E-03
FBgn0036332	<i>CG11261</i>	171.64	-0.69	0.62	0.16	-4.33	1.49E-05	6.54E-04
FBgn0039849	<i>CG11334</i>	1772.52	-0.49	0.71	0.09	-5.35	8.66E-08	8.89E-06
FBgn0039864	<i>CG11550</i>	780.61	0.47	1.38	0.09	4.98	6.52E-07	4.45E-05
FBgn0036847	<i>CG11577</i>	1404.87	0.37	1.29	0.09	4.11	3.89E-05	1.44E-03
FBgn0030545	<i>CG11590</i>	1527.37	-0.53	0.69	0.09	-5.57	2.58E-08	2.90E-06
FBgn0037313	<i>CG1161</i>	2239.50	-0.28	0.82	0.07	-4.03	5.46E-05	1.88E-03
FBgn0030292	<i>CG11752</i>	544.42	-0.60	0.66	0.17	-3.59	3.33E-04	8.59E-03
FBgn0039305	<i>CG11858</i>	1032.41	-0.38	0.77	0.10	-3.75	1.78E-04	5.12E-03
FBgn0035430	<i>CG12009</i>	997.78	0.55	1.46	0.09	6.23	4.60E-10	7.50E-08
FBgn0037386	<i>CG1208</i>	117.13	0.63	1.55	0.15	4.32	1.54E-05	6.75E-04
FBgn0033232	<i>CG12159</i>	1180.24	-0.38	0.77	0.08	-4.88	1.04E-06	6.29E-05
FBgn0033158	<i>CG12164</i>	50.10	-0.70	0.62	0.19	-3.76	1.68E-04	4.89E-03
FBgn0037354	<i>CG12171</i>	910.21	-0.33	0.79	0.10	-3.30	9.81E-04	2.11E-02
FBgn0031048	<i>CG12237</i>	1832.22	-0.53	0.69	0.10	-5.13	2.92E-07	2.17E-05
FBgn0037811	<i>CG12592</i>	43.43	-0.74	0.60	0.18	-4.23	2.32E-05	9.48E-04
FBgn0035522	<i>CG1273</i>	2062.97	0.40	1.32	0.13	3.10	1.95E-03	3.48E-02
FBgn0033184	<i>CG12736</i>	701.42	-0.31	0.80	0.11	-2.98	2.86E-03	4.61E-02
FBgn0026566	<i>CG1307</i>	1958.10	-0.28	0.82	0.09	-3.02	2.53E-03	4.23E-02
FBgn0032614	<i>CG13284</i>	78.55	0.99	1.98	0.19	5.31	1.11E-07	1.04E-05
FBgn0029529	<i>CG13365</i>	298.16	-0.54	0.69	0.13	-4.10	4.05E-05	1.48E-03
FBgn0027507	<i>CG1344</i>	2808.60	0.20	1.15	0.07	2.98	2.86E-03	4.61E-02
FBgn0040658	<i>CG13516</i>	215.45	-1.14	0.45	0.16	-6.94	3.81E-12	8.57E-10
FBgn0040660	<i>CG13551</i>	4309.06	-0.49	0.71	0.09	-5.22	1.79E-07	1.50E-05
FBgn0036717	<i>CG13731</i>	258.92	-0.60	0.66	0.18	-3.31	9.32E-04	2.03E-02
FBgn0035173	<i>CG13907</i>	207.74	0.75	1.68	0.18	4.07	4.72E-05	1.66E-03
FBgn0035246	<i>CG13928</i>	118.86	0.55	1.46	0.17	3.15	1.63E-03	3.05E-02
FBgn0031770	<i>CG13995</i>	329.94	3.11	8.64	0.18	17.04	4.34E-65	1.81E-61
FBgn0039482	<i>CG14258</i>	140.61	-0.52	0.70	0.16	-3.18	1.47E-03	2.87E-02

FBgn0037149	CG14561	767.80	-0.33	0.79	0.10	-3.22	1.26E-03	2.54E-02
FBgn0037127	CG14566	472.71	-0.87	0.55	0.18	-4.71	2.46E-04	1.36E-04
FBgn0037822	CG14683	2553.41	0.29	1.22	0.09	3.33	8.55E-04	1.91E-02
FBgn0037853	CG14696	352.18	-0.49	0.71	0.13	-3.64	2.72E-04	7.27E-03
FBgn0035409	CG14963	113.28	-0.71	0.61	0.16	-4.52	6.22E-06	3.10E-04
FBgn0030040	CG15347	130.33	1.04	2.06	0.18	5.87	4.39E-09	5.89E-07
FBgn0040718	CG15353	627.38	-0.68	0.62	0.18	-3.72	2.02E-04	5.72E-03
FBgn0031161	CG15445	1474.98	0.49	1.41	0.12	3.99	6.73E-05	2.28E-03
FBgn0039807	CG15546	357.76	0.53	1.45	0.16	3.43	6.04E-04	1.43E-02
FBgn0039809	CG15547	182.69	0.57	1.49	0.16	3.61	3.11E-04	8.19E-03
FBgn0029814	CG15765	393.00	1.88	3.67	0.14	13.67	1.54E-42	3.21E-39
FBgn0029766	CG15784	1538.94	0.50	1.41	0.16	3.04	2.37E-03	4.03E-02
FBgn0033446	CG1648	2116.68	-0.59	0.66	0.13	-4.58	4.66E-06	2.43E-04
FBgn0033451	CG1665	1183.52	-0.27	0.83	0.08	-3.49	4.91E-04	1.20E-02
FBgn0028544	CG16884	1627.71	-0.96	0.51	0.15	-6.50	8.27E-11	1.49E-08
FBgn0032538	CG16885	1759.92	-1.02	0.49	0.16	-6.57	5.09E-11	9.94E-09
FBgn0033883	CG16935	769.06	-0.46	0.73	0.11	-4.35	1.34E-05	5.96E-04
FBgn0033443	CG1698	188.88	0.73	1.66	0.16	4.60	4.25E-06	2.24E-04
FBgn0025621	CG16989	1952.03	-0.23	0.85	0.07	-3.32	8.88E-04	1.96E-02
FBgn0039972	CG17018	149.59	0.78	1.72	0.17	4.73	2.25E-06	1.27E-04
FBgn0036547	CG17032	4276.88	-0.50	0.71	0.08	-6.04	1.59E-09	2.33E-07
FBgn0032449	CG17036	125.42	-0.68	0.62	0.17	-4.08	4.56E-05	1.62E-03
FBgn0031170	CG1718	201.89	-0.58	0.67	0.17	-3.34	8.44E-04	1.89E-02
FBgn0032032	CG17294	601.02	0.37	1.30	0.11	3.34	8.28E-04	1.86E-02
FBgn0032713	CG17323	1529.83	-0.46	0.73	0.10	-4.79	1.64E-06	9.67E-05
FBgn0032774	CG17549	1354.77	-0.43	0.74	0.12	-3.60	3.17E-04	8.29E-03
FBgn0263780	CG17684	340.34	1.20	2.29	0.15	7.85	4.02E-15	1.45E-12
FBgn0040899	CG17776	512.79	-0.42	0.75	0.13	-3.27	1.07E-03	2.25E-02
FBgn0028394	CG17834	1210.01	0.66	1.58	0.11	5.81	6.37E-09	8.27E-07
FBgn0032124	CG17855	45.31	0.52	1.44	0.16	3.19	1.40E-03	2.78E-02
FBgn0023537	CG17896	5157.69	-0.39	0.76	0.10	-4.00	6.36E-05	2.17E-03
FBgn0037433	CG17919	2278.96	-0.24	0.84	0.07	-3.49	4.81E-04	1.18E-02
FBgn0038470	CG18213	938.57	0.29	1.22	0.09	3.25	1.14E-03	2.33E-02
FBgn0033205	CG2064	224.36	0.97	1.96	0.15	6.63	3.42E-11	7.10E-09
FBgn0037369	CG2100	1081.59	-0.51	0.70	0.11	-4.54	5.53E-06	2.82E-04
FBgn0030251	CG2145	1205.84	-0.75	0.60	0.13	-5.63	1.77E-08	2.10E-06
FBgn0030447	CG2200	744.99	-0.44	0.74	0.09	-4.61	3.96E-06	2.10E-04
FBgn0034753	CG2852	40954.63	-0.41	0.75	0.12	-3.51	4.55E-04	1.13E-02
FBgn0031459	CG2862	3814.65	-0.52	0.70	0.08	-6.16	7.40E-10	1.16E-07
FBgn0031643	CG3008	2220.33	0.46	1.37	0.08	5.96	2.53E-09	3.50E-07
FBgn0050159	CG30159	1880.54	-0.49	0.71	0.11	-4.39	1.15E-05	5.26E-04
FBgn0260477	CG30283	95.78	0.59	1.51	0.18	3.22	1.28E-03	2.57E-02
FBgn0050291	CG30291	1158.96	-0.32	0.80	0.10	-3.29	9.86E-04	2.11E-02
FBgn0050403	CG30403	372.45	-0.46	0.72	0.11	-4.05	5.17E-05	1.80E-03
FBgn0250838	CG30415	3347.01	-0.39	0.76	0.09	-4.39	1.14E-05	5.26E-04
FBgn0050428	CG30428	256.70	-0.74	0.60	0.15	-4.98	6.52E-07	4.45E-05
FBgn0050463	CG30463	2387.47	0.37	1.29	0.11	3.46	5.50E-04	1.33E-02
FBgn0029804	CG3097	2060.48	-0.85	0.56	0.11	-7.39	1.49E-13	4.13E-11
FBgn0051028	CG31028	1499.74	-0.50	0.71	0.13	-3.95	7.85E-05	2.57E-03
FBgn0051125	CG31125	684.52	-0.54	0.69	0.11	-4.94	7.99E-07	5.15E-05
FBgn0051324	CG31324	120.85	0.70	1.63	0.18	3.92	8.74E-05	2.78E-03
FBgn0051373	CG31373	64.68	-0.57	0.67	0.18	-3.10	1.94E-03	3.48E-02
FBgn0051548	CG31548	805.24	-0.42	0.75	0.10	-4.28	1.90E-05	7.99E-04
FBgn0051549	CG31549	788.24	-0.35	0.78	0.11	-3.12	1.83E-03	3.33E-02
FBgn0051673	CG31673	771.45	-0.42	0.75	0.12	-3.36	7.68E-04	1.76E-02
FBgn0051869	CG31869	1877.66	0.41	1.32	0.08	5.30	1.17E-07	1.06E-05
FBgn0031360	CG31937	894.81	-0.47	0.72	0.09	-5.05	4.35E-07	3.09E-05
FBgn0051997	CG31997	4805.71	-0.56	0.68	0.12	-4.68	2.80E-06	1.54E-04
FBgn0052017	CG32017	122.68	1.33	2.51	0.18	7.56	3.98E-14	1.27E-11
FBgn0052214	CG32214	24.85	-0.92	0.53	0.17	-5.35	8.87E-08	8.89E-06
FBgn0029885	CG3224	1558.67	0.27	1.20	0.08	3.24	1.18E-03	2.41E-02
FBgn0052249	CG32249	169.75	-0.50	0.71	0.15	-3.31	9.28E-04	2.03E-02
FBgn0052365	CG32365	256.67	0.48	1.40	0.16	2.95	3.18E-03	4.99E-02
FBgn0052437	CG32437	168.00	1.02	2.03	0.17	6.03	1.60E-09	2.33E-07
FBgn0052512	CG32512	676.53	0.55	1.46	0.15	3.66	2.51E-04	6.90E-03
FBgn0053217	CG33217	885.39	0.31	1.24	0.09	3.52	4.35E-04	1.09E-02
FBgn0053225	CG33225	53.37	0.71	1.64	0.18	4.07	4.77E-05	1.67E-03
FBgn0053460	CG33460	98.79	0.70	1.62	0.17	4.01	5.96E-05	2.05E-03
FBgn0054057	CG34057	111.87	0.71	1.63	0.18	3.84	1.22E-04	3.74E-03
FBgn0085249	CG34220	39.12	0.56	1.48	0.18	3.11	1.89E-03	3.41E-02
FBgn0085325	CG34296	168.08	0.84	1.78	0.17	5.05	4.41E-07	3.11E-05
FBgn0085376	CG34347	1417.13	0.52	1.43	0.15	3.52	4.27E-04	1.07E-02
FBgn0085384	CG34355	488.84	0.38	1.30	0.12	3.15	1.61E-03	3.04E-02
FBgn0085453	CG34424	223.80	-0.61	0.66	0.17	-3.57	3.60E-04	9.17E-03
FBgn0022343	CG3760	5299.21	-0.33	0.80	0.09	-3.73	1.90E-04	5.45E-03
FBgn0034800	CG3788	347.59	-0.68	0.62	0.13	-5.12	3.07E-07	2.26E-05
FBgn0036842	CG3797	3549.83	-0.27	0.83	0.08	-3.26	1.12E-03	2.31E-02
FBgn0036824	CG3902	3584.21	-0.38	0.77	0.10	-3.91	9.37E-05	2.96E-03
FBgn0058160	CG40160	5734.41	0.38	1.30	0.09	4.37	1.25E-05	5.62E-04
FBgn0029821	CG4020	86.99	0.61	1.53	0.18	3.35	8.04E-04	1.82E-02
FBgn0020312	CG4050	2881.80	-0.33	0.79	0.10	-3.36	7.79E-04	1.78E-02
FBgn0036648	CG4098	163.32	-0.62	0.65	0.18	-3.50	4.59E-04	1.14E-02
FBgn0250868	CG42239	1025.09	-0.46	0.72	0.13	-3.64	2.71E-04	7.27E-03
FBgn0250869	CG42240	721.78	0.49	1.40	0.14	3.57	3.52E-04	9.03E-03

FBgn0259167	CG42272	823.51	-0.30	0.81	0.10	-3.08	2.07E-03	3.66E-02
FBgn0261995	CG42813	717.78	-0.42	0.75	0.10	-4.10	4.14E-05	1.50E-03
FBgn0032138	CG4364	14514.86	0.88	1.84	0.09	9.71	2.61E-22	1.97E-19
FBgn0037024	CG4365	1442.02	-0.47	0.72	0.13	-3.69	2.21E-04	6.18E-03
FBgn0032132	CG4382	4258.07	0.61	1.53	0.13	4.66	3.10E-06	1.67E-04
FBgn0038771	CG4390	4184.73	-0.27	0.83	0.08	-3.50	4.68E-04	1.15E-02
FBgn0266410	CG45050	8248.47	0.35	1.28	0.11	3.16	1.59E-03	3.02E-02
FBgn0033814	CG4670	1689.82	-0.33	0.80	0.11	-3.02	2.54E-03	4.25E-02
FBgn0038739	CG4686	595.58	-0.40	0.76	0.13	-3.13	1.75E-03	3.22E-02
FBgn0027546	CG4766	3139.98	0.40	1.32	0.08	5.33	9.67E-08	9.35E-06
FBgn0030792	CG4789	2026.47	-0.26	0.84	0.07	-3.45	5.67E-04	1.35E-02
FBgn0030799	CG4872	316.60	-0.40	0.76	0.13	-3.00	2.68E-03	4.42E-02
FBgn0031319	CG4896	1607.98	-0.34	0.79	0.11	-3.08	2.04E-03	3.61E-02
FBgn0036587	CG4950	187.51	0.60	1.52	0.17	3.45	5.62E-04	1.35E-02
FBgn0039563	CG4951	1604.25	-0.37	0.78	0.08	-4.76	1.92E-06	1.11E-04
FBgn0032225	CG5022	113.14	-1.32	0.40	0.17	-7.62	2.49E-14	8.28E-12
FBgn0034145	CG5065	601.23	0.57	1.48	0.12	4.57	4.78E-06	2.48E-04
FBgn0032235	CG5096	436.69	0.72	1.65	0.14	5.13	2.90E-07	2.17E-05
FBgn0040382	CG5273	2110.60	-0.42	0.75	0.10	-4.37	1.22E-05	5.56E-04
FBgn0036986	CG5282	143.71	-0.61	0.66	0.18	-3.39	6.88E-04	1.61E-02
FBgn0032213	CG5390	8345.46	-0.25	0.84	0.06	-3.86	1.14E-04	3.56E-03
FBgn0031327	CG5397	1189.97	0.47	1.38	0.13	3.49	4.90E-04	1.20E-02
FBgn0038353	CG5399	422.87	0.65	1.57	0.17	3.76	1.70E-04	4.92E-03
FBgn0039564	CG5527	230.82	-1.77	0.29	0.18	-9.59	8.51E-22	5.44E-19
FBgn0034902	CG5532	2453.37	-0.49	0.71	0.11	-4.26	2.04E-05	8.49E-04
FBgn0039537	CG5590	3334.74	-0.36	0.78	0.12	-2.97	2.96E-03	4.72E-02
FBgn0039527	CG5639	481.33	0.51	1.42	0.16	3.16	1.59E-03	3.02E-02
FBgn0038046	CG5641	3138.76	-0.24	0.84	0.07	-3.33	8.77E-04	1.94E-02
FBgn0036258	CG5642	13042.59	0.43	1.35	0.06	7.08	1.44E-12	3.52E-10
FBgn0035293	CG5687	108.41	1.01	2.02	0.17	5.80	6.67E-09	8.53E-07
FBgn0032196	CG5708	2031.04	0.28	1.22	0.09	3.00	2.72E-03	4.46E-02
FBgn0032191	CG5734	1348.04	-0.29	0.82	0.10	-3.01	2.60E-03	4.32E-02
FBgn0038924	CG6028	992.58	-0.33	0.80	0.09	-3.60	3.14E-04	8.24E-03
FBgn0031918	CG6055	82.93	0.86	1.82	0.18	4.79	1.63E-06	9.67E-05
FBgn0029828	CG6067	25.56	0.47	1.39	0.15	3.11	1.84E-03	3.35E-02
FBgn0032453	CG6180	6137.11	-0.47	0.72	0.08	-5.57	2.50E-08	2.85E-06
FBgn0033866	CG6280	457.42	0.49	1.40	0.12	4.08	4.55E-05	1.62E-03
FBgn0033875	CG6357	781.61	0.85	1.80	0.16	5.28	1.28E-07	1.13E-05
FBgn0033879	CG6543	5017.74	-0.50	0.71	0.10	-4.90	9.79E-07	6.03E-05
FBgn0036402	CG6650	2809.15	-0.29	0.82	0.09	-3.19	1.42E-03	2.80E-02
FBgn0033889	CG6701	2483.78	-0.52	0.70	0.11	-4.77	1.89E-06	1.10E-04
FBgn0031926	CG6739	656.86	-0.44	0.74	0.11	-3.89	1.02E-04	3.19E-03
FBgn0038941	CG7080	25.45	0.60	1.51	0.18	3.38	7.25E-04	1.67E-02
FBgn0035865	CG7201	240.64	-0.58	0.67	0.14	-4.17	3.10E-05	1.20E-03
FBgn0038272	CG7265	1509.58	-0.30	0.81	0.08	-3.66	2.53E-04	6.93E-03
FBgn0032284	CG7294	71.86	-0.76	0.59	0.19	-4.10	4.12E-05	1.49E-03
FBgn0032283	CG7296	49.40	-0.62	0.65	0.18	-3.40	6.62E-04	1.55E-02
FBgn0037135	CG7414	12729.52	-0.44	0.74	0.10	-4.31	1.62E-05	6.98E-04
FBgn0038727	CG7432	286.73	-0.58	0.67	0.14	-4.11	4.04E-05	1.48E-03
FBgn0034432	CG7461	2415.56	-0.28	0.83	0.09	-3.04	2.37E-03	4.03E-02
FBgn0035833	CG7565	402.10	-0.45	0.73	0.13	-3.44	5.77E-04	1.37E-02
FBgn0032026	CG7627	2947.94	-0.29	0.82	0.09	-3.28	1.05E-03	2.22E-02
FBgn0040793	CG7630	2815.16	-0.46	0.73	0.10	-4.73	2.29E-06	1.29E-04
FBgn0027525	CG7686	4208.32	0.46	1.37	0.07	6.55	5.94E-11	1.12E-08
FBgn0038652	CG7720	1352.02	0.57	1.48	0.13	4.37	1.23E-05	5.56E-04
FBgn0034447	CG7744	1344.46	0.27	1.21	0.08	3.52	4.30E-04	1.08E-02
FBgn0039697	CG7834	3407.38	-0.54	0.69	0.10	-5.52	3.33E-08	3.65E-06
FBgn0037548	CG7900	164.67	2.11	4.31	0.19	11.33	9.40E-30	1.56E-26
FBgn0039737	CG7920	6048.78	-0.30	0.81	0.08	-3.63	2.87E-04	7.58E-03
FBgn0035252	CG7970	2876.05	-0.41	0.75	0.08	-5.29	1.24E-07	1.11E-05
FBgn0033356	CG8229	671.63	0.65	1.57	0.12	5.61	2.00E-08	2.34E-06
FBgn0034045	CG8249	228.97	0.61	1.52	0.17	3.53	4.16E-04	1.05E-02
FBgn0038126	CG8483	928.79	0.34	1.26	0.11	3.03	2.47E-03	4.16E-02
FBgn0033751	CG8818	3048.16	-0.46	0.73	0.10	-4.54	5.67E-06	2.87E-04
FBgn0033702	CG8854	54.58	-0.59	0.67	0.18	-3.17	1.51E-03	2.91E-02
FBgn0034493	CG8908	38.94	0.59	1.50	0.19	3.14	1.67E-03	3.11E-02
FBgn0040931	CG9034	551.16	-0.45	0.73	0.14	-3.13	1.72E-03	3.19E-02
FBgn0030793	CG9125	985.51	-0.35	0.79	0.10	-3.59	3.29E-04	8.51E-03
FBgn0035206	CG9186	2148.07	-0.26	0.83	0.07	-3.78	1.55E-04	4.55E-03
FBgn0032889	CG9331	5645.69	-0.92	0.53	0.18	-5.21	1.85E-07	1.52E-05
FBgn0032899	CG9338	442.26	-0.52	0.70	0.14	-3.68	2.33E-04	6.47E-03
FBgn0034564	CG9344	1614.08	-0.34	0.79	0.09	-3.70	2.18E-04	6.11E-03
FBgn0034438	CG9416	5116.14	0.38	1.30	0.11	3.39	6.93E-04	1.61E-02
FBgn0033101	CG9436	1030.46	-0.51	0.70	0.14	-3.65	2.61E-04	7.08E-03
FBgn0037749	CG9471	946.25	-0.35	0.78	0.10	-3.39	6.95E-04	1.62E-02
FBgn0031817	CG9531	221.76	-0.46	0.73	0.14	-3.35	8.05E-04	1.82E-02
FBgn0031092	CG9577	2161.43	-0.59	0.67	0.07	-8.03	1.00E-15	3.97E-13
FBgn0031093	CG9581	696.39	-0.50	0.71	0.16	-3.04	2.36E-03	4.03E-02
FBgn0030763	CG9782	1772.69	-0.49	0.71	0.14	-3.45	5.60E-04	1.35E-02
FBgn0034860	CG9812	484.41	0.50	1.42	0.17	2.97	3.02E-03	4.78E-02
FBgn0032781	CG9987	2070.92	-0.40	0.76	0.13	-3.17	1.51E-03	2.91E-02
FBgn0030744	CG9992	1679.62	0.23	1.18	0.08	3.03	2.45E-03	4.15E-02
FBgn0035398	<i>Cht7</i>	1245.51	-0.57	0.67	0.12	-4.90	9.55E-07	5.93E-05
FBgn0001977	<i>CIAPIN1</i>	1683.74	0.23	1.17	0.08	3.05	2.27E-03	3.91E-02

FBgn0027598	<i>cindr</i>	3166.83	0.27	1.20	0.07	3.67	2.45E-04	6.77E-03
FBgn0062442	<i>Cisd2</i>	2408.47	-0.47	0.72	0.08	-5.73	9.96E-09	1.22E-06
FBgn0000318	<i>cl</i>	2351.96	-0.32	0.80	0.07	-4.52	6.12E-06	3.07E-04
FBgn0019830	<i>colt</i>	2322.51	-0.31	0.81	0.08	-3.80	1.45E-04	4.34E-03
FBgn0032833	<i>COX4</i>	4623.11	-0.34	0.79	0.11	-3.16	1.58E-03	3.02E-02
FBgn0019624	<i>COX5A</i>	3627.31	-0.60	0.66	0.12	-4.94	7.97E-07	5.15E-05
FBgn0031066	<i>COX6B</i>	6481.41	-0.39	0.76	0.08	-4.81	1.52E-06	9.12E-05
FBgn0040529	<i>COX7A</i>	5146.46	-0.66	0.63	0.09	-7.52	5.69E-14	1.69E-11
FBgn0040773	<i>COX7C</i>	2948.67	-0.54	0.69	0.10	-5.34	9.18E-08	9.08E-06
FBgn0263911	<i>COX8</i>	1629.31	-0.73	0.60	0.11	-6.41	1.47E-10	2.55E-08
FBgn0030494	<i>Cpr12A</i>	3265.99	0.35	1.28	0.10	3.65	2.65E-04	7.15E-03
FBgn0033725	<i>Cpr49Ac</i>	14675.72	0.55	1.47	0.16	3.54	4.01E-04	1.02E-02
FBgn0033730	<i>Cpr49Ag</i>	1078.90	0.48	1.40	0.12	4.12	3.75E-05	1.40E-03
FBgn0033731	<i>Cpr49Ah</i>	453.64	-0.81	0.57	0.16	-4.97	6.77E-07	4.58E-05
FBgn0034499	<i>Cpr56F</i>	72.58	-0.76	0.59	0.18	-4.20	2.71E-05	1.07E-03
FBgn0035510	<i>Cpr64Aa</i>	1098.22	-0.58	0.67	0.17	-3.31	9.25E-04	2.03E-02
FBgn0085732	<i>CR40190</i>	331.71	-0.99	0.50	0.13	-7.53	4.89E-14	1.51E-11
FBgn0262532	<i>CR43086</i>	64.23	0.86	1.82	0.19	4.64	3.48E-06	1.85E-04
FBgn0262620	<i>CR43144</i>	137.74	0.75	1.68	0.17	4.51	6.59E-06	3.24E-04
FBgn0263768	<i>CR43685</i>	691.56	-0.55	0.68	0.11	-5.17	2.34E-07	1.80E-05
FBgn0266211	<i>CR44906</i>	228.43	-0.67	0.63	0.14	-4.75	2.06E-06	1.18E-04
FBgn0266632	<i>CR45139</i>	241.10	0.62	1.54	0.15	4.12	3.77E-05	1.40E-03
FBgn0267073	<i>CR45517</i>	80.77	0.90	1.87	0.19	4.86	1.20E-06	7.25E-05
FBgn0267798	<i>CR46123</i>	173.18	-1.10	0.47	0.17	-6.36	2.05E-10	3.47E-08
FBgn0267920	<i>CR46201</i>	43.20	0.71	1.63	0.19	3.80	1.45E-04	4.34E-03
FBgn0023023	<i>CRMP</i>	424.01	-0.38	0.77	0.13	-2.96	3.11E-03	4.88E-02
FBgn0027054	<i>CSN4</i>	2416.52	-0.23	0.86	0.07	-3.44	5.92E-04	1.41E-02
FBgn0028836	<i>CSN7</i>	2665.79	-0.25	0.84	0.08	-3.05	2.27E-03	3.91E-02
FBgn0039867	<i>CstF-50</i>	1134.45	-0.31	0.81	0.08	-3.67	2.45E-04	6.77E-03
FBgn0032956	<i>Cul2</i>	3803.87	0.22	1.16	0.06	3.85	1.18E-04	3.67E-03
FBgn0039858	<i>CycG</i>	24661.26	0.38	1.30	0.09	4.42	9.84E-06	4.59E-04
FBgn0025674	<i>CycK</i>	2805.89	0.19	1.14	0.06	3.00	2.73E-03	4.46E-02
FBgn0001992	<i>Cyp303a1</i>	39.28	0.57	1.49	0.18	3.10	1.95E-03	3.48E-02
FBgn0014469	<i>Cyp4e2</i>	943.63	0.57	1.49	0.18	3.11	1.90E-03	3.41E-02
FBgn0015714	<i>Cyp6a17</i>	39.31	-0.62	0.65	0.14	-4.28	1.85E-05	7.85E-04
FBgn0033696	<i>Cyp6g2</i>	226.08	1.61	3.05	0.16	10.01	1.35E-23	1.25E-20
FBgn0033697	<i>Cyp6t3</i>	177.90	1.67	3.19	0.16	10.23	1.46E-24	1.52E-21
FBgn0015031	<i>cype</i>	2860.63	-0.57	0.67	0.10	-5.76	8.30E-09	1.03E-06
FBgn0023507	<i>D2hgdh</i>	214.12	-0.79	0.58	0.16	-4.93	8.39E-07	5.36E-05
FBgn0039802	<i>dj-1beta</i>	1548.63	-0.58	0.67	0.11	-5.20	1.98E-07	1.59E-05
FBgn0032474	<i>DnaJ-H</i>	1029.60	-0.37	0.78	0.11	-3.27	1.09E-03	2.27E-02
FBgn0024245	<i>dnt</i>	3114.19	0.23	1.17	0.07	3.47	5.16E-04	1.26E-02
FBgn0266518	<i>Dpit47</i>	2115.59	-0.23	0.85	0.08	-2.96	3.09E-03	4.88E-02
FBgn0000490	<i>dpp</i>	2217.16	0.30	1.23	0.10	3.06	2.19E-03	3.80E-02
FBgn0015380	<i>drl</i>	9294.13	0.28	1.21	0.07	3.81	1.40E-04	4.22E-03
FBgn0027594	<i>drpr</i>	4093.64	0.35	1.27	0.09	3.98	6.82E-05	2.30E-03
FBgn0038071	<i>Dtg</i>	3947.88	0.30	1.23	0.09	3.45	5.61E-04	1.35E-02
FBgn0020445	<i>E23</i>	499.53	0.58	1.50	0.18	3.30	9.70E-04	2.09E-02
FBgn0000533	<i>ea</i>	337.74	-0.66	0.63	0.13	-4.92	8.81E-07	5.59E-05
FBgn0000556	<i>Ef1alpha48D</i>	601736.06	0.44	1.36	0.10	4.31	1.61E-05	6.96E-04
FBgn0000559	<i>EF2</i>	226298.08	0.29	1.22	0.09	3.07	2.16E-03	3.77E-02
FBgn0001942	<i>elF-4a</i>	92277.21	0.51	1.43	0.07	7.35	2.05E-13	5.51E-11
FBgn0034967	<i>elF-5A</i>	68663.31	0.46	1.38	0.09	5.00	5.77E-07	4.00E-05
FBgn0029629	<i>elF3ga</i>	8809.30	0.27	1.20	0.09	3.09	2.00E-03	3.56E-02
FBgn0000565	<i>Eip71CD</i>	1985.90	-0.32	0.80	0.10	-3.13	1.75E-03	3.22E-02
FBgn0004865	<i>Eip78C</i>	1876.25	0.69	1.62	0.13	5.25	1.50E-07	1.27E-05
FBgn0000579	<i>Eno</i>	17807.85	-0.42	0.75	0.10	-4.19	2.85E-05	1.11E-03
FBgn0027496	<i>epsilonCOP</i>	1942.85	-0.28	0.82	0.09	-3.18	1.47E-03	2.87E-02
FBgn0037913	<i>fabp</i>	2587.09	-0.50	0.71	0.16	-3.13	1.75E-03	3.22E-02
FBgn0035859	<i>FBgn0001942</i>	287.63	-0.72	0.61	0.17	-4.28	1.87E-05	7.91E-04
FBgn0032820	<i>fbp</i>	2194.91	-0.56	0.68	0.09	-6.14	8.51E-10	1.31E-07
FBgn0013954	<i>FK506-bp2</i>	15765.60	-0.33	0.80	0.07	-4.44	8.80E-06	4.23E-04
FBgn0086675	<i>fnr</i>	60.63	-0.61	0.65	0.18	-3.31	9.45E-04	2.05E-02
FBgn0000810	<i>fs(1)K10</i>	3375.66	1.64	3.11	0.09	17.63	1.58E-69	1.31E-65
FBgn0259108	<i>futsch</i>	473.13	0.69	1.61	0.18	3.82	1.32E-04	3.98E-03
FBgn0029818	<i>GAA1</i>	3397.16	-0.56	0.68	0.10	-5.53	3.26E-08	3.61E-06
FBgn0001091	<i>Gapdh1</i>	7264.73	-0.99	0.50	0.06	-15.74	8.49E-56	2.35E-52
FBgn0001092	<i>Gapdh2</i>	28190.84	-0.30	0.81	0.05	-5.68	1.38E-08	1.66E-06
FBgn0036428	<i>Gbs-70E</i>	1084.50	0.51	1.42	0.16	3.23	1.25E-03	2.52E-02
FBgn0030289	<i>GCS1</i>	1762.72	-0.35	0.79	0.10	-3.59	3.27E-04	8.50E-03
FBgn0004868	<i>Gdi</i>	11767.87	-0.27	0.83	0.08	-3.29	1.00E-03	2.14E-02
FBgn0020300	<i>geko</i>	647.16	0.39	1.31	0.12	3.24	1.22E-03	2.47E-02
FBgn0011770	<i>Gip</i>	1106.74	-0.36	0.78	0.09	-3.83	1.26E-04	3.86E-03
FBgn0036144	<i>GlcAT-P</i>	255.60	0.69	1.61	0.19	3.70	2.15E-04	6.03E-03
FBgn0283450	<i>Glo1</i>	1497.09	-0.64	0.64	0.11	-5.57	2.50E-08	2.85E-06
FBgn0265191	<i>Glycogenin</i>	2359.74	-0.24	0.85	0.07	-3.23	1.26E-03	2.53E-02
FBgn0004507	<i>GlyP</i>	6246.58	-0.46	0.73	0.11	-4.33	1.46E-05	6.46E-04
FBgn0022160	<i>Gpo-1</i>	153.74	-0.81	0.57	0.16	-4.91	9.13E-07	5.75E-05
FBgn0260798	<i>Gprk1</i>	4061.31	0.38	1.30	0.10	3.96	7.58E-05	2.50E-03
FBgn0035167	<i>Gr61a</i>	71.84	-0.68	0.62	0.18	-3.72	2.02E-04	5.72E-03
FBgn0027590	<i>GstE12</i>	3648.07	-0.34	0.79	0.10	-3.33	8.64E-04	1.92E-02
FBgn0033381	<i>GstE13</i>	1835.98	-0.39	0.76	0.10	-3.93	8.41E-05	2.69E-03
FBgn0063492	<i>GstE8</i>	103.49	-0.54	0.69	0.18	-2.99	2.77E-03	4.52E-02
FBgn0010226	<i>GstS1</i>	14064.05	-0.36	0.78	0.08	-4.52	6.07E-06	3.06E-04

FBgn0041630	<i>Hexo1</i>	5696.62	-0.37	0.77	0.11	-3.27	1.09E-03	2.26E-02
FBgn0014857	<i>His3.3A</i>	6092.03	-0.38	0.77	0.08	-4.72	2.37E-06	1.32E-04
FBgn0013981	<i>His4r</i>	23601.99	-0.35	0.78	0.08	-4.48	7.55E-06	3.69E-04
FBgn0035829	<i>HP4</i>	1674.77	-0.25	0.84	0.08	-3.16	1.59E-03	3.02E-02
FBgn0264562	<i>Hr4</i>	2937.14	0.56	1.48	0.18	3.20	1.39E-03	2.77E-02
FBgn0001225	<i>Hsp26</i>	21697.61	0.45	1.37	0.15	3.12	1.83E-03	3.33E-02
FBgn0026417	<i>Hus1-like</i>	262.87	0.56	1.47	0.17	3.27	1.07E-03	2.25E-02
FBgn0031294	<i>IA-2</i>	52.54	0.44	1.36	0.14	3.15	1.65E-03	3.09E-02
FBgn0001253	<i>ImpE1</i>	13163.28	0.44	1.36	0.14	3.22	1.28E-03	2.56E-02
FBgn0025582	<i>Int6</i>	15170.00	0.52	1.44	0.06	9.37	7.28E-21	4.32E-18
FBgn0025366	<i>Ip259</i>	11691.43	0.43	1.35	0.07	6.20	5.61E-10	8.97E-08
FBgn0266375	<i>IP3K2</i>	1436.59	0.44	1.36	0.09	5.07	3.96E-07	2.84E-05
FBgn0016672	<i>lpp</i>	924.46	-0.34	0.79	0.12	-2.97	2.95E-03	4.71E-02
FBgn0259683	<i>Ir40a</i>	66.86	0.70	1.63	0.19	3.78	1.60E-04	4.66E-03
FBgn0034005	<i>ItgaPS4</i>	66.90	0.84	1.78	0.17	4.90	9.39E-07	5.87E-05
FBgn0040309	<i>Jafrac1</i>	12374.11	-0.25	0.84	0.06	-4.20	2.69E-05	1.07E-03
FBgn0051363	<i>Jupiter</i>	10894.71	0.25	1.19	0.08	3.21	1.35E-03	2.69E-02
FBgn0001323	<i>knrl</i>	769.44	0.41	1.33	0.13	3.16	1.59E-03	3.02E-02
FBgn0028336	<i>l(1)G0255</i>	5332.46	-0.56	0.68	0.11	-5.17	2.37E-07	1.81E-05
FBgn0011297	<i>l(2)not</i>	370.66	-0.38	0.77	0.13	-2.98	2.93E-03	4.68E-02
FBgn0010397	<i>LamC</i>	1672.94	-0.38	0.77	0.12	-3.02	2.52E-03	4.22E-02
FBgn0040102	<i>lectin-24Db</i>	145.31	0.58	1.50	0.18	3.17	1.51E-03	2.91E-02
FBgn0034877	<i>levy</i>	2953.90	-0.66	0.63	0.13	-5.19	2.13E-07	1.67E-05
FBgn0052699	<i>LPCAT</i>	1733.43	0.22	1.17	0.07	3.35	8.16E-04	1.84E-02
FBgn0010602	<i>lwr</i>	9316.09	-0.21	0.86	0.07	-3.04	2.35E-03	4.03E-02
FBgn0002736	<i>mago</i>	3178.11	-0.48	0.72	0.08	-5.92	3.26E-09	4.44E-07
FBgn0002643	<i>mam</i>	4899.49	0.33	1.26	0.09	3.71	2.07E-04	5.84E-03
FBgn0260986	<i>mei-38</i>	711.96	-0.44	0.74	0.14	-3.12	1.79E-03	3.27E-02
FBgn0030731	<i>Mfe2</i>	3408.49	-0.36	0.78	0.12	-3.08	2.09E-03	3.66E-02
FBgn0019985	<i>mGluR</i>	74.17	1.58	2.98	0.19	8.46	2.61E-17	1.20E-14
FBgn0025814	<i>Mgstl</i>	228.68	-0.54	0.69	0.14	-3.79	1.49E-04	4.45E-03
FBgn0027111	<i>mip1e1</i>	2351.78	-0.25	0.84	0.07	-3.66	2.56E-04	6.97E-03
FBgn0002772	<i>Mlc1</i>	149.27	-0.87	0.55	0.18	-4.77	1.85E-06	1.08E-04
FBgn0002773	<i>Mlc2</i>	713.36	-0.93	0.52	0.18	-5.21	1.87E-07	1.52E-05
FBgn0259209	<i>Mlp60A</i>	50.35	-0.58	0.67	0.18	-3.33	8.72E-04	1.93E-02
FBgn0002789	<i>Mp20</i>	169.65	-0.49	0.71	0.17	-2.97	2.99E-03	4.75E-02
FBgn0261380	<i>mRpL37</i>	1686.22	-0.40	0.76	0.09	-4.55	5.40E-06	2.77E-04
FBgn0036486	<i>Msh6</i>	2000.93	-0.33	0.79	0.09	-3.66	2.56E-04	6.97E-03
FBgn0028479	<i>Mtpalpha</i>	10743.30	-0.37	0.77	0.07	-5.26	1.41E-07	1.21E-05
FBgn0260795	<i>NaPI-III</i>	1792.06	-0.21	0.87	0.07	-2.98	2.87E-03	4.62E-02
FBgn0031228	<i>ND-15</i>	1942.86	-0.33	0.80	0.08	-3.91	9.29E-05	2.95E-03
FBgn0266582	<i>ND-30</i>	2102.21	-0.40	0.76	0.09	-4.45	8.46E-06	4.09E-04
FBgn0034645	<i>ND-B12</i>	1243.82	-0.68	0.63	0.10	-6.86	6.67E-12	1.46E-09
FBgn0033570	<i>ND-B14</i>	934.24	-0.36	0.78	0.10	-3.65	2.67E-04	7.17E-03
FBgn0025839	<i>ND-B14.5A</i>	466.60	-0.60	0.66	0.15	-3.93	8.39E-05	2.69E-03
FBgn0034576	<i>ND-B14.7</i>	1503.98	-0.30	0.81	0.08	-3.59	3.37E-04	8.67E-03
FBgn0033961	<i>ND-B15</i>	741.63	-0.43	0.74	0.14	-3.01	2.64E-03	4.37E-02
FBgn0029868	<i>ND-B16.6</i>	2329.06	-0.27	0.83	0.09	-3.07	2.17E-03	3.78E-02
FBgn0001989	<i>ND-B17</i>	1205.08	-0.49	0.71	0.13	-3.85	1.20E-04	3.70E-03
FBgn0030605	<i>ND-B18</i>	928.35	-0.39	0.77	0.12	-3.27	1.09E-03	2.26E-02
FBgn0083167	<i>Neb-cGP</i>	2319.90	-0.51	0.70	0.09	-5.47	4.59E-08	4.83E-06
FBgn0261673	<i>nemy</i>	494.68	0.53	1.45	0.13	4.14	3.45E-05	1.30E-03
FBgn0051658	<i>Nnf1b</i>	221.69	-0.44	0.74	0.14	-3.14	1.69E-03	3.14E-02
FBgn0028473	<i>Non1</i>	29641.95	0.95	1.94	0.10	9.81	1.06E-22	8.83E-20
FBgn0035370	<i>Non2</i>	14963.12	-0.40	0.76	0.10	-4.09	4.22E-05	1.52E-03
FBgn0033224	<i>Nop17l</i>	4164.06	-0.25	0.84	0.09	-2.99	2.83E-03	4.58E-02
FBgn0044028	<i>Notum</i>	1563.63	0.25	1.19	0.08	2.98	2.91E-03	4.67E-02
FBgn0027785	<i>NP15.6</i>	1433.72	-0.52	0.70	0.13	-3.89	1.00E-04	3.16E-03
FBgn0034243	<i>Ns2</i>	4616.78	0.36	1.28	0.07	5.09	3.67E-07	2.65E-05
FBgn0013718	<i>nuf</i>	4561.12	0.19	1.14	0.06	3.15	1.61E-03	3.04E-02
FBgn0039852	<i>nyo</i>	3825.54	0.37	1.29	0.11	3.24	1.19E-03	2.42E-02
FBgn0004646	<i>ogre</i>	22128.58	0.33	1.26	0.07	4.68	2.82E-06	1.54E-04
FBgn0033179	<i>p47</i>	3163.77	-0.33	0.79	0.10	-3.19	1.44E-03	2.83E-02
FBgn0037138	<i>P5CDh1</i>	3158.58	-0.54	0.69	0.10	-5.34	9.35E-08	9.15E-06
FBgn0010247	<i>Parp</i>	3156.06	-0.71	0.61	0.07	-9.64	5.41E-22	3.75E-19
FBgn0036271	<i>Pbgs</i>	964.74	-0.27	0.83	0.09	-3.11	1.90E-03	3.41E-02
FBgn0024841	<i>Pcd</i>	996.68	-0.46	0.73	0.09	-4.95	7.46E-07	4.92E-05
FBgn0086768	<i>Pcmt</i>	2230.67	-0.32	0.80	0.08	-4.14	3.46E-05	1.30E-03
FBgn0020386	<i>Pdk1</i>	3334.40	0.42	1.33	0.11	3.63	2.85E-04	7.55E-03
FBgn0031969	<i>pes</i>	688.32	0.44	1.36	0.14	3.26	1.11E-03	2.30E-02
FBgn0003071	<i>Pfk</i>	4337.01	-0.32	0.80	0.11	-2.96	3.10E-03	4.88E-02
FBgn0004654	<i>Pgd</i>	1849.81	-0.40	0.76	0.13	-3.03	2.44E-03	4.14E-02
FBgn0003074	<i>Pgi</i>	5000.56	-0.32	0.80	0.09	-3.51	4.48E-04	1.12E-02
FBgn0250906	<i>Pgk</i>	8014.32	-0.38	0.77	0.13	-3.01	2.60E-03	4.32E-02
FBgn0014869	<i>Pglym78</i>	2302.32	-0.36	0.78	0.08	-4.32	1.59E-05	6.92E-04
FBgn0035975	<i>PGRP-LA</i>	93.55	0.58	1.50	0.18	3.27	1.07E-03	2.25E-02
FBgn0035089	<i>Phk-3</i>	5938.78	0.32	1.25	0.08	4.08	4.51E-05	1.62E-03
FBgn0003089	<i>pip</i>	831.18	0.59	1.51	0.12	4.95	7.52E-07	4.92E-05
FBgn0086706	<i>pix</i>	14805.10	0.68	1.60	0.08	8.45	2.88E-17	1.26E-14
FBgn0000489	<i>Pka-C3</i>	284.35	0.60	1.52	0.15	3.97	7.30E-05	2.43E-03
FBgn0036354	<i>Poc1</i>	2132.05	-0.43	0.74	0.10	-4.43	9.47E-06	4.50E-04
FBgn0032884	<i>Pomp</i>	2399.10	-0.44	0.74	0.12	-3.79	1.51E-04	4.48E-03
FBgn0065109	<i>ppk11</i>	42.17	1.64	3.12	0.18	9.01	1.98E-19	1.10E-16
FBgn0003149	<i>Prm</i>	139.55	-0.50	0.71	0.17	-3.00	2.69E-03	4.43E-02

FBgn0010590	<i>Prosbeta1</i>	4597.67	-0.30	0.81	0.09	-3.27	1.09E-03	2.26E-02
FBgn0029134	<i>Prosbeta5</i>	6998.02	-0.26	0.84	0.09	-2.99	2.76E-03	4.51E-02
FBgn0031888	<i>Pvf2</i>	843.20	0.34	1.27	0.11	3.18	1.50E-03	2.91E-02
FBgn0032006	<i>Pvr</i>	2461.55	0.28	1.21	0.08	3.31	9.36E-04	2.04E-02
FBgn0267385	<i>PyK</i>	7962.85	-0.45	0.73	0.11	-3.95	7.90E-05	2.58E-03
FBgn0025382	<i>Rab27</i>	380.56	-0.57	0.67	0.17	-3.28	1.05E-03	2.22E-02
FBgn0020618	<i>Rack1</i>	108044.76	0.24	1.18	0.07	3.16	1.59E-03	3.02E-02
FBgn0024194	<i>rasp</i>	1399.19	-0.42	0.75	0.08	-5.14	2.75E-07	2.08E-05
FBgn0260944	<i>Rbp1</i>	3489.56	-0.41	0.75	0.08	-5.41	6.46E-08	6.71E-06
FBgn0031047	<i>Rcd-1</i>	6419.61	-0.27	0.83	0.07	-3.57	3.58E-04	9.16E-03
FBgn0014018	<i>Rel</i>	2585.88	0.33	1.26	0.11	3.15	1.65E-03	3.09E-02
FBgn0035574	<i>RhoGEF64C</i>	2431.40	1.26	2.39	0.15	8.19	2.66E-16	1.10E-13
FBgn0025638	<i>Roc1a</i>	4815.17	-0.34	0.79	0.08	-4.10	4.06E-05	1.48E-03
FBgn0019661	<i>roX1</i>	536.01	-1.31	0.40	0.19	-7.08	1.39E-12	3.51E-10
FBgn0050410	<i>Rpi</i>	1972.91	-0.60	0.66	0.14	-4.21	2.59E-05	1.04E-03
FBgn0036213	<i>RpL10Ab</i>	86319.81	0.30	1.23	0.08	3.83	1.30E-04	3.94E-03
FBgn0013325	<i>RpL11</i>	54882.19	0.26	1.20	0.09	2.97	2.98E-03	4.74E-02
FBgn0017579	<i>RpL14</i>	51999.57	0.28	1.22	0.09	3.05	2.32E-03	3.99E-02
FBgn0028697	<i>RpL15</i>	75087.76	0.53	1.44	0.10	5.30	1.13E-07	1.05E-05
FBgn0032987	<i>RpL21</i>	65075.97	0.36	1.29	0.12	3.15	1.62E-03	3.05E-02
FBgn0037899	<i>RpL24-like</i>	6383.75	0.51	1.42	0.10	5.35	8.78E-08	8.89E-06
FBgn0261606	<i>RpL27A</i>	69353.82	0.27	1.21	0.08	3.41	6.46E-04	1.52E-02
FBgn0031980	<i>RpL36A</i>	43049.97	0.33	1.26	0.08	4.26	2.04E-05	8.49E-04
FBgn0030616	<i>RpL37a</i>	52720.94	0.21	1.16	0.07	3.05	2.30E-03	3.96E-02
FBgn0003941	<i>RpL40</i>	55101.10	0.28	1.22	0.07	4.21	2.57E-05	1.04E-03
FBgn0064225	<i>RpL5</i>	133711.28	0.56	1.48	0.10	5.79	7.13E-09	8.98E-07
FBgn0005593	<i>RpL7</i>	100024.84	0.44	1.36	0.07	6.46	1.04E-10	1.84E-08
FBgn0014026	<i>RpL7A</i>	101970.39	0.29	1.22	0.09	3.18	1.48E-03	2.88E-02
FBgn0015756	<i>RpL9</i>	71791.35	0.35	1.28	0.08	4.39	1.14E-05	5.26E-04
FBgn0002593	<i>RpLP1</i>	68944.05	0.33	1.25	0.10	3.36	7.89E-04	1.80E-02
FBgn0033699	<i>RpS11</i>	62512.25	0.22	1.17	0.06	3.88	1.05E-04	3.28E-03
FBgn0034138	<i>RpS15</i>	65162.92	0.27	1.20	0.08	3.33	8.59E-04	1.92E-02
FBgn0033555	<i>RpS15Ab</i>	2360.75	-0.70	0.62	0.09	-7.46	8.81E-14	2.53E-11
FBgn0005533	<i>RpS17</i>	55216.40	0.24	1.18	0.06	4.14	3.40E-05	1.30E-03
FBgn0010411	<i>RpS18</i>	62131.21	0.26	1.20	0.07	3.99	6.74E-05	2.28E-03
FBgn0019936	<i>RpS20</i>	48027.62	0.32	1.25	0.08	4.04	5.30E-05	1.83E-03
FBgn0033912	<i>RpS23</i>	69519.69	0.26	1.20	0.08	3.37	7.52E-04	1.73E-02
FBgn0261596	<i>RpS24</i>	61495.83	0.36	1.28	0.07	5.09	3.60E-07	2.63E-05
FBgn0039300	<i>RpS27</i>	34477.47	0.36	1.28	0.11	3.34	8.42E-04	1.89E-02
FBgn0261599	<i>RpS29</i>	61259.15	0.30	1.23	0.07	4.25	2.13E-05	8.77E-04
FBgn0017545	<i>RpS3A</i>	109993.41	0.54	1.45	0.08	7.01	2.33E-12	5.37E-10
FBgn0011284	<i>RpS4</i>	118668.08	0.36	1.29	0.07	5.47	4.56E-08	4.83E-06
FBgn0033785	<i>Sans</i>	2754.64	0.25	1.19	0.08	2.99	2.79E-03	4.54E-02
FBgn0035298	<i>SCOT</i>	1243.90	-0.35	0.79	0.11	-3.12	1.82E-03	3.33E-02
FBgn0035390	<i>scramb2</i>	5447.56	-0.29	0.82	0.05	-5.30	1.15E-07	1.05E-05
FBgn0004888	<i>Scsalpha</i>	5210.54	-0.30	0.81	0.10	-3.11	1.85E-03	3.35E-02
FBgn0021765	<i>scu</i>	3968.02	-0.56	0.68	0.14	-4.14	3.41E-05	1.30E-03
FBgn0041094	<i>scyl</i>	16134.28	-0.21	0.87	0.06	-3.76	1.71E-04	4.94E-03
FBgn0037873	<i>SdhC</i>	2051.63	-0.43	0.74	0.10	-4.14	3.46E-05	1.30E-03
FBgn0039112	<i>SdhD</i>	1328.56	-0.44	0.74	0.10	-4.20	2.68E-05	1.07E-03
FBgn0038279	<i>Sdr</i>	1146.56	-0.34	0.79	0.11	-3.07	2.16E-03	3.77E-02
FBgn0036804	<i>Sgf11</i>	584.55	-0.32	0.80	0.11	-2.99	2.81E-03	4.57E-02
FBgn0029761	<i>SK</i>	189.42	-0.63	0.65	0.18	-3.45	5.60E-04	1.35E-02
FBgn0052484	<i>Sk2</i>	1628.15	-0.44	0.74	0.12	-3.53	4.14E-04	1.05E-02
FBgn0264087	<i>Slob</i>	27.46	0.66	1.58	0.18	3.64	2.77E-04	7.38E-03
FBgn0011288	<i>Snap25</i>	61.92	1.21	2.31	0.19	6.50	8.12E-11	1.49E-08
FBgn0003462	<i>Sod</i>	6851.22	-0.43	0.74	0.09	-4.96	7.10E-07	4.72E-05
FBgn0010213	<i>Sod2</i>	3127.27	-0.30	0.81	0.07	-4.20	2.72E-05	1.07E-03
FBgn0033631	<i>Sod3</i>	7079.95	-0.21	0.86	0.05	-3.93	8.34E-05	2.69E-03
FBgn0035710	<i>SP1173</i>	2902.42	-0.48	0.72	0.10	-4.65	3.35E-06	1.80E-04
FBgn0026562	<i>SPARC</i>	1637.75	-0.60	0.66	0.14	-4.31	1.67E-05	7.14E-04
FBgn0260440	<i>spdo</i>	99.45	0.54	1.46	0.18	3.08	2.08E-03	3.66E-02
FBgn0039795	<i>Spn100A</i>	4240.24	0.59	1.50	0.18	3.26	1.13E-03	2.32E-02
FBgn0033115	<i>Spn42De</i>	188.42	-0.59	0.67	0.15	-3.85	1.19E-04	3.68E-03
FBgn0024294	<i>Spn43Aa</i>	8370.63	0.37	1.30	0.11	3.29	1.02E-03	2.17E-02
FBgn0015818	<i>Spx</i>	1872.48	-0.35	0.79	0.10	-3.38	7.22E-04	1.67E-02
FBgn0031959	<i>spz3</i>	675.01	-0.44	0.74	0.11	-3.97	7.27E-05	2.43E-03
FBgn0014388	<i>sty</i>	2462.67	0.33	1.26	0.11	3.10	1.97E-03	3.50E-02
FBgn0040271	<i>Sulf1</i>	2986.73	0.35	1.27	0.08	4.07	4.62E-05	1.63E-03
FBgn0014391	<i>sun</i>	2386.92	-0.49	0.71	0.12	-4.14	3.42E-05	1.30E-03
FBgn0028563	<i>sut1</i>	1867.51	-0.33	0.79	0.08	-4.22	2.41E-05	9.84E-04
FBgn0023477	<i>Taldo</i>	5484.15	-0.32	0.80	0.08	-4.26	2.09E-05	8.63E-04
FBgn0033902	<i>Tango7</i>	15108.46	0.45	1.37	0.07	6.59	4.44E-11	9.00E-09
FBgn0021795	<i>Tapdelta</i>	6465.38	-0.34	0.79	0.08	-4.01	6.02E-05	2.06E-03
FBgn0037874	<i>Tctp</i>	52182.75	0.30	1.23	0.06	5.19	2.06E-07	1.63E-05
FBgn0041183	<i>Tep1</i>	241.11	0.54	1.45	0.17	3.20	1.36E-03	2.71E-02
FBgn0034223	<i>Tes</i>	2276.53	-0.26	0.83	0.09	-3.00	2.68E-03	4.42E-02
FBgn0031975	<i>Tg</i>	77.05	0.65	1.57	0.18	3.65	2.65E-04	7.15E-03
FBgn0025352	<i>Thiolase</i>	6056.94	-0.34	0.79	0.09	-3.78	1.56E-04	4.57E-03
FBgn0003716	<i>tkv</i>	16567.46	0.22	1.17	0.06	3.47	5.19E-04	1.26E-02
FBgn0262473	<i>Tl</i>	2135.92	0.29	1.22	0.09	3.02	2.51E-03	4.22E-02
FBgn0004117	<i>Tm2</i>	151.96	-0.69	0.62	0.18	-3.79	1.50E-04	4.46E-03
FBgn0262624	<i>Tmhs</i>	1100.41	0.36	1.29	0.10	3.73	1.93E-04	5.53E-03
FBgn0033357	<i>Tom7</i>	1896.66	-0.45	0.73	0.12	-3.94	8.18E-05	2.66E-03

FBgn0003733	<i>tor</i>	91.78	-1.58	0.33	0.18	-8.86	8.18E-19	4.25E-16
FBgn0086355	<i>Tpi</i>	4134.27	-0.68	0.62	0.15	-4.42	9.69E-06	4.55E-04
FBgn0015834	<i>Trip1</i>	14850.22	0.30	1.23	0.06	5.22	1.81E-07	1.51E-05
FBgn0031760	<i>Tsp26A</i>	959.34	-0.27	0.83	0.09	-2.96	3.04E-03	4.81E-02
FBgn0034046	<i>tun</i>	2553.39	-0.46	0.73	0.09	-5.18	2.18E-07	1.70E-05
FBgn0263697	<i>Uba3</i>	1510.14	-0.22	0.86	0.07	-3.08	2.09E-03	3.66E-02
FBgn0015321	<i>Ubc4</i>	2227.19	-0.28	0.82	0.08	-3.31	9.40E-04	2.04E-02
FBgn0040091	<i>Ugt58Fa</i>	714.33	-0.38	0.77	0.12	-3.27	1.09E-03	2.26E-02
FBgn0040251	<i>Ugt86Di</i>	2430.39	0.71	1.63	0.11	6.57	5.14E-11	9.94E-09
FBgn0003950	<i>unc</i>	327.06	1.54	2.91	0.14	10.93	8.62E-28	1.02E-24
FBgn0025726	<i>unc-13</i>	6249.12	0.57	1.49	0.15	3.83	1.28E-04	3.90E-03
FBgn0010812	<i>unc-45</i>	2166.48	0.31	1.24	0.07	4.21	2.56E-05	1.04E-03
FBgn0004169	<i>up</i>	334.67	-0.72	0.61	0.18	-3.93	8.35E-05	2.69E-03
FBgn0033428	<i>Updo</i>	2316.12	-0.33	0.79	0.11	-3.17	1.50E-03	2.91E-02
FBgn0036728	<i>UQCR-Q</i>	2124.47	-0.65	0.64	0.09	-7.70	1.37E-14	4.75E-12
FBgn0029819	<i>Usp30</i>	1715.03	-0.27	0.83	0.09	-2.98	2.86E-03	4.61E-02
FBgn0004055	<i>uzip</i>	2158.68	0.26	1.20	0.08	3.08	2.04E-03	3.61E-02
FBgn0035103	<i>Vdup1</i>	6977.52	-0.24	0.85	0.06	-3.72	1.99E-04	5.67E-03
FBgn0262524	<i>ver</i>	310.89	0.38	1.30	0.12	3.04	2.35E-03	4.03E-02
FBgn0026753	<i>Vha13</i>	2257.45	-0.44	0.74	0.06	-7.08	1.48E-12	3.52E-10
FBgn0016078	<i>wun</i>	1328.21	0.28	1.22	0.09	3.25	1.17E-03	2.40E-02
FBgn0283471	<i>wupA</i>	185.42	-0.54	0.69	0.18	-3.04	2.37E-03	4.03E-02
FBgn0031972	<i>Wwox</i>	593.81	0.54	1.46	0.10	5.48	4.22E-08	4.56E-06
FBgn0261113	<i>Xrp1</i>	15232.79	0.32	1.25	0.10	3.29	9.93E-04	2.12E-02
FBgn0041713	<i>yellow-c</i>	32.15	-0.55	0.68	0.17	-3.17	1.50E-03	2.91E-02
FBgn0041711	<i>yellow-e</i>	311.79	-0.54	0.69	0.14	-3.95	7.66E-05	2.52E-03
FBgn0038150	<i>yellow-e3</i>	354.27	-1.02	0.49	0.12	-8.51	1.67E-17	8.15E-15
FBgn0045842	<i>yuri</i>	622.23	0.40	1.32	0.13	3.16	1.58E-03	3.02E-02
FBgn0260486	<i>Ziz</i>	1766.97	0.38	1.30	0.12	3.19	1.41E-03	2.79E-02
FBgn0037000	<i>ZnT77C</i>	483.55	0.42	1.34	0.14	3.14	1.68E-03	3.13E-02

Table S3: Measure of endogenous CycG expression by RT-qPCR.

AE: amplification efficiency. Expression of *RPL15*, *RPL7* and *Rack1* were normalized on the geometric mean of *Lam* and *rin*.

Primers	AE						
<i>3'UTR-G1</i>		1.9944					
<i>Lam</i>		1.9902					
<i>rin</i>		1.9962					
Amplicon	Genotype	mean Cq	AE ^Δ mean Cq	normalization/ <i>lam-rin</i>	mean	sd	
<i>CycG-3'UTR</i>	<i>da-Gal4/+ - 1</i>	23.26	9.41E+06	0.8503	0.8683	0.0254	
	<i>da-Gal4/+ - 2</i>	23.60	1.19E+07	0.8862			
Amplicon	Genotype	mean Cq	<i>Lam rin</i> geometric mean				
<i>Lam</i>	<i>da-Gal4/+ - 1</i>	22.96	8.00E+06				
	<i>da-Gal4/+ - 2</i>	23.19	1.05E+07				
<i>rin</i>	<i>da-Gal4/+ - 1</i>	23.13					
	<i>da-Gal4/+ - 2</i>	23.70					
Amplicon	Genotype	mean Cq	AE ^Δ mean Cq	normalization/ <i>lam-rin</i>	mean	sd	p-value
<i>CycG-3'UTR</i>	<i>da-Gal4. UAS-CycG^{ΔP}/+ - 1</i>	30.20	1.13E+09	0.1646	0.1384	0.0371	1.89E-03
	<i>da-Gal4. UAS-CycG^{ΔP}/+ - 2</i>	30.33	1.24E+09	0.1122			
Amplicon	Genotype	mean Cq	<i>Lam rin</i> geometric mean				
<i>Lam</i>	<i>da-Gal4. UAS-CycG^{ΔP}/+ - 1</i>	27.20	1.87E+08				
	<i>da-Gal4. UAS-CycG^{ΔP}/+ - 2</i>	26.95	1.39E+08				
<i>rin</i>	<i>da-Gal4. UAS-CycG^{ΔP}/+ - 1</i>	28.02					
	<i>da-Gal4. UAS-CycG^{ΔP}/+ - 2</i>	27.42					

Table S4: Ontology of genes deregulated in *UAS-CycG^{ΔP}*, *da-Gal4/+* wing imaginal discs.
Gene ontology analyses were performed with DAVID (<https://david.ncifcrf.gov/home.jsp>).

Up-regulated genes									
Annotation Cluster 1		Enrichment Score: 13.41							
Category	Term	Count	%	p-value	List Total	Pop Hits	Pop Total	Fold Enrichment	Bonferroni
GOTERM_BP_DIRECT	GO:0002181~cytoplasmic translation	26	12.04	7.69E-24	171	100	10996	16.72	4.20E-21
GOTERM_CC_DIRECT	GO:0005840~ribosome	21	9.72	1.82E-16	174	98	10026	12.35	2.82E-14
KEGG_PATHWAY	dme03010:Ribosome	26	12.04	2.38E-13	57	233	2752	5.39	8.10E-12
GOTERM_MF_DIRECT	GO:0003735~structural constituent of ribosome	26	12.04	1.68E-10	161	319	9284	4.70	3.27E-08
GOTERM_BP_DIRECT	GO:0006412~translation	27	12.50	1.68E-06	171	601	10996	2.89	9.17E-04
Annotation Cluster 2		Enrichment Score: 4.78							
Category	Term	Count	%	p-value	List Total	Pop Hits	Pop Total	Fold Enrichment	Bonferroni
GOTERM_CC_DIRECT	GO:0005852~eukaryotic translation initiation factor 3 complex	7	3.24	2.56E-07	174	17	10026	23.73	3.25E-05
GOTERM_CC_DIRECT	GO:0033290~eukaryotic 48S preinitiation complex	6	2.78	7.55E-06	174	17	10026	20.34	9.59E-04
GOTERM_BP_DIRECT	GO:0006446~regulation of translational initiation	6	2.78	1.07E-05	171	20	10996	19.29	5.82E-03
GOTERM_CC_DIRECT	GO:0016282~eukaryotic 43S preinitiation complex	6	2.78	1.81E-05	174	20	10026	17.29	2.30E-03
GOTERM_BP_DIRECT	GO:0001731~formation of translation preinitiation complex	6	2.78	2.79E-05	171	24	10996	16.08	1.51E-02
GOTERM_BP_DIRECT	GO:0006413~translational initiation	7	3.24	8.96E-05	171	48	10996	9.38	4.77E-02
GOTERM_MF_DIRECT	GO:0003743~translation initiation factor activity	7	3.24	3.80E-04	161	56	9284	7.21	7.14E-02
Down-regulated genes									
Annotation Cluster 1		Enrichment Score: 5.84							
Category	Term	Count	%	p-value	List Total	Pop Hits	Pop Total	Fold Enrichment	Bonferroni
GOTERM_CC_DIRECT	GO:0005751~mitochondrial respiratory chain complex IV	7	2.23	4.75E-07	243	14	10026	20.63	7.69E-05
GOTERM_MF_DIRECT	GO:0004129~cytochrome-c oxidase activity	8	2.55	1.78E-06	243	24	9284	12.74	4.90E-04
GOTERM_BP_DIRECT	GO:0006123~mitochondrial electron transport, cytochrome c to oxygen	6	1.91	3.53E-06	244	12	10996	22.53	1.76E-03

Table S5: Validation of RNA-seq experiments by RT-qPCR.

AE: amplification efficiency. Expression of *RPL15*, *RPL7* and *Rack1* were normalized on the geometric mean of *Lam* and *rin*.

Primers	AE
<i>RPL15</i>	1.9941
<i>RPL7</i>	2.0014
<i>Rack1</i>	2.0138
<i>Lam</i>	1.9902
<i>rin</i>	1.9962

Amplicon	Genotype	mean Cq	AE^mean Cq	normalization/ <i>lam-rin</i>	mean	sd
<i>RPL15</i>	<i>da-Gal4/+ - 1</i>	24.07	1.64E+07	0.4878	0.5756	0.1241
	<i>da-Gal4/+ - 2</i>	23.50	1.11E+07	0.6633		
<i>RPL7</i>	<i>da-Gal4/+ - 1</i>	20.87	1.94E+06	4.1149	4.0389	0.1074
	<i>da-Gal4/+ - 2</i>	20.80	1.85E+06	3.9630		
<i>Rack1</i>	<i>da-Gal4/+ - 1</i>	21.72	4.01E+06	1.9951	2.1187	0.1748
	<i>da-Gal4/+ - 2</i>	21.43	3.27E+06	2.2423		

Amplicon	Genotype	mean Cq	<i>Lam rin</i> geometric mean
<i>Lam</i>	<i>da-Gal4/+ - 1</i>	22.96	8.00E+06
	<i>da-Gal4/+ - 2</i>	22.81	7.34E+06
<i>rin</i>	<i>da-Gal4/+ - 1</i>	23.13	
	<i>da-Gal4/+ - 2</i>	23.03	

Amplicon	Genotype	mean Cq	AE^mean Cq	normalization/ <i>lam-rin</i>	mean	sd	p-value
<i>RPL15</i>	<i>da-Gal4, UAS-CycG^{AP}/+ - 1</i>	23.16	8.75E+06	21.3165	21.6519	0.4744	2.71E-04
	<i>da-Gal4, UAS-CycG^{AP}/+ - 2</i>	22.69	6.33E+06	21.9874			
<i>RPL7</i>	<i>da-Gal4, UAS-CycG^{AP}/+ - 1</i>	23.15	9.46E+06	19.7231	19.2369	0.6876	1.05E-03
	<i>da-Gal4, UAS-CycG^{AP}/+ - 2</i>	22.80	7.42E+06	18.7507			
<i>Rack1</i>	<i>da-Gal4, UAS-CycG^{AP}/+ - 1</i>	22.72	8.08E+06	23.0995	25.3168	3.1357	9.04E-03
	<i>da-Gal4, UAS-CycG^{AP}/+ - 2</i>	22.05	5.05E+06	27.5341			

Amplicon	Genotype	mean Cq	<i>Lam rin</i> geometric mean
<i>Lam</i>	<i>da-Gal4, UAS-CycG^{AP}/+ - 1</i>	27.20	1.87E+08
	<i>da-Gal4, UAS-CycG^{AP}/+ - 2</i>	26.95	1.39E+08
<i>rin</i>	<i>da-Gal4, UAS-CycG^{AP}/+ - 1</i>	28.02	
	<i>da-Gal4, UAS-CycG^{AP}/+ - 2</i>	27.42	

Table S6: List of the 889 genes bound by Cyclin G in wing imaginal discs.

Gene ID	Gene name	Location	Peak coordinates		Strand
FBgn0011710	<i>Sep1</i>	X	21358286	21361688	+
FBgn0020238	<i>14-3-3epsilon</i>	3R	18242531	18250550	+
FBgn0260793	<i>2mit</i>	3R	13121951	13155687	-
FBgn0052016	<i>4E-T</i>	4	951542	958392	-
FBgn0053100	<i>4EHP</i>	3R	24063077	24108960	-
FBgn0261929	<i>5-HT2B</i>	3R	8578205	8629996	+
FBgn0000017	<i>Abl</i>	3L	16615866	16647882	-
FBgn0024150	<i>Ac78C</i>	3L	21136447	21171930	-
FBgn0038363	<i>Acyp2</i>	3R	15792688	15793487	+
FBgn0262739	<i>AGO1</i>	2R	13943387	13958089	-
FBgn0250816	<i>AGO3</i>	3L	23554593	23689640	+
FBgn0010548	<i>Aldh-III</i>	2R	7466879	7477162	-
FBgn0086361	<i>alph</i>	3R	29591831	29617157	+
FBgn0010215	<i>alpha-Cat</i>	3L	23318646	23338100	-
FBgn0039378	<i>alpha4GT2</i>	3R	25832230	25842878	+
FBgn0003884	<i>alphaTub84B</i>	3R	7086599	7088839	+
FBgn0038535	<i>alt</i>	3R	17673732	17682515	-
FBgn0052626	<i>AMPdeam</i>	X	13830741	13845866	-
FBgn0266111	<i>ana3</i>	2R	12344983	12351325	+
FBgn0025111	<i>Ant2</i>	X	10778954	10786907	-
FBgn0000108	<i>Appl</i>	X	530501	579044	+
FBgn0039889	<i>Arl4</i>	4	177348	179389	-
FBgn0001961	<i>Arpc1</i>	2L	13827941	13829741	-
FBgn0000119	<i>arr</i>	2R	13453640	13483229	-
FBgn0032329	<i>Art8</i>	2L	11009821	11011086	-
FBgn0039908	<i>Asator</i>	4	469409	488994	-
FBgn0034606	<i>ASPP</i>	2R	21217856	21251150	-
FBgn0015905	<i>ast</i>	2L	1077948	1080803	+
FBgn0266429	<i>AstA-R1</i>	X	3574536	3666724	+
FBgn0261823	<i>Asx</i>	2R	14503958	14512493	+
FBgn0029943	<i>Atg5</i>	X	7314622	7323770	-
FBgn0052672	<i>Atg8a</i>	X	10764878	10768338	-
FBgn0039213	<i>atl</i>	3R	24625671	24634714	+
FBgn0052446	<i>Atox1</i>	3L	21640995	21642599	+
FBgn0002921	<i>Atpalpha</i>	3R	20948714	20976239	+
FBgn0039830	<i>ATPsynC</i>	3R	31216145	31219630	-
FBgn0035032	<i>ATPsynF</i>	2R	24599088	24599821	-
FBgn0041188	<i>Atx2</i>	3R	15408423	15417277	+
FBgn0037218	<i>aux</i>	3R	4211783	4227518	+
FBgn0050476	<i>ave</i>	2R	14752521	14753269	+
FBgn0026597	<i>Axn</i>	3R	30022842	30035311	+
FBgn0000152	<i>Axs</i>	X	16680089	16683895	-
FBgn0004870	<i>bab1</i>	3L	1036369	1101089	-
FBgn0027889	<i>ball</i>	3R	26864605	26866807	-
FBgn0000163	<i>baz</i>	X	17160006	17200705	+
FBgn0033844	<i>bbc</i>	2R	13486634	13494862	-
FBgn0087007	<i>bbg</i>	3L	14412828	14536276	-
FBgn0034049	<i>bdg</i>	2R	15923040	15931935	-
FBgn0038498	<i>beat-Ila</i>	3R	17320004	17366119	-
FBgn0038092	<i>beat-Vb</i>	3R	12916056	12934813	+
FBgn0263231	<i>bel</i>	3R	8654975	8660761	-
FBgn0260859	<i>Bet3</i>	3L	9438482	9442267	-
FBgn0039175	<i>beta-PheRS</i>	3R	24250460	24252679	-
FBgn0008635	<i>betaCOP</i>	X	18381549	18385242	-
FBgn0004581	<i>bgn</i>	2R	23853270	23858921	-
FBgn0036199	<i>Bmcp</i>	3L	11720934	11728118	+
FBgn0086694	<i>Bre1</i>	3L	5789831	5794192	-
FBgn0000221	<i>brn</i>	X	4104342	4105791	+
FBgn0264001	<i>bru-3</i>	3L	13521907	13803400	-
FBgn0266717	<i>Bruce</i>	3R	10312039	10331353	-
FBgn0004101	<i>bs</i>	2R	24342861	24376473	+
FBgn0030228	<i>BTBD9</i>	X	10768537	10772154	+
FBgn0023096	<i>btv</i>	2L	17962625	17982472	-
FBgn0259176	<i>bun</i>	2L	12455540	12546611	-
FBgn0000241	<i>bw</i>	2R	23527805	23538499	-
FBgn0040236	<i>c11.1</i>	X	9275318	9283117	-
FBgn0040235	<i>c12.1</i>	X	9317915	9319223	-
FBgn0040234	<i>c12.2</i>	X	9319359	9324458	+
FBgn0259228	<i>C3G</i>	X	6780790	6803593	-
FBgn0015609	<i>CadN</i>	2L	17647053	17778340	-
FBgn0053653	<i>Cadps</i>	4	1230837	1271759	+
FBgn0030054	<i>Caf1-180</i>	X	8602137	8606304	-
FBgn0012051	<i>CalpA</i>	2R	19425113	19430564	+

FBgn0037831	<i>Cap-H2</i>	3R	10761310	10766756	+
FBgn0020224	<i>Cbl</i>	3L	8424954	8432246	+
FBgn0052183	<i>Ccn</i>	3L	17690015	17748839	+
FBgn0051973	<i>Cda5</i>	2L	25402	65404	-
FBgn0004107	<i>Cdk2</i>	3R	20735623	20738414	+
FBgn0030269	<i>CDK2AP1</i>	X	11137859	11139689	+
FBgn0028509	<i>CenG1A</i>	2L	13835564	13898712	+
FBgn0027569	<i>cert</i>	3L	8282528	8289870	-
FBgn0039590	<i>CG10011</i>	3R	28607939	28635099	-
FBgn0039084	<i>CG10175</i>	3R	23522264	23530986	-
FBgn0032796	<i>CG10188</i>	2L	19502335	19508764	-
FBgn0033019	<i>CG10395</i>	2R	5350477	5351972	+
FBgn0033021	<i>CG10417</i>	2R	5360331	5363104	-
FBgn0034570	<i>CG10543</i>	2R	20996220	21007740	+
FBgn0032717	<i>CG10600</i>	2L	18833710	18839679	-
FBgn0032721	<i>CG10602</i>	2L	18855126	18859248	-
FBgn0036286	<i>CG10616</i>	3L	12471728	12474428	+
FBgn0029980	<i>CG10778</i>	X	7931745	7933351	-
FBgn0031395	<i>CG10874</i>	2L	2189914	2192386	-
FBgn0038769	<i>CG10889</i>	3R	20033881	20036056	-
FBgn0034307	<i>CG10914</i>	2R	18158257	18160310	+
FBgn0032857	<i>CG10947</i>	2L	20385293	20414800	-
FBgn0030400	<i>CG11138</i>	X	12569169	12583193	-
FBgn0039936	<i>CG11148</i>	4	853557	867025	-
FBgn0037279	<i>CG1129</i>	3R	4811444	4816025	+
FBgn0039920	<i>CG11360</i>	4	671142	690650	+
FBgn0026876	<i>CG11403</i>	X	1236873	1239884	-
FBgn0029715	<i>CG11444</i>	X	4553117	4554398	-
FBgn0038683	<i>CG11779</i>	3R	19154097	19159878	-
FBgn0030346	<i>CG11802</i>	X	11871299	11872779	-
FBgn0039293	<i>CG11851</i>	3R	25221589	25224118	+
FBgn0039635	<i>CG11876</i>	3R	29113071	29116197	+
FBgn0039642	<i>CG11882</i>	3R	29147016	29148172	-
FBgn0033538	<i>CG11883</i>	2R	10617662	10641807	+
FBgn0037644	<i>CG11964</i>	3R	8942954	8945020	-
FBgn0035285	<i>CG12025</i>	3L	1865430	1869491	+
FBgn0030052	<i>CG12065</i>	X	8574306	8588528	+
FBgn0260742	<i>CG12213</i>	3R	11964674	11967691	-
FBgn0029822	<i>CG12236</i>	X	5908135	5913079	+
FBgn0029930	<i>CG12541</i>	X	7021608	7066052	-
FBgn0030055	<i>CG12772</i>	X	8677063	8680912	+
FBgn0039523	<i>CG12885</i>	3R	27520866	27533934	+
FBgn0037065	<i>CG12974</i>	3L	21281752	21285962	-
FBgn0037061	<i>CG12975</i>	3L	21215995	21216839	-
FBgn0040877	<i>CG12994</i>	X	17422320	17443994	-
FBgn0032050	<i>CG13096</i>	2L	8509069	8511866	-
FBgn0036406	<i>CG13484</i>	3L	14052428	14053079	-
FBgn0040658	<i>CG13516</i>	2R	22669145	22670622	+
FBgn0030151	<i>CG1354</i>	X	9778742	9782094	+
FBgn0040660	<i>CG13551</i>	2R	23377866	23383424	-
FBgn0033374	<i>CG13741</i>	2R	9092506	9094658	-
FBgn0035237	<i>CG13917</i>	3L	1576699	1600845	+
FBgn0035287	<i>CG13937</i>	3L	1876551	1883041	-
FBgn0033405	<i>CG13954</i>	2R	9309296	9389467	-
FBgn0036851	<i>CG14082</i>	3L	19105381	19138975	-
FBgn0031023	<i>CG14200</i>	X	19495505	19518402	+
FBgn0039462	<i>CG14252</i>	3R	26945534	26947248	+
FBgn0038629	<i>CG14304</i>	3R	18592801	18621327	-
FBgn0037171	<i>CG14459</i>	3L	22573114	22637916	-
FBgn0033000	<i>CG14464</i>	2R	4829246	4830587	+
FBgn0037920	<i>CG14710</i>	3R	11620090	11621728	+
FBgn0025393	<i>CG14795</i>	X	1512227	1512803	-
FBgn0041702	<i>CG15107</i>	2R	18971309	18972537	-
FBgn0029746	<i>CG15465</i>	X	5085759	5254864	+
FBgn0030466	<i>CG15744</i>	X	13288051	13294433	+
FBgn0029858	<i>CG15896</i>	X	6291303	6294177	+
FBgn0029941	<i>CG1677</i>	X	7281089	7405797	-
FBgn0037728	<i>CG16817</i>	3R	9677927	9679658	+
FBgn0040394	<i>CG16903</i>	X	2078343	2080405	-
FBgn0266917	<i>CG16941</i>	3R	16999384	17002355	-
FBgn0030321	<i>CG1703</i>	X	11611927	11615128	+
FBgn0035140	<i>CG17180</i>	3L	540851	542147	+
FBgn0038829	<i>CG17271</i>	3R	20819129	20821848	-
FBgn0259979	<i>CG17337</i>	2R	5697872	5700212	+
FBgn0032997	<i>CG17486</i>	2R	4619030	4620833	+
FBgn0039959	<i>CG17514</i>	3L	27967244	28012599	-
FBgn0261387	<i>CG17528</i>	2R	4815426	4824319	-

FBgn0033777	CG17574	2R	12849358	12869423	-
FBgn0262115	CG17683	2R	4130974	4133484	+
FBgn0263780	CG17684	2R	1866080	2262115	-
FBgn0040056	CG17698	3L	23737960	23749058	+
FBgn0029877	CG17717	X	6589290	6590646	+
FBgn0035425	CG17746	3L	3236805	3239578	-
FBgn0036454	CG17839	3L	14805136	14882224	+
FBgn0040005	CG17883	2R	4671853	4673639	+
FBgn0033491	CG18011	2R	10142338	10146206	+
FBgn0033426	CG1814	2R	9577427	9581847	+
FBgn0030956	CG18259	X	18781265	18783494	-
FBgn0039189	CG18528	3R	24358095	24360144	-
FBgn0027561	CG18659	2R	9123304	9132030	-
FBgn0040964	CG18661	2L	8997605	8998544	+
FBgn0042185	CG18769	3L	6550738	6593940	+
FBgn0042132	CG18809	X	19741224	19744335	-
FBgn0030485	CG1998	X	13409369	13413074	-
FBgn0037292	CG2022	3R	4986500	5011031	-
FBgn0029942	CG2059	X	7286358	7288117	+
FBgn0030003	CG2116	X	8129812	8131783	+
FBgn0033289	CG2121	2R	8396397	8411767	-
FBgn0035211	CG2211	3L	1333239	1335359	-
FBgn0030320	CG2247	X	11606290	11611652	-
FBgn0039890	CG2316	4	184076	193829	-
FBgn0029672	CG2875	X	3571456	3573622	-
FBgn0023529	CG2918	X	2271008	2275068	-
FBgn0023528	CG2924	X	2264657	2270761	-
FBgn0040373	CG3038	X	243954	245856	-
FBgn0050428	CG30428	2R	25251927	25254535	+
FBgn0050438	CG30438	2R	5496674	5549543	+
FBgn0034703	CG3045	2R	22172803	22174691	-
FBgn0034816	CG3085	2R	23074823	23076857	+
FBgn0051038	CG31038	3R	29877059	29903231	+
FBgn0033005	CG3107	2R	5090581	5095090	+
FBgn0051103	CG31103	3R	25219318	25221444	+
FBgn0051221	CG31221	3R	19412689	19460311	+
FBgn0051406	CG31406	3R	10348761	10350010	+
FBgn0051457	CG31457	3R	23126581	23127981	-
FBgn0051542	CG31542	3R	5369540	5371744	+
FBgn0051637	CG31637	2L	6498647	6526996	+
FBgn0051752	CG31752	2L	18839628	18841310	-
FBgn0051998	CG31998	4	196675	205945	-
FBgn0052000	CG32000	4	132220	143123	+
FBgn0267795	CG32138	3L	14053215	14071583	+
FBgn0052206	CG32206	3L	19340321	19412912	-
FBgn0052365	CG32365	3L	7869042	7894814	+
FBgn0052369	CG32369	3L	7777105	7809825	-
FBgn0052473	CG32473	3R	13302648	13312785	+
FBgn0266918	CG32486	3L	3055908	3070839	-
FBgn0052676	CG32676	X	10711163	10744943	-
FBgn0267253	CG32700	X	9502826	9550838	-
FBgn0052758	CG32758	X	5719374	5738031	-
FBgn0052767	CG32767	X	5071027	5084768	-
FBgn0052816	CG32816	X	316576	470726	-
FBgn0052850	CG32850	4	314923	331387	+
FBgn0053057	CG33057	3L	8402168	8405277	-
FBgn0053111	CG33111	3R	23801714	23819237	-
FBgn0053155	CG33155	2R	13954195	13955664	+
FBgn0053169	CG33169	3L	22863864	22864496	+
FBgn0053217	CG33217	3L	23126025	23132209	+
FBgn0053267	CG33267	3L	11564483	11572796	+
FBgn0053926	CG33926	3L	9443232	9446388	+
FBgn0066303	CG33932	X	19744431	19745898	+
FBgn0083966	CG34130	3R	26189004	26189977	-
FBgn0085201	CG34172	2L	2192525	2197912	-
FBgn0085306	CG34277	3R	5369540	5371744	+
FBgn0085382	CG34353	3R	27767966	27905843	-
FBgn0085383	CG34354	3R	28146880	28240526	+
FBgn0085384	CG34355	3R	23803859	23859167	+
FBgn0085391	CG34362	3R	28026615	28090740	+
FBgn0085430	CG34401	X	18863950	18884075	+
FBgn0085451	CG34422	X	18843663	18855858	+
FBgn0085464	CG34435	X	5613325	5614467	-
FBgn0085478	CG34449	X	9324508	9356227	-
FBgn0035033	CG3548	2R	24599947	24602367	+
FBgn0029708	CG3556	X	4530231	4535464	+
FBgn0029706	CG3626	X	4366417	4371136	+

FBgn0261444	CG3638	X	1215289	1236684	-
FBgn0032974	CG3651	2L	22121338	22126614	+
FBgn0036684	CG3764	3L	16994717	17012565	-
FBgn0035088	CG3776	2R	24969678	24970855	+
FBgn0024989	CG3777	X	279703	350504	+
FBgn0036842	CG3797	3L	19059400	19062816	-
FBgn0036838	CG3808	3L	18997875	19000608	-
FBgn0029867	CG3847	X	6347103	6349236	+
FBgn0029873	CG3918	X	6524464	6526342	+
FBgn0031574	CG3964	2L	3862668	3867507	+
FBgn0058045	CG40045	3L	24028515	24035859	+
FBgn0058178	CG40178	3L	25798441	26014112	-
FBgn0058191	CG40191	2R	1264140	1267747	+
FBgn0029821	CG4020	X	5905746	5908001	+
FBgn0063670	CG40228	3L	27082091	27083906	-
FBgn0058439	CG40439	2L	22797519	22798276	-
FBgn0058470	CG40470	3L	23839860	23986410	-
FBgn0085521	CG40813	X	22143102	22143816	+
FBgn0085638	CG41378	2R	2770380	2846708	-
FBgn0087011	CG41520	2R	1649061	1778937	+
FBgn0259101	CG42249	X	11096273	11108148	+
FBgn0259229	CG42329	2L	1219293	1229802	+
FBgn0259242	CG42340	X	6423123	6524323	-
FBgn0261570	CG42684	X	17710144	17752007	+
FBgn0263354	CG42784	2L	13415431	13500427	+
FBgn0261859	CG42788	3R	15095957	15131926	-
FBgn0031287	CG4291	2L	851251	852730	-
FBgn0262570	CG43110	2R	17477565	17486220	-
FBgn0262599	CG43129	2L	10850141	10854604	+
FBgn0038787	CG4360	3R	20324274	20328003	-
FBgn0032138	CG4364	2L	9708921	9711271	-
FBgn0037024	CG4365	3L	20798645	20800081	+
FBgn0263996	CG43739	2L	20871335	20918931	-
FBgn0264090	CG43759	X	18930335	19028629	+
FBgn0264449	CG43867	X	808217	927975	-
FBgn0265002	CG44153	2L	10064121	10180256	-
FBgn0266100	CG44837	3L	11850645	11938872	-
FBgn0031896	CG4502	2L	7194908	7204264	-
FBgn0266486	CG45085	2R	9186670	9192096	-
FBgn0266696	CG45186	3L	2377655	2499226	+
FBgn0267428	CG45781	2R	432219	705848	+
FBgn0267429	CG45782	3L	25236940	25670980	-
FBgn0032364	CG4970	2L	11517391	11519783	+
FBgn0035953	CG5087	3L	8998184	9002566	+
FBgn0031912	CG5261	2L	7426866	7430329	+
FBgn0039160	CG5510	3R	24167675	24169562	-
FBgn0032656	CG5674	2L	17963379	17974868	+
FBgn0036560	CG5895	3L	16035485	16037227	+
FBgn0032587	CG5953	2L	16508078	16532877	-
FBgn0039492	CG6051	3R	27124759	27151069	-
FBgn0039417	CG6073	3R	26187018	26188807	-
FBgn0039451	CG6420	3R	26719847	26725216	-
FBgn0036710	CG6479	3L	17337172	17339262	-
FBgn0032363	CG6509	2L	11508399	11517081	-
FBgn0037855	CG6621	3R	10889768	10893531	-
FBgn0036062	CG6685	3L	9966603	9968317	-
FBgn0037878	CG6693	3R	11220268	11221639	-
FBgn0036843	CG6812	3L	19063165	19066151	+
FBgn0036240	CG6928	3L	12003155	12008051	+
FBgn0038286	CG6966	3R	15079320	15095631	-
FBgn0030085	CG6999	X	9088367	9089314	+
FBgn0039026	CG7029	3R	22750901	22794030	+
FBgn0030086	CG7033	X	9089513	9092826	+
FBgn0032521	CG7110	2L	13398991	13411047	+
FBgn0030970	CG7326	X	18861197	18863776	-
FBgn0031374	CG7337	2L	1884622	1944289	+
FBgn0038108	CG7518	3R	12998089	13008404	+
FBgn0036734	CG7564	3L	17514298	17524740	+
FBgn0033548	CG7637	2R	10810556	10810936	-
FBgn0038536	CG7655	3R	17682669	17683773	+
FBgn0039743	CG7946	3R	30052514	30054697	+
FBgn0033391	CG8026	2R	9186670	9192096	-
FBgn0037702	CG8176	3R	9516007	9527237	+
FBgn0037624	CG8223	3R	8747798	8754104	+
FBgn0034050	CG8297	2R	15934825	15935938	+
FBgn0037720	CG8312	3R	9591309	9625073	+
FBgn0035707	CG8368	3L	6603684	6608739	+

FBgn0027495	<i>CG8378</i>	2R	12140631	12143272	+
FBgn0034073	<i>CG8414</i>	2R	16099306	16102608	-
FBgn0027602	<i>CG8611</i>	X	17413267	17422145	-
FBgn0033309	<i>CG8735</i>	2R	8596972	8599962	-
FBgn0036900	<i>CG8765</i>	3L	19683941	19687353	-
FBgn0037676	<i>CG8861</i>	3R	9293642	9328511	-
FBgn0030812	<i>CG8949</i>	X	17068717	17077897	-
FBgn0031738	<i>CG9171</i>	2L	5767002	5800253	-
FBgn0031779	<i>CG9175</i>	2L	6096698	6098966	-
FBgn0032919	<i>CG9253</i>	2L	21143229	21145146	+
FBgn0032524	<i>CG9267</i>	2L	13444103	13445651	-
FBgn0032883	<i>CG9323</i>	2L	20754579	20757985	-
FBgn0035094	<i>CG9380</i>	2R	25183628	25255318	-
FBgn0031813	<i>CG9527</i>	2L	6426724	6448403	-
FBgn0031826	<i>CG9550</i>	2L	6497053	6498466	+
FBgn0030768	<i>CG9723</i>	X	16653220	16655015	-
FBgn0027866	<i>CG9776</i>	3R	4327814	4334071	-
FBgn0037623	<i>CG9801</i>	3R	8735879	8747675	-
FBgn0037636	<i>CG9821</i>	3R	8813490	8820682	-
FBgn0030757	<i>CG9902</i>	X	16542124	16547520	-
FBgn0032781	<i>CG9987</i>	2L	19430643	19432444	+
FBgn0021760	<i>chb</i>	3L	21172853	21183278	+
FBgn0053194	<i>CheA29a</i>	2L	8477349	8478088	+
FBgn0086758	<i>chinmo</i>	2L	1651258	1704682	+
FBgn0026084	<i>cib</i>	X	4106113	4110981	+
FBgn0262582	<i>cic</i>	3R	20252770	20303942	+
FBgn0027598	<i>cindr</i>	3R	30808617	30827005	+
FBgn0035533	<i>Cip4</i>	3L	4322491	4364102	-
FBgn0015024	<i>Cklalpha</i>	X	12653626	12657834	+
FBgn0264492	<i>Cklalpha</i>	3L	23097072	23103460	+
FBgn0000259	<i>Ckillbeta</i>	X	11792533	11801587	+
FBgn0010314	<i>Cks30A</i>	2L	9330763	9331981	+
FBgn0032979	<i>Clamp</i>	2L	22165720	22169143	-
FBgn0040232	<i>cmet</i>	2L	11261026	11269002	-
FBgn0263257	<i>Cngl</i>	X	15386038	15441252	-
FBgn0259212	<i>cno</i>	3R	5170004	5217456	-
FBgn0005775	<i>Con</i>	3L	4936758	5079033	-
FBgn0031066	<i>COX6B</i>	X	19740537	19744335	-
FBgn0263911	<i>COX8</i>	3L	21538859	21539447	-
FBgn0013770	<i>Cp1</i>	2R	13960675	13967981	+
FBgn0036680	<i>Cpr73D</i>	3L	16939100	16957689	-
FBgn0261429	<i>CR42646</i>	2R	5363253	5367357	+
FBgn0265784	<i>CrebB</i>	X	18366357	18377864	+
FBgn0024811	<i>Crk</i>	4	210224	213165	+
FBgn0001994	<i>crp</i>	2L	16263556	16287730	-
FBgn0036746	<i>Crtc</i>	3L	17659818	17669234	-
FBgn0028837	<i>CSN6</i>	3R	22580773	22582033	+
FBgn0000382	<i>csw</i>	X	2094234	2115701	+
FBgn0015509	<i>Cul1</i>	2R	7916856	7921579	+
FBgn0000405	<i>CycB</i>	2R	22803521	22806948	-
FBgn0025455	<i>CycT</i>	3L	17551004	17557788	-
FBgn0032378	<i>CycY</i>	2L	11810092	11813780	-
FBgn0004432	<i>Cyp1</i>	X	16317673	16320370	-
FBgn0035141	<i>Cypl</i>	3L	542122	542931	-
FBgn0030001	<i>cyr</i>	X	8121280	8135713	-
FBgn0264294	<i>Cyt-b5</i>	2R	7533506	7535936	+
FBgn0262029	<i>d</i>	2L	8466817	8488671	+
FBgn0033015	<i>d4</i>	2R	5259004	5295965	+
FBgn0019643	<i>Dat</i>	2R	24139563	24157762	+
FBgn0031820	<i>Daxx</i>	2L	6480929	6487576	+
FBgn0024804	<i>Dbp80</i>	3L	27279316	27422159	+
FBgn0013799	<i>Deaf1</i>	3L	19818174	19830686	+
FBgn0033160	<i>Dhx15</i>	2R	7387187	7391023	+
FBgn0011202	<i>dia</i>	2L	20758144	20768053	+
FBgn0260635	<i>Diap1</i>	3L	16038410	16051034	-
FBgn0015247	<i>Diap2</i>	2R	15932170	15934825	-
FBgn0033486	<i>dmpd</i>	2R	10117694	10121451	+
FBgn0259113	<i>DNAPol-alpha180</i>	3R	21666562	21671750	-
FBgn0037554	<i>DNAPol-iota</i>	3R	8233507	8237389	+
FBgn0024245	<i>dnt</i>	2L	19338669	19363227	-
FBgn0043903	<i>dome</i>	X	19676061	19683518	-
FBgn0011582	<i>Dop1R1</i>	3R	14165379	14214810	-
FBgn0266137	<i>Dop1R2</i>	3R	29630304	29659984	-
FBgn0027835	<i>Dp1</i>	2R	18412027	18421124	+
FBgn0040726	<i>dpr1</i>	2R	20698483	20750442	+
FBgn0261871	<i>dpr2</i>	2L	10917015	10964153	-
FBgn0260995	<i>dpr21</i>	2R	3066499	3191011	+

FBgn0040823	<i>dpr6</i>	3L	9974651	10139360	+
FBgn0052600	<i>dpr8</i>	X	14322226	14462351	+
FBgn0053196	<i>dpy</i>	2L	4477462	4614300	-
FBgn0002183	<i>dre4</i>	3L	1871574	1876312	-
FBgn0038145	<i>Droj2</i>	3R	13382106	13385283	+
FBgn0026404	<i>Dronc</i>	3L	9968479	9971002	+
FBgn0020304	<i>drongo</i>	2L	833584	851071	-
FBgn0026479	<i>Drp1</i>	2L	2581281	2585430	-
FBgn0000524	<i>dx</i>	X	6533999	6538575	+
FBgn0027101	<i>Dyrk3</i>	4	1225089	1230713	-
FBgn0000541	<i>E(bx)</i>	3L	233926	246912	-
FBgn0087008	<i>e(y)3</i>	X	19626548	19638369	-
FBgn0033166	<i>Eaf</i>	2R	7396850	7407819	-
FBgn0000543	<i>ecd</i>	3L	2263581	2265857	-
FBgn0027506	<i>EDTP</i>	2R	17432173	17444938	-
FBgn0000556	<i>Ef1alpha48D</i>	2R	11891135	11895762	+
FBgn0011217	<i>eff</i>	3R	14732414	14741319	-
FBgn0000562	<i>egl</i>	2R	23734904	23746829	-
FBgn0040227	<i>elF-3p66</i>	3R	23680039	23682317	+
FBgn0001942	<i>elF-4a</i>	2L	5981764	5985909	+
FBgn0020660	<i>elF-4B</i>	3L	27842669	27858271	-
FBgn0015218	<i>elF-4E</i>	3L	9399618	9402460	-
FBgn0034967	<i>elF-5A</i>	2R	24057798	24059483	+
FBgn0034258	<i>elF3-S8</i>	2R	17665678	17669275	+
FBgn0023213	<i>elF4G</i>	4	915297	930715	-
FBgn0260634	<i>elF4G2</i>	3R	23808285	23819237	-
FBgn0000567	<i>Eip74EF</i>	3L	17558672	17619325	-
FBgn0000568	<i>Eip75B</i>	3L	17950953	18064696	-
FBgn0004865	<i>Eip78C</i>	3L	21226609	21266503	+
FBgn0023212	<i>EloB</i>	3R	20578222	20579850	-
FBgn0020497	<i>emb</i>	2L	8403573	8408853	+
FBgn0028515	<i>EndoG1</i>	2L	16257688	16259511	+
FBgn0025936	<i>Eph</i>	4	610684	622470	+
FBgn0000588	<i>esc</i>	2L	11827204	11829405	-
FBgn0004510	<i>Ets97D</i>	3R	26910775	26912886	-
FBgn0262740	<i>Evi5</i>	X	11430523	11454386	-
FBgn0025608	<i>Faf2</i>	2L	18706010	18708688	-
FBgn0037760	<i>FBXO11</i>	3R	9803486	9809368	-
FBgn0045063	<i>fdl</i>	2R	12487451	12507333	-
FBgn0003062	<i>Fib</i>	2R	23072909	23074725	-
FBgn0039969	<i>Fis1</i>	2R	5603587	5604834	-
FBgn0013269	<i>FK506-bp1</i>	3R	15331584	15333133	-
FBgn0000662	<i>fl(2)d</i>	2R	13819624	13824553	-
FBgn0086675	<i>fne</i>	X	12917477	12950417	+
FBgn0011592	<i>fra</i>	2R	12529053	12564184	+
FBgn0031815	<i>frj</i>	2L	6456052	6459008	+
FBgn0004656	<i>fs(1)h</i>	X	8037808	8061436	-
FBgn0001078	<i>ftz-f1</i>	3L	18750607	18801309	-
FBgn0001087	<i>g</i>	X	13727204	13736278	-
FBgn0040372	<i>G9a</i>	X	245978	254650	+
FBgn0001104	<i>Galphai</i>	3L	6972750	6980044	-
FBgn0029667	<i>Gas8</i>	X	3491011	3504851	-
FBgn0260743	<i>GC1</i>	3R	11967708	11971686	+
FBgn0266465	<i>GckIII</i>	3R	17085513	17087988	+
FBgn0030141	<i>Gga</i>	X	9601030	9604280	+
FBgn0032135	<i>GlcAT-S</i>	2L	9616469	9623109	+
FBgn0264574	<i>Glut1</i>	3L	914074	993788	+
FBgn0027528	<i>goe</i>	X	16727304	16751910	-
FBgn0013272	<i>Gp150</i>	2R	22317662	22329416	+
FBgn0264495	<i>gpp</i>	3R	6406855	6449274	+
FBgn0260798	<i>Gprk1</i>	2R	4322295	4471060	-
FBgn0261278	<i>grp</i>	2L	16680054	16699926	+
FBgn0010226	<i>GstS1</i>	2R	17093246	17099501	-
FBgn0026239	<i>gukh</i>	3R	18984025	19022436	+
FBgn0051992	<i>gw</i>	4	649041	663103	-
FBgn0038295	<i>Gyc88E</i>	3R	15150375	15191242	+
FBgn0261509	<i>haf</i>	2L	1555129	1608404	+
FBgn0026575	<i>hang</i>	X	16422831	16438454	+
FBgn0046706	<i>Haspin</i>	2R	4014111	4049342	+
FBgn0029082	<i>hbs</i>	2R	15011396	15042134	+
FBgn0042712	<i>HBS1</i>	3L	1862881	1865240	-
FBgn0039904	<i>Hcf</i>	4	359938	375554	+
FBgn0011224	<i>heph</i>	3R	31846987	32015520	-
FBgn0052529	<i>Hers</i>	X	19866146	19908108	+
FBgn0035142	<i>Hljk</i>	3L	543060	581099	+
FBgn0053855	<i>His1:CG33855</i>	2L	21521616	21522638	+
FBgn0053853	<i>His2A:CG33853</i>	2L	21518655	21519147	+

FBgn0053856	<i>His2A:CG33856</i>	2L	21523498	21523990	+
FBgn0053859	<i>His2A:CG33859</i>	2L	21528341	21528833	+
FBgn0053862	<i>His2A:CG33862</i>	2L	21533184	21533676	+
FBgn0053900	<i>His2B:CG33900</i>	2L	21457272	21457866	-
FBgn0053854	<i>His3:CG33854</i>	2L	21520109	21520637	+
FBgn0053857	<i>His3:CG33857</i>	2L	21524952	21525480	+
FBgn0025639	<i>Hmt4-20</i>	X	648483	656033	-
FBgn0261456	<i>hpo</i>	2R	19493996	19496856	-
FBgn0263395	<i>hppy</i>	2R	19178738	19227193	+
FBgn0261239	<i>Hr39</i>	2L	21237250	21259675	+
FBgn0264562	<i>Hr4</i>	X	1941940	2007956	+
FBgn0015240	<i>Hr96</i>	3R	25025235	25029351	+
FBgn0266599	<i>Hsc70-4</i>	3R	15242687	15246614	+
FBgn0015245	<i>Hsp60</i>	X	11108482	11112308	+
FBgn0061198	<i>HSPC300</i>	2R	24027717	24028789	-
FBgn0263391	<i>hts</i>	2R	19397032	19424903	-
FBgn0028427	<i>Ilk</i>	3L	21216901	21219240	+
FBgn0013983	<i>imd</i>	2R	18409796	18413599	-
FBgn0025394	<i>inc</i>	X	1483479	1517615	+
FBgn0030945	<i>Ing3</i>	X	18650718	18653091	-
FBgn0011674	<i>insc</i>	2R	20821262	20836028	-
FBgn0030858	<i>IntS2</i>	X	17652761	17656818	-
FBgn0262117	<i>IntS3</i>	2R	4235779	4242934	-
FBgn0086359	<i>Invadolysin</i>	3R	10144668	10159134	+
FBgn0025366	<i>Ip259</i>	2L	10408352	10409610	+
FBgn0051718	<i>Ir31a</i>	2L	10405565	10408197	+
FBgn0040849	<i>Ir41a</i>	2R	4917519	5021955	+
FBgn0259215	<i>Ir93a</i>	3R	20851709	20859945	-
FBgn0036999	<i>isoQC</i>	3L	20474466	20477003	+
FBgn0040309	<i>Jafrac1</i>	X	13329824	13331994	+
FBgn0011225	<i>jar</i>	3R	24252826	24271233	-
FBgn0037703	<i>JHDM2</i>	3R	9516007	9520938	+
FBgn0003357	<i>Jon99Ciii</i>	3R	29922216	29923455	+
FBgn0001291	<i>Jra</i>	2R	10096480	10098556	+
FBgn0015396	<i>jumu</i>	3R	10350182	10361612	+
FBgn0051363	<i>Jupiter</i>	3R	11590386	11619906	-
FBgn0263929	<i>jvl</i>	3R	14741582	14795868	+
FBgn0040208	<i>Kat60</i>	3R	5227289	5232209	-
FBgn0261794	<i>kcc</i>	2R	23907654	23925066	+
FBgn0033494	<i>KCNQ</i>	2R	10145897	10192394	-
FBgn0015400	<i>kek2</i>	2L	11581937	11626883	+
FBgn0019968	<i>Khc-73</i>	2R	15515778	15532259	-
FBgn0262127	<i>kibra</i>	3R	14697689	14724261	-
FBgn0028369	<i>kirre</i>	X	2740384	3134532	+
FBgn0267432	<i>kl-3</i>	Y	336381	563165	+
FBgn0267433	<i>kl-5</i>	Y	22250	137486	-
FBgn0001316	<i>klar</i>	3L	434083	540614	-
FBgn0038476	<i>kuk</i>	3R	17080244	17084781	+
FBgn0033032	<i>kune</i>	2R	5671741	5672800	+
FBgn0259984	<i>kuz</i>	2L	13550139	13639411	+
FBgn0028331	<i>l(1)G0289</i>	X	10348680	10366273	-
FBgn0010607	<i>l(2)05714</i>	2L	4970135	4973921	-
FBgn0262123	<i>l(2)41Ab</i>	2R	1349392	1443935	+
FBgn0010238	<i>Lac</i>	2R	12453190	12465630	+
FBgn0002524	<i>lace</i>	2L	15499127	15505018	+
FBgn0086372	<i>lap</i>	3R	7186994	7200941	+
FBgn0000464	<i>Lar</i>	2L	19586623	19732069	+
FBgn0037856	<i>Leash</i>	3R	10885540	10896418	+
FBgn0034877	<i>levy</i>	2R	23548239	23548982	+
FBgn0034720	<i>Liprin-gamma</i>	2R	22333500	22373109	-
FBgn0017581	<i>Lk6</i>	3R	11750931	11764457	-
FBgn0028717	<i>Lnk</i>	3R	25888542	25893270	+
FBgn0263594	<i>lost</i>	3R	4403076	4407182	+
FBgn0052699	<i>LPCAT</i>	X	9571537	9579987	-
FBgn0051092	<i>LpR2</i>	3R	25698727	25740465	-
FBgn0040765	<i>luna</i>	2R	10977956	11116378	-
FBgn0035640	<i>mad2</i>	3L	5812135	5813093	-
FBgn0002645	<i>Map205</i>	3R	32055279	32068441	-
FBgn0034282	<i>Mapmodulin</i>	2R	17866178	17872015	-
FBgn0015513	<i>mbc</i>	3R	23781765	23801634	+
FBgn0004419	<i>me31B</i>	2L	10239341	10242172	+
FBgn0036761	<i>MED19</i>	3L	17843725	17846501	-
FBgn0040020	<i>MED21</i>	3L	25114924	25115946	-
FBgn0051390	<i>MED7</i>	3R	10760071	10761032	-
FBgn0002715	<i>mei-S332</i>	2R	22122101	22124566	+
FBgn0265140	<i>Meltrin</i>	3R	14664907	14697292	-
FBgn0029155	<i>Men-b</i>	3R	27151662	27157603	+

FBgn0058263	<i>MFS17</i>	2R	2494742	2565385	-
FBgn0053988	<i>Mid1</i>	2R	24695378	24736657	-
FBgn0033846	<i>mip120</i>	2R	13506430	13513112	+
FBgn0263112	<i>Mitf</i>	4	1198852	1224467	+
FBgn0035889	<i>mkg-p</i>	3L	8402168	8405277	-
FBgn0033549	<i>mms4</i>	2R	10811078	10812215	+
FBgn0259168	<i>mnb</i>	X	17862697	17887222	-
FBgn0011661	<i>Moe</i>	X	8873012	8898332	-
FBgn0002783	<i>mor</i>	3R	15968134	15972913	-
FBgn0026409	<i>Mpcp</i>	3L	14537651	14540441	+
FBgn0035107	<i>mri</i>	3L	200174	202152	+
FBgn0032456	<i>MRP</i>	2L	12719045	12766546	+
FBgn0032720	<i>mRpL13</i>	2L	18858028	18859248	-
FBgn0014023	<i>mRpL47</i>	3R	9514822	9515908	-
FBgn0050481	<i>mRpL53</i>	2R	13954195	13955664	+
FBgn0044511	<i>mRpS21</i>	3R	13381276	13381809	-
FBgn0010909	<i>msn</i>	3L	2554847	2586540	-
FBgn0040305	<i>MTF-1</i>	3L	9430312	9439490	+
FBgn0030766	<i>mth1</i>	X	16640968	16650309	+
FBgn0013756	<i>Mtor</i>	2R	11852617	11861202	+
FBgn0050361	<i>mtt</i>	2R	8473956	8532294	-
FBgn0052580	<i>Muc14A</i>	X	16009114	16061722	+
FBgn0264272	<i>mwh</i>	3L	1200786	1232700	+
FBgn0086347	<i>Myo31DF</i>	2L	10491814	10506779	-
FBgn0267431	<i>Myo81F</i>	3R	567076	2532932	+
FBgn0004657	<i>mys</i>	X	8061645	8070237	+
FBgn0004647	<i>N</i>	X	3134870	3172221	+
FBgn0086904	<i>Nacalpa</i>	2R	12759693	12760999	-
FBgn0085434	<i>NaCP60E</i>	2R	24891614	24921677	+
FBgn0260795	<i>NaPi-III</i>	3L	11123348	11134663	+
FBgn0010352	<i>Nc73EF</i>	3L	16954822	16968724	+
FBgn0028704	<i>Nckx30C</i>	2L	9711512	9746495	-
FBgn0030718	<i>ND-20</i>	X	15985473	15986808	-
FBgn0039909	<i>ND-49</i>	4	568296	571554	-
FBgn0058002	<i>ND-AGGG</i>	3L	24976254	24977118	+
FBgn0083167	<i>Neb-cGP</i>	X	10460736	10461878	+
FBgn0017430	<i>Nelf-E</i>	3L	8599442	8600879	-
FBgn0015773	<i>NetA</i>	X	14604012	14653928	-
FBgn0035993	<i>Nf-YA</i>	3L	9440056	9442267	-
FBgn0029905	<i>Nf-YC</i>	X	6818178	6820919	-
FBgn0053554	<i>Nipped-A</i>	2R	5177965	5251022	-
FBgn0083975	<i>Nlg4</i>	3R	20204809	20245473	+
FBgn0011817	<i>nmo</i>	3L	7979046	8054147	+
FBgn0002948	<i>nod</i>	X	11580772	11585750	+
FBgn0262738	<i>norpA</i>	X	4322626	4365408	+
FBgn0085436	<i>Not1</i>	2R	9566146	9579007	-
FBgn0033029	<i>Not3</i>	2R	5656406	5663222	-
FBgn0024320	<i>Npc1a</i>	2L	10213812	10221216	-
FBgn0264975	<i>Nrg</i>	X	8517373	8555170	+
FBgn0262527	<i>ns1</i>	3R	15793782	15802102	+
FBgn0050104	<i>NT5E-2</i>	2R	17485002	17493169	+
FBgn0031886	<i>Nuf2</i>	2L	7064431	7065837	-
FBgn0031078	<i>Nup205</i>	X	19852214	19859379	+
FBgn0039120	<i>Nup98-96</i>	3R	23774225	23781621	-
FBgn0051501	<i>nxf4</i>	3R	7346730	7347836	+
FBgn0014184	<i>Oda</i>	2R	12166295	12174264	-
FBgn0259175	<i>ome</i>	3L	14672839	14747868	+
FBgn0015271	<i>Orc5</i>	2L	13829837	13831576	+
FBgn0261885	<i>osa</i>	3R	17687818	17718350	-
FBgn0031829	<i>Osm6</i>	2L	6555717	6557502	-
FBgn0033179	<i>p47</i>	2R	7465018	7466759	-
FBgn0037718	<i>P58IPK</i>	3R	9586942	9589581	+
FBgn0038100	<i>Paip2</i>	3R	12980792	12985488	+
FBgn0044826	<i>Pak3</i>	3R	16445007	16453821	-
FBgn0085432	<i>pan</i>	4	69326	114270	+
FBgn0020389	<i>Papss</i>	3L	19845293	19860925	+
FBgn0029878	<i>Pat1</i>	X	6590776	6596954	+
FBgn0003042	<i>Pc</i>	3L	21306138	21318020	-
FBgn0033988	<i>pcs</i>	2R	14981263	14991336	+
FBgn0264815	<i>Pde1c</i>	2L	11814156	11928572	-
FBgn0014002	<i>Pdi</i>	3L	15137738	15142840	-
FBgn0029958	<i>Pdp</i>	X	7731779	7734651	-
FBgn0032407	<i>Pex19</i>	2L	12091822	12095250	+
FBgn0027621	<i>Pfrx</i>	X	19495505	19509350	+
FBgn0014869	<i>Pglym78</i>	3R	29148248	29149901	+
FBgn0039776	<i>PH4alphaEFB</i>	3R	30466050	30485799	+
FBgn0031091	<i>Phf7</i>	X	20160355	20165830	-

FBgn0011754	<i>PhKgamma</i>	X	11695137	11704394	+
FBgn0267350	<i>PI4KIIIalpha</i>	X	2624804	2633672	+
FBgn0261811	<i>pico</i>	X	19830215	19852059	-
FBgn0000273	<i>Pka-C1</i>	2L	9682315	9699297	-
FBgn0004611	<i>Plc21C</i>	2L	305935	355566	+
FBgn0025741	<i>PlexA</i>	4	1009895	1027101	-
FBgn0025740	<i>PlexB</i>	4	32478	43778	-
FBgn0062928	<i>pncr009:3L</i>	3L	19486746	19488439	-
FBgn0029903	<i>pod1</i>	X	6803684	6813830	+
FBgn0032884	<i>Pomp</i>	2L	20787656	20789098	+
FBgn0004363	<i>porin</i>	2L	10847227	10850848	-
FBgn0004103	<i>Pp1-87B</i>	3R	12423621	12425917	-
FBgn0046697	<i>Ppr-Y</i>	Y	1636574	1884846	+
FBgn0003139	<i>PpV</i>	X	6371065	6372915	-
FBgn0024734	<i>PRL-1</i>	2L	16245835	16257606	-
FBgn0014269	<i>prod</i>	2R	18969404	18971133	-
FBgn0026189	<i>prominin-like</i>	3L	3114450	3127724	-
FBgn0004595	<i>pros</i>	3R	11328480	11407627	+
FBgn0261394	<i>Prosalpha3</i>	2R	20994900	20996118	+
FBgn0250843	<i>Prosalpha6</i>	2L	10221351	10222546	+
FBgn0010590	<i>Prosbeta1</i>	2R	16013805	16014787	-
FBgn0004370	<i>Ptp10D</i>	X	11622015	11677338	+
FBgn0004369	<i>Ptp99A</i>	3R	29377646	29487131	+
FBgn0032006	<i>Pvr</i>	2L	8220980	8239878	-
FBgn0003174	<i>pwn</i>	2R	7282572	7300806	+
FBgn0003175	<i>px</i>	2R	22494297	22562065	-
FBgn0034918	<i>Pym</i>	2R	23855954	23856936	-
FBgn0259785	<i>pzg</i>	3L	21286099	21290310	+
FBgn0267430	<i>Pzl</i>	3R	2554162	3263582	-
FBgn0263974	<i>qin</i>	3R	18591027	18650137	+
FBgn0003189	<i>r</i>	X	16655359	16668712	+
FBgn0003257	<i>r-l</i>	3R	21070557	21073319	-
FBgn0031090	<i>Rab35</i>	X	20155766	20159872	-
FBgn0035255	<i>RabX5</i>	3L	1668901	1670108	-
FBgn0020618	<i>Rack1</i>	2L	7825347	7827315	-
FBgn0026777	<i>Rad23</i>	4	308093	310822	+
FBgn0015286	<i>Rala</i>	X	3704610	3719635	-
FBgn0020255	<i>Ran</i>	X	11144852	11148716	-
FBgn0003204	<i>ras</i>	X	10744502	10749097	+
FBgn0003206	<i>Ras64B</i>	3L	4139076	4141398	+
FBgn0262734	<i>Rbp2</i>	X	16448665	16454972	+
FBgn0261064	<i>Rbsn-5</i>	2L	8159832	8161800	+
FBgn0261549	<i>rdgA</i>	X	8907068	9029476	+
FBgn0027872	<i>rdgBbeta</i>	2R	17695776	17698362	-
FBgn0243486	<i>rdo</i>	2L	18012380	18070246	+
FBgn0031814	<i>retm</i>	2L	6448464	6455929	-
FBgn0004795	<i>retn</i>	2R	23632610	23654820	+
FBgn0087002	<i>Rfabg</i>	4	1060969	1077273	+
FBgn0021906	<i>RFeSP</i>	2L	1612429	1614160	-
FBgn0266098	<i>rg</i>	X	5085759	5254864	+
FBgn0267792	<i>rgr</i>	2R	8600415	8612295	+
FBgn0041191	<i>Rheb</i>	3R	5568921	5570491	+
FBgn0014020	<i>Rho1</i>	2R	16102687	16107229	+
FBgn0261461	<i>RhoGAP18B</i>	X	19136107	19167082	-
FBgn0031118	<i>RhoGAP19D</i>	X	20469955	20510694	-
FBgn0038853	<i>RhoGAP93B</i>	3R	21083043	21097827	-
FBgn0026375	<i>RhoGAPp190</i>	X	17639147	17652562	-
FBgn0083940	<i>RhoU</i>	X	10086527	10148876	+
FBgn0032189	<i>Ripalpha</i>	2L	10199401	10200974	-
FBgn0003256	<i>rl</i>	2R	1071462	1125927	+
FBgn0262116	<i>RNASEK</i>	2R	4186835	4188127	-
FBgn0035106	<i>rno</i>	3L	187207	199762	-
FBgn0014024	<i>Rnp4F</i>	X	5318928	5322696	-
FBgn0026181	<i>Rok</i>	X	16624012	16637414	-
FBgn0004574	<i>Rop</i>	3L	4136359	4138996	-
FBgn0003275	<i>Rpl18</i>	3R	5371795	5372397	+
FBgn0024733	<i>RpL10</i>	3L	23093190	23095471	-
FBgn0013325	<i>RpL11</i>	2R	19442342	19443825	+
FBgn0037351	<i>RpL13A</i>	3R	5624474	5625947	+
FBgn0017579	<i>RpL14</i>	3L	8601006	8602392	+
FBgn0028697	<i>RpL15</i>	3L	27267255	27268445	+
FBgn0029897	<i>RpL17</i>	X	6741537	6744238	-
FBgn0002607	<i>RpL19</i>	2R	24967877	24969547	-
FBgn0032987	<i>RpL21</i>	2L	22247111	22247875	-
FBgn0015288	<i>RpL22</i>	X	762560	765130	-
FBgn0010078	<i>RpL23</i>	2R	22854383	22855694	+
FBgn0026372	<i>RpL23A</i>	3L	1667192	1668654	-

FBgn0261606	<i>RpL27A</i>	2L	4457186	4458364	-
FBgn0035422	<i>RpL28</i>	3L	3220911	3222960	-
FBgn0016726	<i>RpL29</i>	2R	21293768	21294404	+
FBgn0020910	<i>RpL3</i>	3R	11221894	11225173	+
FBgn0086710	<i>RpL30</i>	2L	19008031	19009306	-
FBgn0025286	<i>RpL31</i>	2R	9587193	9587989	+
FBgn0002626	<i>RpL32</i>	3R	30045229	30046161	-
FBgn0037686	<i>RpL34b</i>	3R	9400237	9401226	-
FBgn0031980	<i>RpL36A</i>	2L	8041873	8042909	-
FBgn0030616	<i>RpL37a</i>	X	15137870	15139367	-
FBgn0261608	<i>RpL37A</i>	2L	5070957	5072055	+
FBgn0040007	<i>RpL38</i>	2R	4515388	4516458	-
FBgn0066084	<i>RpL41</i>	2R	24903416	24903935	-
FBgn0064225	<i>RpL5</i>	2L	22532279	22536884	-
FBgn0005593	<i>RpL7</i>	2L	10201004	10202321	+
FBgn0014026	<i>RpL7A</i>	X	6530897	6533348	-
FBgn0261602	<i>RpL8</i>	3L	2587456	2588883	+
FBgn0000100	<i>RpLP0</i>	3L	22075867	22077487	+
FBgn0003274	<i>RpLP2</i>	2R	16586129	16586732	+
FBgn0028695	<i>Rpn1</i>	3L	19915051	19918160	+
FBgn0015283	<i>Rpn10</i>	3L	21537000	21538582	+
FBgn0028689	<i>Rpn6</i>	2R	14750166	14752910	-
FBgn0028691	<i>Rpn9</i>	3R	23731375	23733462	-
FBgn0066304	<i>Rpp20</i>	X	19744431	19745898	+
FBgn0004403	<i>RpS14a</i>	X	7933742	7934677	+
FBgn0010198	<i>RpS15Aa</i>	X	13335637	13337705	-
FBgn0034743	<i>RpS16</i>	2R	22605745	22607995	+
FBgn0005533	<i>RpS17</i>	3L	9428795	9429821	-
FBgn0010412	<i>RpS19a</i>	X	16637894	16639249	+
FBgn0015521	<i>RpS21</i>	2L	2856070	2857029	+
FBgn0086472	<i>RpS25</i>	3R	11215028	11216287	-
FBgn0003942	<i>RpS27A</i>	2L	10408352	10410456	+
FBgn0030136	<i>RpS28b</i>	X	9554623	9555661	+
FBgn0261599	<i>RpS29</i>	3R	9778042	9779528	+
FBgn0038834	<i>RpS30</i>	3R	20850516	20851427	+
FBgn0017545	<i>RpS3A</i>	4	65225	67207	-
FBgn0011284	<i>RpS4</i>	3L	13041756	13044234	+
FBgn0002590	<i>RpS5a</i>	X	17143588	17148264	-
FBgn0039757	<i>RpS7</i>	3R	30206447	30209020	-
FBgn0028685	<i>Rpt4</i>	X	6289470	6291245	-
FBgn0034065	<i>Rrp42</i>	2R	16014908	16016050	+
FBgn0053113	<i>Rtnl1</i>	2L	4992808	5009720	-
FBgn0261277	<i>rtv</i>	X	11152484	11153990	-
FBgn0003301	<i>rut</i>	X	14787478	14826073	-
FBgn0003302	<i>rux</i>	X	6035753	6037800	-
FBgn0034763	<i>RYBP</i>	2R	22670587	22673212	+
FBgn0003310	<i>S</i>	2L	1049674	1077815	-
FBgn0000416	<i>Sap-r</i>	3R	30883464	30889062	-
FBgn0038947	<i>Sar1</i>	3R	22356685	22360711	+
FBgn0016754	<i>sba</i>	3R	23894174	23922973	-
FBgn0040918	<i>schlank</i>	X	6257668	6267228	-
FBgn0020908	<i>Scp1</i>	2R	2932595	2968052	-
FBgn0263289	<i>scrib</i>	3R	26536350	26604051	+
FBgn0010638	<i>Sec61beta</i>	2R	14618771	14619681	+
FBgn0031049	<i>Sec61gamma</i>	X	19643327	19644518	+
FBgn0011259	<i>Sema-1a</i>	2L	8542147	8672041	+
FBgn0011260	<i>Sema-2a</i>	2R	16500178	16533459	+
FBgn0003360	<i>sesB</i>	X	10780893	10786958	-
FBgn0030486	<i>Set2</i>	X	13413242	13421024	+
FBgn0050390	<i>Sgf29</i>	2R	21292239	21293646	-
FBgn0003371	<i>sgg</i>	X	2633952	2679553	+
FBgn0265101	<i>Sgt1</i>	3R	8304190	8305274	-
FBgn0085395	<i>Shawl</i>	2L	9370309	9415156	-
FBgn0003391	<i>shg</i>	2R	21049654	21057197	-
FBgn0003392	<i>shi</i>	X	15892116	15906716	+
FBgn0013733	<i>shot</i>	2R	13864237	13942110	-
FBgn0037802	<i>Sirt6</i>	3R	10255349	10261849	-
FBgn0026179	<i>siz</i>	3L	21034535	21075444	+
FBgn0037643	<i>skap</i>	3R	8938724	8943027	+
FBgn0025637	<i>SkpA</i>	X	656114	657899	+
FBgn0016984	<i>skt1</i>	2R	20827282	20836028	-
FBgn0032901	<i>sky</i>	2L	20871335	20918931	-
FBgn0040011	<i>Slmap</i>	2L	22579072	22585843	+
FBgn0086906	<i>sfs</i>	3L	2039681	2115611	-
FBgn0023167	<i>SmD3</i>	2R	12168731	12170003	+
FBgn0016070	<i>smg</i>	3L	8990317	8997989	-
FBgn0264922	<i>smt3</i>	2L	6966780	6967644	-

FBgn0011288	<i>Snap25</i>	3L	24074180	24299205	+
FBgn0003449	<i>snf</i>	X	5309242	5310501	+
FBgn0264357	<i>SNF4Agamma</i>	3R	21140739	21214269	+
FBgn0265630	<i>sno</i>	X	13195499	13211674	-
FBgn0016978	<i>snRNP-U1-70K</i>	2L	6968711	6971737	-
FBgn0038065	<i>Snx3</i>	3R	12628031	12630495	+
FBgn0030869	<i>Socs16D</i>	X	17820764	17827564	-
FBgn0041184	<i>Socs36E</i>	2L	18138675	18152417	-
FBgn0001965	<i>Sos</i>	2L	13813816	13819824	+
FBgn0086683	<i>Spf45</i>	2L	23066874	23068386	-
FBgn0264324	<i>spg</i>	3R	28845270	28870439	+
FBgn0086676	<i>spin</i>	2R	16124981	16138238	+
FBgn0010905	<i>Spn</i>	3L	2505245	2554292	-
FBgn0052451	<i>SPoCk</i>	3L	22749444	22787631	+
FBgn0263987	<i>spoon</i>	X	5412386	5420867	-
FBgn0029768	<i>SPR</i>	X	5446656	5494012	+
FBgn0085443	<i>spri</i>	X	10490069	10585422	-
FBgn0036374	<i>Spt20</i>	3L	13502707	13511541	+
FBgn0259678	<i>sqa</i>	2R	9716348	9748121	-
FBgn0267347	<i>squ</i>	2L	16680054	16681653	+
FBgn0038320	<i>Sra-1</i>	3R	15333266	15338365	+
FBgn0036340	<i>SRm160</i>	3L	13036821	13040976	+
FBgn0038808	<i>Srp14</i>	3R	20580115	20580764	+
FBgn0010747	<i>Srp54k</i>	3L	5152678	5154777	+
FBgn0003512	<i>Sry-delta</i>	3R	30043341	30044886	+
FBgn0003517	<i>sta</i>	X	1481797	1483413	-
FBgn0044817	<i>Ste12DOR</i>	X	14000210	14000889	+
FBgn0086779	<i>step</i>	2L	21740041	21757466	-
FBgn0259817	<i>SteXh.CG42398</i>	2.11E+14	1449	2180	+
FBgn0003557	<i>Su(dx)</i>	2L	2037714	2044372	+
FBgn0003638	<i>su(w[a])</i>	X	1012779	1046040	+
FBgn0264270	<i>Sxl</i>	X	7074550	7098053	-
FBgn0024187	<i>syd</i>	3L	7916650	7936120	-
FBgn0039212	<i>Syx18</i>	3R	24623802	24625562	-
FBgn0013343	<i>Syx1A</i>	3R	24101600	24105763	-
FBgn0004359	<i>T48</i>	3R	26881734	26910997	+
FBgn0010355	<i>Taf1</i>	3R	6646889	6656048	+
FBgn0037792	<i>TAF1B</i>	3R	10140103	10144184	-
FBgn0024909	<i>Taf7</i>	3R	7907333	7909721	+
FBgn0086674	<i>Tango13</i>	X	13563823	13593224	+
FBgn0052675	<i>Tango5</i>	X	10760048	10764413	-
FBgn0037766	<i>Teh1</i>	3R	9826081	9868120	-
FBgn0023479	<i>Tequila</i>	3L	9074643	9092131	+
FBgn0261014	<i>TER94</i>	2R	9989159	9993559	+
FBgn0263392	<i>Tet</i>	3L	2786207	2879158	-
FBgn0011289	<i>TfIIA-L</i>	3R	27251112	27256463	+
FBgn0013347	<i>TfIIA-S</i>	3R	23890388	23891060	-
FBgn0015828	<i>TfIIealpha</i>	3L	11682038	11683805	+
FBgn0010422	<i>TfIIS</i>	2L	15058919	15060757	-
FBgn0031975	<i>Tg</i>	2L	8011405	8026898	+
FBgn0036373	<i>Tgi</i>	3L	13486797	13502492	+
FBgn0032988	<i>Tif-IA</i>	2L	22249876	22258260	+
FBgn0038118	<i>timeout</i>	3R	13088651	13163876	+
FBgn0003714	<i>tko</i>	X	2442313	2443976	-
FBgn0086899	<i>Tlk</i>	X	3720007	3789770	+
FBgn0015600	<i>toc</i>	2L	3068345	3144786	-
FBgn0004885	<i>tok</i>	3R	24719697	24749125	+
FBgn0004924	<i>Top1</i>	X	15319479	15328029	+
FBgn0037751	<i>topi</i>	3R	9775121	9777943	+
FBgn0032586	<i>Tpr2</i>	2L	16491540	16507621	+
FBgn0040340	<i>TRAM</i>	X	935232	937822	+
FBgn0037734	<i>trbd</i>	3R	9705996	9711037	-
FBgn0003744	<i>trc</i>	3L	19830864	19834304	-
FBgn0039668	<i>Trc8</i>	3R	29499025	29503797	-
FBgn0030049	<i>Trf4-1</i>	X	8560322	8570159	+
FBgn0003862	<i>trx</i>	3R	14263358	14286903	-
FBgn0029506	<i>Tsp42Ee</i>	2R	7012254	7018362	+
FBgn0027865	<i>Tsp96F</i>	3R	25872900	25881427	-
FBgn0011726	<i>tsr</i>	2R	24044453	24046805	-
FBgn0034046	<i>tun</i>	2R	15794000	15855645	+
FBgn0003896	<i>tup</i>	2L	18859507	18881261	-
FBgn0029128	<i>tyn</i>	X	142208	200663	+
FBgn0023143	<i>Uba1</i>	2R	9688289	9693328	-
FBgn0004436	<i>Ubc6</i>	3R	4948755	4952682	-
FBgn0029996	<i>UbcE2H</i>	X	8087544	8094064	-
FBgn0262124	<i>uex</i>	2R	3900285	3949425	-
FBgn0036136	<i>Ufd1-like</i>	3L	11121966	11123216	-

FBgn0031879	<i>uif</i>	2L	6972828	7010359	-
FBgn0025549	<i>unc-119</i>	X	7288367	7291298	-
FBgn0040395	<i>Unc-76</i>	X	2080610	2093948	+
FBgn0004395	<i>unk</i>	3R	23149653	23157862	-
FBgn0036398	<i>upSET</i>	3L	14002127	14020148	+
FBgn0260008	<i>UQCR-11</i>	3L	25120709	25126171	+
FBgn0036728	<i>UQCR-Q</i>	3L	17474761	17476124	+
FBgn0003963	<i>ush</i>	2L	476220	540560	+
FBgn0028476	<i>Usp1</i>	3R	29229161	29235302	+
FBgn0039025	<i>Usp12-46</i>	3R	22750901	22776374	+
FBgn0032216	<i>Usp14</i>	2L	10312265	10314396	-
FBgn0050421	<i>Usp15-31</i>	2R	24743749	24756976	+
FBgn0031187	<i>Usp2</i>	X	22455803	22470146	+
FBgn0030366	<i>Usp7</i>	X	12022837	12029032	-
FBgn0003969	<i>vap</i>	X	15999951	16005812	-
FBgn0262736	<i>Vha16-1</i>	2R	6625242	6633090	-
FBgn0015324	<i>Vha26</i>	3R	5591763	5595356	+
FBgn0005671	<i>Vha55</i>	3R	12623762	12627829	-
FBgn0039058	<i>VhaAC39-2</i>	3R	23158017	23159316	-
FBgn0028662	<i>VhaPPA1-1</i>	3R	14902330	14904061	-
FBgn0024183	<i>vig</i>	2L	15062931	15070316	-
FBgn0259978	<i>vlc</i>	2R	5702112	5705439	+
FBgn0003984	<i>vn</i>	3L	5813338	5845664	-
FBgn0052350	<i>Vps11</i>	3L	23147656	23150499	-
FBgn0034744	<i>Vps20</i>	2R	22608310	22609419	+
FBgn0243516	<i>Vrp1</i>	2R	22106107	22122562	-
FBgn0260987	<i>vtd</i>	3L	27136525	27157999	+
FBgn0267449	<i>WDY</i>	Y	2273422	2487777	+
FBgn0011737	<i>Wee1</i>	2L	6911090	6914138	-
FBgn0034876	<i>wmd</i>	2R	23544823	23548151	-
FBgn0031902	<i>Wnt6</i>	2L	7333714	7352542	+
FBgn0052677	<i>X11Lbeta</i>	X	10627737	10710947	+
FBgn0028554	<i>x16</i>	2L	6914301	6920210	-
FBgn0029906	<i>xit</i>	X	6821016	6822840	+
FBgn0004832	<i>Xpac</i>	X	4102955	4104197	-
FBgn0038150	<i>yellow-e3</i>	3R	13403423	13404870	-
FBgn0267398	<i>Yeti</i>	2R	1343403	1345119	-
FBgn0022959	<i>yps</i>	3L	12121274	12125150	-
FBgn0004049	<i>yrt</i>	3R	13428867	13434984	-
FBgn0265434	<i>zip</i>	2R	24990570	25011965	-
FBgn0039902	<i>Zip102B</i>	4	310930	314087	-
FBgn0039714	<i>Zip99C</i>	3R	29863701	29868895	-
FBgn0260486	<i>Ziz</i>	2L	7472513	7496307	-
FBgn0037000	<i>ZnT77C</i>	3L	20484293	20494921	-
FBgn0024177	<i>zpg</i>	3L	6604366	6606032	-
FBgn0011642	<i>Zyx</i>	4	1057365	1065001	-

Table S7: Validation of ChIP-seq experiments by RT-QPCR.

AE: amplification efficiency. Cq of the Input were adjusted taking dilution into account.

Results were normalized in comparison to the Input.

		AE
RPL7	TSS	2.00
	Gene body	2.00
RPL5	TSS	1.9560
	Gene body	1.9810
Rack1	TSS	2.0389
	Gene body	1.9886
CycG	TSS	2.0122
	Gene body	2.0277

	ChIP	Amplicon	Cq mean			% Input			mean % Input	CV % Input
			replicate 1	replicate 2	replicate 3	replicate 1	replicate 2	replicate 3		
RPL7	a-Myc	TSS	25.51	25.36	28.57	6.94	5.94	1.10	4.66	0.67
		Gene body	29.41	26.55	30.31	0.52	3.74	0.32	1.53	1.26
	mock	TSS	35.32	34.88	33.84	0.01	0.01	0.03	0.01	0.80
		Gene body	37.91	35.74	32.90	0.00	0.01	0.05	0.02	1.41
	INPUT	TSS	21.65	21.28	22.05					
		Gene body	21.83	21.82	22.07					
RPL5	a-Myc	TSS	27.36	24.52	26.95	4.75	15.16	12.66	10.86	0.50
		Gene body	31.00	30.04	28.05	0.34	0.29	1.56	0.73	0.98
	mock	TSS	36.36	35.79	36.60	0.01	0.02	0.02	0.02	0.26
		Gene body	34.54	36.33	35.30	0.03	0.01	0.01	0.02	0.71
	INPUT	TSS	22.82	21.71	23.87					
		Gene body	22.70	21.48	21.96					
Rack1	a-Myc	TSS	24.20	25.00	29.11	5.39	3.05	0.16	2.86	1.09
		Gene body	25.76	27.31	31.07	2.55	0.88	0.07	1.16	0.92
	mock	TSS	28.72	30.88	33.85	0.22	0.05	0.01	0.09	0.80
		Gene body	30.00	33.06	38.62	0.14	0.02	0.00	0.05	0.69
	INPUT	TSS	20.10	19.63	23.61					
		Gene body	20.42	20.52	22.61					
CycG	a-Myc	TSS	30.15	28.71	30.84	0.64	13.71	5.50	6.61	1.00
		Gene body	29.23	24.96	34.85	0.34	4.16	0.01	1.50	1.53
	mock	TSS	32.38	32.74	37.27	0.13	0.82	0.06	0.34	1.24
		Gene body	32.77	29.21	35.67	0.03	0.21	0.01	0.08	1.36
	INPUT	TSS	22.92	25.87	26.69					
		Gene body	21.20	20.46	22.10					

Table S8: List of the 62 genes deregulated in *da-Gal4, UAS-CycGΔP/+* wing imaginal discs and bound by Cyclin G at the TSS.

Gene ID	Gene	Coordinates	Fold change
FBgn0040658	<i>CG13516</i>	2R:22,669,145-22,670,622	0.45461
FBgn0038150	<i>yellow-e3</i>	3R:13,403,423-13,404,870	0.49374
FBgn0050428	<i>CG30428</i>	2R:25,251,927-25,254,535	0.59934
FBgn0263911	<i>COX8</i>	3L:21,538,859-21,539,447	0.60255
FBgn0035032	<i>ATPsynF</i>	2R:24,599,088-24,599,821	0.61090
FBgn0034877	<i>levy</i>	2R:23,548,239-23,548,982	0.63459
FBgn0036728	<i>UQCR-Q</i>	3L:17,474,761-17,476,124	0.63510
FBgn0086675	<i>fne</i>	X:12,917,477-12,950,417	0.65489
FBgn0083167	<i>Neb-cGP</i>	X:10,460,736-10,461,878	0.70284
FBgn0040660	<i>CG13551</i>	2R:23,377,866-23,383,424	0.71449
FBgn0037024	<i>CG4365</i>	3L:20,798,645-20,800,081	0.72118
FBgn0034046	<i>tun</i>	2R:15,794,000-15,855,645	0.72857
FBgn0032884	<i>Pomp</i>	2L:20,787,656-20,789,098	0.73631
FBgn0032781	<i>CG9987</i>	2L:19,430,643-19,432,444	0.75731
FBgn0031066	<i>COX6B</i>	X:19,740,537-19,744,335	0.76360
FBgn0010226	<i>GstS1</i>	2R:17,093,246-17,099,501	0.78064
FBgn0014869	<i>Pglym78</i>	3R:29,148,248-29,149,901	0.78130
FBgn0003884	<i>α-Tubulin at 84B</i>	3R:7,086,599-7,088,839	0.79238
FBgn0033179	<i>p47</i>	2R:7,465,018-7,466,759	0.79458
FBgn0010590	<i>Proteasome β1 subunit</i>	2R:16,013,805-16,014,787	0.81354
FBgn0036842	<i>CG3797</i>	3L:19,059,400-19,062,816	0.82732
FBgn0040309	<i>Jafrac1</i>	X:13,329,824-13,331,994	0.84071
FBgn0260795	<i>NaPi-III</i>	3L:11,123,348-11,134,663	0.86608
FBgn0030616	<i>RpL37a</i>	X:15,137,870-15,139,367	1.15845
FBgn0052699	<i>LPCAT</i>	X:9,571,537-9,579,987	1.16788
FBgn0024245	<i>dnt</i>	2L:19,338,669-19,363,227	1.17348
FBgn0020618	<i>Rack1</i>	2L:7,825,347-7,827,315	1.17770
FBgn0005533	<i>RpS17</i>	3L:9,428,795-9,429,821	1.17829
FBgn0051363	<i>Jupiter</i>	3R:11,590,386-11,619,906	1.19014
FBgn0013325	<i>Rpl11</i>	2R:19,442,342-19,443,825	1.19740
FBgn0263780	<i>CG17684</i>	2R:1,866,080-2,262,115	1.19822
FBgn0027598	<i>cindr</i>	3R:30,808,617-30,827,005	1.20242
FBgn0261606	<i>RpL27A</i>	2L:4,457,186-4,458,364	1.20657
FBgn0032006	<i>Pvr</i>	2L:8,220,980-8,239,878	1.21189
FBgn0017579	<i>RpL14</i>	3L:8,601,006-8,602,392	1.21528
FBgn0014026	<i>RpL7A</i>	X:6,530,897-6,533,348	1.22384
FBgn0261599	<i>RpS29</i>	3R:9,778,042-9,779,528	1.23116
FBgn0053217	<i>CG33217</i>	3L:23,126,025-23,132,209	1.24102
FBgn0031980	<i>RpL36A</i>	2L:8,041,873-8,042,909	1.25680
FBgn0011284	<i>RpS4</i>	3L:13,041,756-13,044,234	1.28572
FBgn0032987	<i>RpL21</i>	2L:22,247,111-22,247,875	1.28773

FBgn0260798	<i>Gprk1</i>	2R:4,322,295-4,471,060	1.29892
FBgn0085384	<i>CG34355</i>	3R:23,803,859-23,859,167	1.30261
FBgn0260486	<i>Ziz</i>	2L:7,472,513-7,496,307	1.30393
FBgn0037000	<i>ZnT77C</i>	3L:20,484,293-20,494,921	1.34194
FBgn0025366	<i>Ip259</i>	2L:10,408,352-10,409,610	1.35186
FBgn0005593	<i>RpL7</i>	2L:10,201,004-10,202,321	1.35897
FBgn0000556	<i>EF1α48D</i>	2R:11,891,135-11,895,762	1.36037
FBgn0034967	<i>eIF-5a</i>	2R:24,057,798-24,059,483	1.37526
FBgn0052365	<i>CG32365</i>	3L:7,869,042-7,894,814	1.39938
FBgn0053653	<i>Cadps</i>	4:1,230,837-1,271,759	1.40905
FBgn0001942	<i>eIF-4a</i>	2L:5,981,764-5,985,909	1.42770
FBgn0028697	<i>RpL15</i>	3L:27,267,255-27,268,445	1.44360
FBgn0017545	<i>RpS3A</i>	4:65,225-67,207	1.45457
FBgn0064225	<i>RpL5</i>	2L:22,532,279-22,536,884	1.47580
FBgn0264562	<i>Hr4</i>	X:1,941,940-2,007,956	1.47882
FBgn0029821	<i>CG4020</i>	X:5,905,746-5,908,001	1.52709
FBgn0031975	<i>Tg</i>	2L:8,011,405-8,026,898	1.57445
FBgn0250816	<i>AGO3</i>	3L:23,554,593-23,689,640	1.61253
FBgn0004865	<i>Eip78C</i>	3L:21,226,609-21,266,503	1.61862
FBgn0032138	<i>CG4364</i>	2L:9,708,921-9,711,271	1.83522
FBgn0011288	<i>Snap25</i>	3L:24,074,180-24,299,205	2.31191

Table S9: Comparison of fragments bound by Cyclin G with fragments bound by ASX, Calypso, PC, PH, PSC, RNAPoIII or enriched in H3K27me3 in 3rd instar wing imaginal discs.

ChIP	Observed overlaps between enriched regions (25 nt fragments)	Expected overlaps under the null hypothesis (25 nt fragments)	Minimal expected overlap for 95% confidence interval	Maximal expected overlap for 95% confidence interval	Sd	Fold enrichment	log2Fold enrichment	p-value
ASX	65109	12958	8368	18156	2978.04	5.0242	2.3289	1.00E-005
Calypso	12237	9690	5619	14506	2711.36	1.2628	0.3366	1.69E-001
PC	194860	127465	111782	143702	9707.22	1.5287	0.6123	1.00E-005
PH	203746	140394	124553	156860	9807.03	1.4512	0.5373	1.00E-005
PSC	95129	75494	62889	89085	7959.99	1.2601	0.3335	9.99E-003
RNAPoIII	161849	82710	70297	95804	7772.29	1.9568	0.9685	1.00E-005
H3K27me3	6623	87315	72570	103081	9320.89	0.0759	-3.7205	1.00E-005

Table S10: Primers used in this study. Coordinates on the *Drosophila* genome (dm6, r6.13)

Cloning primers		Oligonucleotides coordinates	
<i>attB-Nsil-F</i>	5'-GCAATGCATCGTCGACGATGT-3'		
<i>attB-Nsil-R</i>	5'-AATATGCATGTCGACATGCC-3'		
<i>CycGn-F</i>	5'-CACCTCTGTCCCTGTACGCTACTCC-3'	3R: 31,602,187 - 31,602,207	
<i>CycGn-R</i>	5'-CTAACATTGTTCGAAAATGGAATTATGGG-3'	3R: 31,599,273 - 31,599,302	
<i>CycG541-R</i>	5'-CTATCTAGAACGCAGGCCATCGTCG-3'	3R: 31,600,389 - 31,600,409	
<i>CycG130-F</i>	5'-CACCGCCGCTGTGCCGCATCC-3'	3R: 31,601,822 - 31,601,803	
RT-qPCR primers		Oligonucleotides coordinates	
<i>CycG-3'UTR-F</i>	5'-GACAGCCAGCAGCAGTAGAGC-3'	3R:31,597,244 - 31,601,264	
<i>CycG-3'UTR-R</i>	5'-CTACTACACTCGCACGCGAAC-3'	3R:31,597,049 - 31,601,070	
<i>Lam-F</i>	5'-GCCGCACGCACATCCAATTCC-3'	2L: 5,544,475 - 5,544,495	
<i>Lam-R</i>	5'-CTATCTCTTGACCGTGGCGTTC-3'	2L: 5,544,658 - 5,544,637	
<i>Rin-F</i>	5'-CGCTCAGTCGCCGGAAGTAC-3'	3R: 13,649,407 - 13,649,428	
<i>Rin-R</i>	5'-GCAACTACATCGCCGGCCACC-3'	3R: 13,649,580 - 13,649,560	
<i>RPL15-F</i>	5'-CCGACCGAGAAGAAGACAGGG-3'	2L: 22,532,913 - 22,532,893	
<i>RPL15-R</i>	5'-CTCACTACAACGATGGCAAGGC-3'	2L: 22,532,787 - 22,532,808	
<i>RPL7-F</i>	5'-CCGCGAGGACCAGATCAACCG-3'	2L: 10,202,016 - 10,202,036	
<i>RPL7-R</i>	5'-GACTAAATCAGCGAATCGAAGCG-3'	2L: 10,202,203 - 10,202,181	
<i>Rack1-F</i>	5'-CCCTGTGCTTCTCGCCCAACC-3'	2L: 7,825,942 - 7,825,922	
<i>Rack1-R</i>	5'-GGAGTAGCCGCGCAACAGAGTC-3'	2L: 7,825,746 - 7,825,767	
ChIP-qPCR primers		Oligonucleotides coordinates	Position of the amplicon with respect to the TSS
<i>CycG-TSS-F</i>	5'-TAGTTAACAGAGAGAATCG-3'	3R: 31,609,967 - 31,609,949	-7516 to -7739 <i>CycG</i> isoform F
<i>CycG-TSS-R</i>	5'-CTATTTTCTATTCCCTAAGC-3'	3R: 31,609,726 - 31,609,744	
<i>CycG-gene body-F</i>	5'-CTGCCGCGGGTGTACGACTC-3'	3R:31,598,729 - 31,602,748	+10240 to +10408 <i>CycG</i> isoform A
<i>CycG-gene body-R</i>	5'-CTACGCCCTCTTCCGCAACTTG-3'	3R:31,598,917 - 31,602,938	
<i>RPL5-TSS-F</i>	5'-AGCGTCAAAGGCACAGCACAAC-3'	2L: 22,536,739 - 22,536,760	-200 to -369 <i>RPL5</i> isoform G
<i>RPL5-TSS-R</i>	5'-ATCGTTCATACCGTTCACATCGC-3'	2L: 22,536,930 - 22,536,908	
<i>RPL5-gene body-F</i>	5'-CCGACCGAGAAGAAGACAGGG-3'	2L:22,529,961 - 22,535,844	+3738 to +3855 <i>RPL5</i> isoform A
<i>RPL5-gene body-R</i>	5'-CTCACTACAACGATGGCAAGGC-3'	2L:22,530,787 - 22,534,808	
<i>RPL7-TSS-F</i>	5'-TGCTGTTGCTCTGCTAGTGGTG-3'	2L: 10,200,938 - 10,200,959	-85 to -271 <i>RPL7</i> isoform B
<i>RPL7-TSS-R</i>	5'-TTACTAGTCACTGCACACGCTGG-3'	2L: 10,201,145 - 10,201,123	
<i>RPL7-gene body-F</i>	5'-CCGCGAGGACCAGATCAACCG-3'	2L: 10,202,016 - 10,202,036	+1011 to +1196 <i>RPL7</i> isoform A
<i>RPL7-gene body-R</i>	5'-GACTAAATCAGCGAATCGAAGCG-3'	2L: 10,202,203 - 10,202,181	
<i>Rack1-TSS-F</i>	5'-AAACACGTCCAAGGCGCTGC-3'	2L: 7,825,205 - 7,829,225	-36 to -188 <i>Rack1</i> isoform B
<i>Rack1-TSS-R</i>	5'-GTTTTTGATATTATTATTGACGTTACA-3'	2L: 7,827,384 - 7,827,357	
<i>Rack1-gene body-F</i>	5'-CCCTGTGCTTCTCGCCCAACC-3'	2L: 7,825,942 - 7,825,922	+1310 to +1482 <i>Rack1</i> isoform A
<i>Rack1-gene body-R</i>	5'-GGAGTAGCCGCGCAACAGAGTC-3'	2L: 7,825,746 - 7,825,767	

Table S11: RNA-seq of wing imaginal discs.

Sample name	Genotype	Total reads	Filtered reads	Aligned reads	Unmap reads	Reads with multiple alignment	Reads with unique alignments	Reads used for analysis
339	<i>UAS-CycG^{ΔP}, da-Gal4/+</i>	3.12E+07	2.90E+07	3.21E+07	2.32E+06	6.15E+06	2.37E+07	2.30E+07
340	<i>UAS-CycG^{ΔP}, da-Gal4/+</i>	3.61E+07	3.37E+07	4.53E+07	2.12E+06	2.32E+07	2.00E+07	1.93E+07
341	<i>UAS-CycG^{ΔP}, da-Gal4/+</i>	3.76E+07	3.40E+07	4.08E+07	2.53E+06	1.35E+07	2.47E+07	2.40E+07
342	<i>da-Gal4/+</i>	4.18E+07	3.76E+07	4.52E+07	3.21E+06	1.54E+07	2.67E+07	2.58E+07
343	<i>da-Gal4/+</i>	4.52E+07	4.09E+07	4.34E+07	3.48E+06	5.14E+06	3.48E+07	3.40E+07
344	<i>da-Gal4/+</i>	3.68E+07	3.40E+07	4.12E+07	2.50E+06	1.45E+07	2.43E+07	2.35E+07

Table S12: ChIP-seq of wing imaginal discs.

Sample name	Genotype	Total reads	Discarded reads	Output reads	Unmap reads	Reads with multiple alignment	Reads with unique alignments	Reads used for analysis
Input 1	<i>UAS-CycG^{ΔP}/+ ; +/-Gal4</i>	7.40E+07	1.22E+07	6.19E+07	6.75E+05	1.88E+07	4.23E+07	4.23E+07
Input 2	<i>UAS-CycG^{ΔP}/+ ; +/-Gal4</i>	6.06E+07	9.57E+06	5.10E+07	5.49E+05	1.55E+07	3.50E+07	3.50E+07
ChIP 1	<i>UAS-CycG^{ΔP}/+ ; +/-Gal4</i>	3.89E+07	5.53E+06	3.33E+07	5.22E+05	9.88E+06	2.29E+07	2.29E+07
ChIP2	<i>UAS-CycG^{ΔP}/+ ; +/-Gal4</i>	4.88E+07	7.08E+06	4.17E+07	5.49E+05	1.55E+07	3.50E+07	3.50E+07